the general science journal

General Relativity Applications in Astronomy and Cosmology, and Alternative Cosmology

Anatoli Vankov
IPPE, Russia; Bethany College, USA
anatolivankov@hotmail.com

Kirill Vankov
Université Grenoble-Alpes, Grenoble, France
kirill.vankov@gmail.com

2020-06-21

Abstract

Nowadays, among General Relativity and Cosmology communities, there are distinct signs of scientific stagnation, first of all, in our understanding of the Nature of Matter in Space and Time. Big questions, not all of them new, are about an existence of a Universe having no Big Bang, or contrarily, many Big Bangs, or multiverse (many universes). New observations raise more questions rather than bring answers. Thereafter, this work presents a critical review of the General Relativity applications to the Standard Cosmological Model. The Alternative is proposed.

Contents

1 General Relativity in Astronomy and Cosmology

1.1 Preamble

The Standard Cosmological Model is based on General Relativity (GR) concepts, which are parts the GR Foundations, namely, the metric expansion of space for description of cosmological space-time scaling, and the Schwarzschild metric describing gravitational orbits and structure of galaxies in GR Dynamics of particle motion. Both concepts have been historically originated from solutions of Einstein's Field Equations (EFE), which are radically different. Testable predictions of the Cosmological Model are related to observations on the possible largest space-time scale, while while in GR Dynamics tests, observations on a local Astronomical scale.

The above interconnection between Cosmological and GR Dynamics conceptions is only a rough picture. In reality, it is much more complicated. Each conception has its own long-standing inherent problems. There are numerous phenomena, which are hard to explain in General Relativity. They used to be labeled by names, for example, Dark Matter and Dark Energy. As a usual practice in Cosmology, to fit unexplained observations, assumptions are made, which are believed to be true without proof.

Not surprisingly, GR-based Cosmology encounters numerous problems and inherent contradictions. They were accumulated over a long period of time due to many modifications made to account for new discoveries in the course of a progress in high-precision observational technologies. Very disturbing is the admittance of different types of New Physics ousting well established Fundamental Physics. In our view, Cosmology and Gravitation, paired in General Relativity lost scientific connection with physical reality of the world we live.

In this work, an unprecedented attempt is made to conduct a detailed critical analysis of current Cosmology and Gravitation altogether to unveil their true scientific values. The Alternative unfolding a natural vision of physical world is proposed.

The work is started with the GR Dynamics followed by Standard Cosmological Model and the Alternative.

1.2 General Relativity Dynamics: introductory notes

The General Relativity Dynamics of particle motion is studied here in the whole range of gravitational field strength. The attention is focused on Einstein's equation of motion [1] and its exact solutions in comparison with Special Relativity Dynamics and Classical theories. Solutions are obtained in the ideal model, in which the test particle motion in the spherical symmetric geometry is used. It is shown further how the test particle concept is fundamentally important in field theories, particularly, in GR and SR theories.

As an example of the weak field condition, the famous problem of Einstein's Mercury perihelion advance is investigated. There is a common opinion among the GR community that the problem is fully studied and understood in all mathematical and physical aspects. Such a statement is supported by the mainstream and mass media, however, in reality, such an opinion is not true. The exact solutions of the GR equation of motion describing orbital motion in space and time have never been studied. Instead, the approximate field models and solutions were used in spite of the fact that errors due to approximations and assumptions cannot be assessed without the knowledge of exact solutions.

Nowadays, high precision and effective computational methods are available. We used them to study consistent formulations of relativistic dynamics problems and their full exact solutions. Contemporary mathematical numerical methods having no restrictions on their numerical precision make a treatment of tiny observable relativistic effects sufficiently reliable.

There is a wide opinion that all GR predictions are successfully confirmed by empirical tests. However, our results based on exact solutions lead us to conclusion that the GR prediction of perihelion angular advance for *the weak field* without studying the corresponding GR temporal shift has no physical sense. Strong field problem along with inherent methodological controversies also were studied. Some of them were actually known in literature, others mostly ignored, forgotten, and remained unresolved. Methodological and technical novelties are outlined throughout the text, in particular, the following:

- the GR exact full (space and time) solutions in the whole range of gravitational field strength;
- similar studies in the alternative SR framework;
- evaluations of precision requirements in theory and observations;
- criteria for empirical tests of theoretical predictions;
- alternative GPS proposal.

1.3 Some GR works of historic interest

We consider the history of GR development essential for understanding the current status of relativistic particle dynamics. Originally, Einstein's non-classical effect in Mercury's orbit was obtained under assumptions and approximations, among which, weak field conditions in "a perturbation" scheme [1]. It is not clear what and how a small parameter in such approximation should be identified.

Most of responding publications of different authors were devoted to confirmations or modifications of Einstein's methodology of particle dynamics, see reviews in [2–4]. An attention deserves the old work by Hagihara [5] (1931), in which elliptic functions for deriving exact analytic solution of Einstein's problem was suggested. In particular, the Mercury's perihelion anomaly, a very small deviation from the classical theory, is discussed there. Because of absence of numerical computer technique at that time, this work contains only qualitative results.

Later on, Chandrasekhar [6] (1983) studied the problem analytically in terms of elliptic function solution in relationship with the GR Black Hole (BH) concept. However, he modified original Einstein's equation in order to obtain its "simplified" numerical solution in terms of classical geometrical parameter, "an effective eccentricity", in combination with "effective" physical parameters. Consequently, the solution deviated from the exact one, and the difference had not been evaluated. Besides, the GR Mercury problem was not studied there.

More recently, Kraniotis and Whitehouse [7] (2003) used the theory of elliptic functions to obtain the exact solution in order to reproduce Einstein's GR prediction of Mercury's anomaly. Even before their publication, there was a wide belief among Physics community that the above Einstein's problem had been fully studied. In fact, the exact angular solution to the Mercury's problem was obtained for the first time.

However, conditions of arbitrary field strength, the time-dependent problems, and criteria of comparison of GR versus Newtonian predictions, the topics of this work, were not studied there. More historical references can be found in [2].

Over time, the GR treatment of the problem has changed after declaration of Schwarzschild metric being an exact solution to Einstein's field equations. Consequently, the original Einstein's equation of particle motion is considered valid in the whole range of field strength. Further, with no more comments, we use this allowance to study weak field GR effects and strong-field phenomena on the same GR Dynamics footing.

2 GR Particle Dynamics

2.1 Einstein's equation

In this work, the GR particle dynamics is studied apart from Einstein's General Relativity theory of gravitational field. We consider the equation of GR particle dynamics originally presented by Einstein in [1] more than a hundred years ago

$$\left(\frac{\mathrm{d}x}{\mathrm{d}\theta}\right)^2 = \frac{2\,A}{B^2} + \frac{\alpha}{B^2}x - x^2 + \alpha\,x^3\,, \tag{1}$$

where $x = 1/r$ is a reciprocal value of radius; A and B are the total energy and the angular momentum, correspondingly; $\alpha = 2\,r_g = 2\,G\,M/c^2$ is the Schwarzschild radius, r_g is called the gravitational radius.

Here, the mass of gravitational field source M is however greater than the mass of the orbiting body, $M \gg m$. In this approximation, such particles in the field do not interact with each other but equally "feel" a field source of given big mass M without a field disturbance. Therefore, a body of mass m can be considered the standard test particle. It should be noted that the GR Particle Dynamics is based on the Schwarzschild metric having two time variables, the proper time τ and the coordinate time t, but the corresponding equations of motion is defined in observable 4-space with the time t. This is a controversial (τ, t) issue discussed later.

Historically, the equation was used for approximate evaluation of the GR Mercury's perihelion advance, but never exactly solved. In this work, a strict derivation of the equation and its exacts solutions are presented. Physics and Mathematics of GR Dynamics are discussed in details.

2.2 Lagrangian solution, and the formulation of initial conditions

2.2.1 The Hamilton Action Principle

There are several approaches to the derivation of the equation in the contemporary presentation. In the work by Kraniotis and Whitehouse [7], it is shown how it comes from Einstein field equations with the use of Christoffel symbols under conditions of spherical symmetry. Alternatively, it can be derived from the Schwarzschild metric [8, 9].

A quick way is based on the Hamiltonian Action Principle S with the Lagrangian L in analogy to classical mechanics [10]

$$\delta S = \delta \int_{t_1}^{t_2} L(q_i, \dot{q}_i, t)\,\mathrm{d}t = 0\,, \tag{2}$$

where q_i and $\dot{q}_i$ are generalized coordinates and their time derivatives $\dot{q}_i = \partial q_i/\partial t$ characterizing the system, $i = 1, 2, \ldots, N$. The Lagrangian is chosen with the idea to find the extremal path between the starting and ending points in the variational integral S:

$$\frac{\partial L}{\partial q_i} - \frac{\mathrm{d}}{\mathrm{d}t}\frac{\partial L}{\partial \dot{q}_i} = 0\,. \tag{3}$$

In General Relativity, the Lagrangian describing the test particle motion is usually taken in the form $L = \mathrm{d}\tau/\mathrm{d}t$, see [10]. It is obtained from the Schwarzschild metric, where $\mathrm{d}s = c\,\mathrm{d}\tau$ is the world line element, τ is the proper time, and t is the coordinate time. The metric in the quadratic form with the signature $[+,\ -,\ -,\ -]$ is given by

$$\mathrm{d}\tau^2 = (1 - 2\,r_g/r)\,\mathrm{d}t^2 - (1 - 2\,r_g/r)^{-1}\,\mathrm{d}r^2 - r^2\,\mathrm{d}\theta^2\,, \tag{4}$$

where the speed of light and the particle mass are taken $c = 1$, $m = 1$.

The Lagrangian is

$$\begin{aligned} |L| &= \mathrm{d}\tau/\mathrm{d}t \\ &= \left((1 - 2\,r_g/r) - (1 - 2\,r_g/r)^{-1}(\mathrm{d}r/\mathrm{d}t)^2 - r^2\,(\mathrm{d}\theta/\mathrm{d}t)^2\right)^{1/2}\,, \end{aligned} \tag{5}$$

where $q_1 = r$ and $q_2 = \theta$. Note, here $c = 1$, therefore, the Lagrangian L is given in a dimensionless form.

Two constants of motion follow from the consideration of the ignorable temporal and angular variables. First, the conserved angular momentum is $l_0 = r\,(\mathrm{d}\theta/\mathrm{d}\tau)$. Second, the conserved total energy comes out from the Hamiltonian

$$H = \sum_i \dot{q}_i \frac{\partial L}{\partial \dot{q}_i} - L\,. \tag{6}$$

When $l_0 = r\,(\mathrm{d}\theta/\mathrm{d}\tau) = 0$, the conserved energy (in a dimensionless form) is

$$\epsilon_{rad} = (1 - 2\,r_g/r)\,\mathrm{d}t/\mathrm{d}\tau\,. \tag{7}$$

The subscript (rad) there stands for the total energy in the particular case of pure radial motion when $l_0^2 = 0$. The corresponding equation of the radial motion is discussed later. This quantity is very strange and its use has never been properly explained.

Finally, the GR equation of motion equations follow, which will be used for the exact solution of the Mercury's problem. The equations have a dynamic time variable τ, the issue to be discussed next.

2.2.2 The proper time τ and the coordinate time t.

Judging by the Hamiltonian Action integration over time limits t_1 and t_2, one can expect that equations will describe an orbital motion in the 4-space with the coordinate time t analogous to that in Classical Mechanics. However, the Schwarzschild quadratic form (4) in the Lagrangian yields coordinate functions dependent on the proper time τ. The $(\tau - t)$ problem is embarrassing in view the fact that the GR Dynamics is based on methodology of relativistic deviations from Classical elliptic motion in terms of the coordinate time t.

Einstein justified the replacement of τ by t by a weak field approximation [8], what is highly arguable, [11]. The matter is that there is no formal definition of time variable in the GR Dynamics. By virtue of Schwarzschild's metric derivation, the

quantities $\Delta\tau$ and Δt are not replaceable. "The proper time" τ must be the affine parameter of world line $\Delta s(\tau) = c\Delta\tau$ in the abstract 4-space. "The coordinate time" t appears in Special Relativity Kinematics in connection with Lorentz transformations of coordinate systems in flat Minkowski space and the corresponding treatments of real observations.

The world line was invented to introduce an undefined metric for a single imaginary observer in the abstract 4-spaces, - the proper space coordinate and the proper time τ. It makes possible to formulate a procedure of transition of abstract to the real physical 4-space [12, 13]. In this way, the coordinate time t is introduced having a specific meaning in the SR Dynamics as an elapsed time Δt recorded by an imaginary standard atomic clock carried by the test particle. Historically, the SR Dynamics theory have been unjustly unappreciated in favor of the GR theory. We return to this issue in more details in a topic of alternatives.

2.2.3 Physical reformulation of Einstein's equation of motion

As noted before, we use the τ denotation pretending it is the coordinate time. Bearing this in mind, we are going to derive the roots of the equations. Let us set the initial conditions at $\tau = \tau_0$, an apsis $r = r_0$: let it be $\theta_0 = 0$, the angular component of the velocity $\beta_\theta = \beta_0 \neq 0$, the radial speed component $\beta_r(r_0) = 0$, recall that the speed of light here is $c = 1$, and the test particle mass $m_0 = 1$. Then, a dimensionless parameter $\rho_0 = r_g/r_0$ characterizes the potential field strength. There is one more degree of freedom allowing to reduce dimensional parameters to dimensionless ones, namely, we can define the initial radius $r_0 = 1$ and return to its physically real value in the final results to be compared with observations. Next, let us introduce a dimensionless variable, the inverted radius, $\xi = r_0/r$, $\xi_0 = 1$.

There must be three roots ξ_i in the GR cubic equation of motion, one of them can be fixed $\xi_0 = 1$, therefore, two other roots can be given by simple algebraic expressions, that is, in terms of elementary functions. This is our technical novelty, which is tremendously helpful in obtaining the exact solutions of equations of motion. Actually, two and only two of any independent parameters (not necessarily roots) will determine the unique solution for a given initial conditions. Once an appropriate set of independent parameters are specified, the connection between any pair of them can be established. A pair of two independent parameters could be, for example, ρ_0 and β_0^2 specified at the periapsis (or apoapsis). It can be also some combination of independent parameters, for example, ρ_0 and $\sigma_0 = \rho_0/\beta_0^2$.

We formulate equations of orbital motion and their independent parameters in the dimensionless form so that all quantities there have a physical meaning. In every equation there are two independent parameters, which could be fixed in the initial conditions. Historically, the equations have been formulated in terms of elliptic correlated parameters that is, in geometrical form, which is not suitable for initial condition formulation. This is one of the reasons, why solutions of the GR Mercury problem have been studied in different forms of approximation but not as exact solutions (more comments later).

Finally, we can get a set of desired equations of motions in the dimensionless form, in which dimensionless parameters are connected with the physical quantities determining the initial conditions $\rho_0 = r_g/r_0$, β_0^2.

Of the importance, there are physical quantities such as the conserved total energy $\epsilon_0 = \epsilon(\xi)$, the effective potential $V_{eff}(\xi)$), and others, which are explicit functions of ξ: V_{eff}^2, β_r^2, β_θ^2, $\beta^2 = \beta_r^2 + \beta_\theta^2$. The conserved squared angular momentum is found

in the form $l_0^2 = r_0^2\,\beta_0^2 = \beta_\theta^2/\xi^2$ (here $\beta_\theta = r\,\mathrm{d}r/\mathrm{d}\tau$). There are other interconnected equations

$$\begin{aligned}\epsilon_0^2 &= 1 - 2\,\rho_0 + \beta_0^2 - 2\,\rho_0\,\beta_0^2 \\ &= 1 - 2\,\rho_0\,\xi + \beta_0^2\,\xi^2 - 2\,\rho_0\,\beta_0^2\,\xi^3 + \beta_r^2(\xi)\,,\end{aligned} \tag{8}$$

and from this

$$\begin{aligned}\beta_r^2(\xi) &= \epsilon_0^2 - 1 + 2\,\rho_0\,\xi - \beta_0^2\,\xi^2 + 2\,\rho_0\,\beta_0^2\,\xi^3 \\ &= \beta_0^2 - 2\,\rho_0 - 2\,\rho_0\,\beta_0^2 + 2\,\rho_0\,\xi - \beta_0^2\,\xi^2 + 2\,\rho_0\,\beta_0^2\,\xi^3\,,\end{aligned} \tag{9}$$

$$\beta_\theta^2(\xi) = (r_0\beta_0)^2\,\xi^2\,, \tag{10}$$

$$\beta^2(\xi) = \beta_r^2(\xi) + \beta_\theta^2(\xi)\,, \tag{11}$$

$$V_{eff}^2(\xi) = \epsilon_0^2 - \beta_r^2(\xi)\,. \tag{12}$$

From the equality $\mathrm{d}\xi/\mathrm{d}\theta = \beta_r(\xi)/\beta_0$ easily proved, the equation of motion $\mathrm{d}\xi/\mathrm{d}\theta = f(\xi)$ follows:

$$\left(\frac{\mathrm{d}\xi}{\mathrm{d}\theta}\right)^2 = \left(1 - \frac{2\,\rho_0}{\beta_0^2} - 2\,\rho_0\right) + \frac{2\,\rho_0}{\beta_0^2}\,\xi - \xi^2 + 2\,\rho_0\,\xi^3\,. \tag{13}$$

Thus we reformulated Einstein's equation (1) to make it solvable. It is the one-body particle problem that is, a motion of test particle in the spherical symmetric field due to point-like source. This problem is the basis of GR Particle Dynamics in GR academic framework.

In (1), a spatial variable is $x = 1/r$ corresponding to our $\xi_0 = r_0/r$. The GR time variable τ is interpreted in term of the coordinate time t in observable space. Thereafter, Einsteins conserved total energy A, taken from Newtonian Physics, corresponds to our relativistic energy ϵ_0 (8), and the conserved angular momentum B corresponds to β_0^2.

Let us reiterate that Einstein's approximate evaluation of the GR Mercury's effect in geometrical (elliptic orbit)terms was actually obtained without solving the equation of motion. Our reformulation of the GR problem and obtaining exact solutions made it possible for the first time to study GR approximations and their controversies and understanding a true value of the Mercury's anomaly explanation. This is a breakthrough in the longstanding GR problem.

2.3 Test particle, Classical and GR orbits, and the Newtonian limit

The question is how to compare predictions of two methodologically different, GR and Classical theories. Our approach to the comparison begins with the above physical reformulation of GR equations, which were traditionally interpreted in geometrical terms of elliptic orbits of a test (point-like) particle motion. This is actually a repetition of the reformulation of classical motion,- traditional Keplerian equations in geometrical terms of elliptic orbit.

In our formulation of the one-body problem of motion in the field due to the source of mass M, the orbit is defined by solution of equation of test particle motion $r(\theta)$. The particle has a mass $m \ll M$ so that it does not disturb the field, so the mass m disappears from the equation. Similarly, the concept of potential energy of the field generated by mass M assumes that the test particle probing the field under static conditions does not disturb the field while measuring it. Unlike the one-body problem, the

Newtonian law of attraction of two bodies of comparable masses M_1 and M_2 is the two body problem where a field generated by two interacting masses can be measured by the test particle.

We avoid the conventional formulation of the classical Keplerian equation in geometrical (elliptic) terms not allowing to fix the initial conditions. We suggest a new form of the equation uniquely solvable in terms of physical parameters fixed in the initial conditions, namely, the one parameter solution in the dimensionless form [2].

$$\theta(\xi) = \int \frac{\mathrm{d}\xi}{\sqrt{(1-2\,\sigma) + 2\,\sigma\,\xi - \xi^2}}\,, \tag{14}$$

therefore

$$\xi(\theta) = \xi_0\ (\sigma_0 - (1-\sigma_0)\,\cos\theta)\ . \tag{15}$$

The dimensionless form presents physical constants of test particle mass $m_0 = 1$, $r_0 = 1$, and the speed of light $c = 1$. The quantity $\sigma = r_g/(r_0\beta_0^2)$ absorbs the initial condition data $r = r_0$, $\beta_r = 0$, $\beta_\theta = \beta_0$, $\theta = \theta_0 = 0$ and serves as the criteria of classification of all possible orbits in Classical Mechanics, bounded and unbounded.

The choice of the initial angle $\theta_0 = 0$ leaves two variable physical parameters ($\rho_0 = r_g/r_0$, β_0), which, after normalization, characterize orbit families by *absolute* orbit sizes, time, speed, and mass (say, in meters, seconds, and masses kg). In the classical equation of motion and its unique solution in the dimensionless form, the only one, necessary and sufficient, parameter σ is needed. The orbit type is determined by a value of σ-parameter, see illustration in Figure 1.

The σ-classification of classical orbits	
$0 < \sigma < 0.5$	hyperbola
$\sigma = 0.5$	parabola
$0.5 < \sigma < 1$	overcircle ellipse
$\sigma = 1$	circle
$1 < \sigma < \infty$	subcircle ellipse

The above physical classification of a family of orbits is advantageous over the conventional geometrical one. A family of orbits with a variable eccentricity e and a fixed semi-latus rectum p are not suitable for our analysis. The parameter σ imposes a physically consistent constraint on a classical family of orbits. As a result, a remarkable σ-gauge symmetry of particle dynamics in a spherical symmetric gravitational field takes place: any change of initial parameters r_g, r_0, β_0^2 preserving σ_0 does not change the character of the particle motion. In geometrical 2-parameter representation form, there is no such categories as sub and over circle orbits, moreover, there is no way to solve the problem starting with initial conditions.

The σ_0 parameter relates to the Virial Theorem in terms of an averaging potential and kinetic energies over time periods. This theorem can be principally generalized in relativistic theories dealing with *unclosed* orbits. Our recommendation to Astronomers is to use the σ_0 classification of orbits instead of traditional two physically correlated geometrical parameters. It is one-body problem, which can be generalized to the 2-body problem in Classical Dynamics, but not in the GR

In our view, the fundamentally wrong statement is often made in GR textbooks with respect to the reduction of GR Dynamics to Newtonian gravitation under the assumptions of low speed and weak field (discussed in [14]). It is stated that Newton's

Universal Law in a general case of arbitrarily distributed matter over the space follows from Einstein's field equations (in some analogy to Electrostatics). The Poisson equation is meant

$$\Delta\phi = 4\pi G\mu\,. \tag{16}$$

where μ is the mass distribution.

A particular case is Newton's law of attraction of two bodies of arbitrary masses m and m' (2-body problem)

$$F = -\frac{Gmm'}{R^2}\,. \tag{17}$$

Any attempted derivation of this law from the GR theory would be flawed.

There is a fundamental cause for the GR theory generally being not reducible to the corresponding classical theory. It is rooted in properties of Einstein's field equations (EFE), as discussed in GR textbooks [15]. The GR equations admit only two types of solutions defined in the infinite 3-space. Here, we are interested in the type of vacuum solutions (zero Ricci tensor). Solutions of the second type (the medium filled with continuously distributed mass, non-zero Ricci tensor) are used in cosmological theories.

The GR Mercury problem in GR Dynamics is necessarily one-body problem that is, the planet is considered the point test particle with the mass however small in comparison with the Solar mass. It is formally reduced to the classical form when the cubic terms is put to zero. The equation with the origin in the center of mass is the two-body problem not allowed in GR Dynamics.

3 Classification of the GR orbits

3.1 Analytic connections between parameters of the motion equation

The advantageous form of our presentation of the GR equation of motion (13) is that it is dimensionless and scaled to the initial condition $\xi_0 = 1$, and as such, it is governed by only two independent physical parameters fixed in the initial conditions. In the integral form, the exact unique solution is given by

$$\theta(\xi) = \int \frac{\mathrm{d}\xi}{\sqrt{\left(1 - \dfrac{2\,\rho_0}{\beta_0^2} - 2\,\rho_0\right) + \dfrac{2\,\rho_0}{\beta_0^2}\,\xi - \xi^2 + 2\,\rho_0\,\xi^3}}\,, \tag{18}$$

where integration is performed within the range between the first root $\xi_1 = \xi_0 = 1$ and the second root ξ_2 if it is real or to infinity. It could be one or three real roots ξ_1, ξ_2, ξ_3. Among three roots of the polynomial, any pair of them are physically independent.

In Einstein's problem, physical constraints are imposed on the equation, first of all, the conservation laws. Additional constraints come from the variable rescaling. The dimensionless form of equations with the first root $\xi_1 = \xi_0 = 1$ allows us to easily determine other two roots without using Tartaglia and Cardano formulas for the roots of a cubic equation and then make a unique physical classification of solutions.

Let

$$f(\xi) = 2\,\rho_0\,\xi^3 - \xi^2 + \frac{2\,\rho_0}{\beta_0^2}\,\xi + \left(1 - \frac{2\,\rho_0}{\beta_0^2} - 2\,\rho_0\right)\,, \tag{19}$$

then

$$\frac{f(\xi)}{\xi-1} = 2\,\rho_0\,\xi^2 - (2\,\rho_0 - 1)\,\xi - \left(1 - \frac{2\,\rho_0}{\beta_0^2} - 2\,\rho_0\right) \tag{20}$$

is a quadratic polynomial in ξ with a simple expression for its roots:

$$\xi_{2,3} = \frac{1 - 2\,\rho_0 \pm \sqrt{1 + 4\,\rho_0 - 12\,\rho_0^2 - 16\,\rho_0^2/\beta_0^2}}{4\,\rho_0}\,. \tag{21}$$

3.2 Types of GR orbits in terms of roots

The Lagrangian problem formulation implies that all GR trajectories are periodic and time reversal, as in classical mechanic. However, while in classical mechanics the angular period is always $2\,\pi$, in GR the angular period takes larger values dependent on initial conditions. The GR perihelion advance effect is valid for any type of GR orbits including unbounded ones.

From the expression (8) for the total energy in the settings of the equation (13), it follows that a condition $\epsilon_0 \geqslant 1$ requires that $\beta_0^2 \geqslant 2\,\rho_0/(1-2\,\rho_0)$. For this condition $\epsilon_0 \geqslant 1$, up to $\rho_0 \leqslant 1/4$, the trajectories are all unbounded: either parabolic or hyperbolic. However, for $\rho_0 > 1/4$ and $2\,\rho_0/(1-2\,\rho_0) \leqslant \beta_0^2 < \rho_0/(1-3\,\rho_0)$, the total energy ϵ_0 is greater or equals to 1, but the trajectory of a particle is of a spiral fall type, i.e. the motion is bounded.

All possible variants of roots are shown in Figure 2. There are several cases when types of orbits depend, firstly, on the roots being real or complex, secondly, on specific values of ξ_2 and ξ_3. The integration of the equation (18) is performed from the first root $\xi_1 = 1$ over the positive part of $f(\xi)$ to the next root or up to the infinity, see example in Section 4.2. There are special cases $\xi_2 = \xi_3$, $\xi_2 = 0$, $\xi_2 = 1$, and $\xi_3 = 1$, for which one needs to find the explicit relationships between ρ_0 and β_0^2 corresponding to three curves on (ρ_0, β_0^2) plane. These curves divide the plane into four regions with a specific trajectory type. Six types of trajectories are possible: hyperbola, parabola, circle, over-circular precessing ellipse, sub-circular precessing ellipse, and spiral fall to the center, see Table 1 and Figure 3.

The regions of the classical orbits in β_0^2 vs ρ_0 plane are shown in Figure 4. While the first root is fixed, $\xi_1 = 1$, the second root is $\xi_2 = 2\,\sigma - 1$ (recall, $r = 1/\xi$). therefore, unbounded motion appears for ξ crossing zero value and going into negative side. The case, when $\xi_2 = 0$, that is when $\sigma = 1/2$, corresponds to a parabolic orbit. The case, when $\xi_2 < 0$, that is when $\sigma < 1/2$, corresponds to a hyperbolic orbit. The other values of σ correspond to elliptic orbits. In particular, for $\sigma = 1$ one has $\xi_2 = 1$, which corresponds to a circular orbit. This picture can be compared with the analogous GR one, see Figure 3.

Notice that types of orbits, which are similar in GR and classical mechanics, have different regions in (ρ_0, β_0^2) diagrams, this is also seen from a comparison of their parameters:

type of orbit	classical mechanics	general relativity
circular	$\beta_0^2 = \rho_0$	$\beta_0^2 = \dfrac{\rho_0}{(1-3\,\rho_0)}$, $\rho_0 \leqslant \frac{1}{4}$
parabolic	$\beta_0^2 = 2\,\rho_0$	$\beta_0^2 = \dfrac{2\,\rho_0}{(1-2\,\rho_0)}$, $\rho_0 < \frac{1}{2}$

It is also seen that in GR a new type of orbits exists, which we call a spiral fall trajectory, it is discussed later. This type of orbits does not exists in classical mechanics.

It is characterized a particle fall on the center under specific conditions. In literature, it is associated with strong fields in the Black Hole environments.

4 Analytic and Numerical Solutions

4.1 Elliptic function method

The equation (18) can be recognized as an elliptic integral of the first kind (see any textbook on elliptic functions and elliptic integrals, for example, [16, 17]). It can be solved by means of the Weierstrass elliptic function $\wp$ [16, §20.6].

The $\wp$-function satisfies the following differential equation

$$(\wp'(z))^2 = 4\,(\wp(z))^3 - g_2\,\wp(z) - g_3\,, \tag{22}$$

where parameters g_2 and g_3 are known as the elliptic invariants. Conversely, given the equation

$$\left(\frac{\partial u}{\partial z}\right)^2 = 4\,u^3 - g_2\,u - g_3\,, \tag{23}$$

One gets the general solution

$$u = \wp(\pm z + \alpha)\,, \tag{24}$$

where α is the constant of integration. The equation $y^2 = 4\,x^3 - g_2\,x - g_3$ is known as the Weierstrass normal form of an elliptic curve. Therefore, the equation (13) can be solved in terms of the Weierstrass elliptic function $\wp$. Moreover, the solution can be given in a convenient form $r(\theta)$.

There are articles, which employed the Weierstrass elliptic function: Hagihara suggested classification of the trajectories in a gravitational field of Schwarzschild [5], Kraniotis and Whitehouse studied the perihelion precession of the orbit of the planet Mercury around the Sun [7], Lämmerzahl discussed the experimental basis of General Relativity [18].

In order to determine the corresponding parameters for $\wp$-function and the expression for the solution of (13), it is necessary to transform our equation into Weierstrass normal form. There are several ways to do this.

Consider the following linear substitution

$$\xi = \frac{2}{\rho_0}\,x + \frac{1}{6\,\rho_0}\,. \tag{25}$$

The equation (13) becomes

$$\left(\frac{\partial x}{\partial \theta}\right)^2 = 4x^3 - \left(\frac{1}{12} - \frac{\rho_0^2}{\beta_0^2}\right)x - \left(\frac{1}{216} - \frac{1+3\beta_0^2}{12\,\beta_0^2}\,\rho_0^2 + \frac{1+\beta_0^2}{2\,\beta_0^2}\,\rho_0^3\right)\,, \tag{26}$$

that is

$$\begin{aligned} g_2 &= \frac{1}{12} - \frac{\rho_0^2}{\beta_0^2}\,, \\ g_3 &= \frac{1}{216} - \frac{1+3\,\beta_0^2}{12\,\beta_0^2}\,\rho_0^2 + \frac{1+\beta_0^2}{2\,\beta_0^2}\,\rho_0^3\,. \end{aligned} \tag{27}$$

Therefore,

$$r(\theta) = \frac{6\,\rho_0\,r_0}{12\,\wp(\theta+\alpha; g_2, g_3) + 1}\,. \tag{28}$$

From the theory of Complex Analysis, it follows that the function $\wp$ is a meromorphic function in the complex plane. It is doubly periodic with two linearly independent periods $2\,\omega_1$ and $2\,\omega_2$. When the roots of the cubic $4\,x^3 - g_2 x - g_3$ are all real, one of the periods is purely imaginary, and another is real. The real period corresponds to the angular period of motion described by the equation (13).

The function $\wp$ is a complex-valued function, however along the line $\alpha + \theta$, where orbital angle θ varies, the imaginary part of it vanishes. The value $\wp(\alpha) = (6\,\rho_0 - 1)/12$ corresponds to the initial condition $(r = r_0, \theta = 0)$ and equals to one of the roots of the cubic polynomial (26). This is the property of the function $\wp$ that values $\wp(\omega_1)$, $\wp(\omega_2)$ and $\wp(-\omega_1 - \omega_2)$ are all three roots of the cubic. Therefore, the value of α is either ω_1, or ω_2, or $-\omega_1 - \omega_2$.

Algorithms for computing the periods for the case of real coefficients may be found in literature, see, for example, [19, Algorithm 7.4.8] or [20, §3.7]. The use of the real arithmeticgeometric mean allow one to compute both values rapidly with a high degree of precision. The theory of this method is described in [21]. It has been generalized in [22] allowing for complex-valued coefficients.

In practice, the software packages produce the corresponding $\wp$-function and compute the periods without requiring a user to transform the equation into the Weierstrass form. Most major mathematical software systems support computation with elliptic functions. We have chosen to use SAGE [23] because it is freely available, highly flexible and very efficient. Calculations can be performed with arbitrary precision, we used precision of 600 significant digits here. Moreover, the computations in SAGE can be performed on-line at `http://cocalc.com` without requiring a user to install software on a personal computer. SAGE also provides access to numerous other open source scientific packages, in particular, we used PARI/GP [24].

4.2 Numerical integration

Recall the integral form of the GR equation of motion (18). As in the above analytical solution, there are several singular cases where the integral does not converge. Depending on values of two parameters ρ_0 and β_0, the integration (18) is performed from $\xi_1 = 1$ to either ξ_2 or ξ_3.

Numerical integration procedure in PARI/GP takes into account the asymptotic behavior of integrating function at end points and compute the result with chosen arbitrary precision. Our direct integration numerical solution is in complete agreement with the solution produced using Weierstrass $\wp$-function.

As an example, consider a case when the cubic has three real roots, e.g. $\rho_0 = 0.05$, $\beta_0 = 0.04$. Then, the cubic polynomial in the equation (18) becomes

$$f(\xi) = 0.1\,\xi^3 - \xi^2 + 2.5\,\xi - 1.6\,, \tag{29}$$

with roots $\xi_1 = 1$, $\xi_2 \approx 2.44$ and $\xi_3 \approx 6.56$, see Figure 6. The initial condition dictates the starting point $r_0 = 1/\xi = 1$, $\theta_0 = 0$, the integration (18) is performed from $\xi = 1$ to $\xi = \xi_2$:

$$\theta(\xi) = \int_1^{\xi_2} \frac{\mathrm{d}\xi}{\sqrt{0.1\,\xi^3 - \xi^2 + 2.5\,\xi - 1.6}}\,. \tag{30}$$

The full integral from 1 to ξ_2 corresponds to the periapsis position $r_p = 1/\xi_2 \approx 0.41$, $\theta_p = \int_1^{\xi_2} 1/\sqrt{f(x)}\,\mathrm{d}\xi \approx 4.53$, which is the closest approach to the central mass. From this point, the test particle motion continues in counter-clock direction. At the apoapsis

point $r_a = r_0 = 1$, $\theta_a = 2\,\theta_p \approx 9.07$, the particle completes the first period, see Figure 7.

4.3 Time dependent exact solution

The time dependent problem in both Newtonian and GR mechanics can be solved only by numerical integration. In GR, the time dependent equation of motion, for example, follows from Eq. (9), where $\beta_r(\xi) = \mathrm{d}r/\mathrm{d}\tau$. Therefore,

$$\tau(\xi) = -\int \frac{\mathrm{d}\xi}{\beta_0\,\xi^2\sqrt{\left(1-\dfrac{2\,\rho_0}{\beta_0^2}-2\,\rho_0\right)+\dfrac{2\,\rho_0}{\beta_0^2}\,\xi-\xi^2+2\,\rho_0\,\xi^3}}\,. \tag{31}$$

The integrand is exactly the same as in (18), and integration is performed along the same ξ interval. The expression (31) corresponds to the elliptic integral of the third type. In contrast to the case of the elliptic integral of the first type, there is no analytical expression similar to (28). Nevertheless, the theory of Complex Analysis implies that the solution $r(\tau)$ exists, and it is periodic. For practical purpose, we compute the integral (31) numerically.

5 GR Mercury's motion in space and time

5.1 The law $\Delta\theta = 3\,\sigma_{gr}\,\rho_0$ in the weak field

Knowledge of exact solutions of Einstein's problem allows us to quantitatively define weak field conditions and assess errors in approximate predictions. Let us consider first the approximate value of the GR perihelion advance $\Delta\theta$ under the weak field conditions $\rho_0 \ll 1$ and compare it with the exact numerical results.

Our original formula provides a precision, which increases when the field strength decreases so that in the limit $\rho_0 \to 0$ its computational error becomes however small.

$$\Delta\theta = 3\,\sigma_{gr}\,\rho_0\,, \tag{32}$$

Here, $\Delta\theta = \theta_{gr}/\theta_{cl} - 1$ is a relative angular shift rad/rad averaged over half a period, $\theta_{cl} = \pi$, $\sigma_{gr} = \sigma_0/(1-3\,\rho_0)$, actually $\sigma_{gr} = \sigma_0 = \rho_0/\beta_0^2$ for $\rho_0 \ll 1$. For Mercury ($\sigma_0 \approx 0.829457$), the calculated effect is exact to the precision, at least, 6 significant figures or 14 decimal places.

The law (32) is illustrated in Figure 8. The plotted data are positive angular deviations from π in $\%$. There are two plots: the line for $\rho_0 = 0.001$ (a weak field), and the curve for $\rho_0 = 0.05$ (a mildly strong field). The line demonstrates the law (32) in the whole range of bounded motion. At $\rho_0 = 0.001$, the angular relative shift is 0.300% at $\sigma_{gr} = 1$.

For $\rho_0 > 0.050$, the GR effect is not linear with σ_{gr} anymore because of the field strength growing with σ_{gr}. For convenience of comparison, the normalization coefficient is selected $k = 1$ for $\rho_0 = 0.01$, so that $k = 10$ for $\rho_0 = 0.001$, and $k = 1/5$ for $\rho_0 = 0.05$. For $\rho_0 = 0.05$ the law is not good in the region of the sub-circle motion $\sigma_{gr} > 1$ and partly in the over-circle region $\sigma_{gr} > 0.7$.

Einstein claimed in [1] that his equation can explain the perihelion precession of the planet Mercury. Kraniotis and Whitehouse discussed in [7] this GR effect in greater details and showed the range of free parameters for which astronomer's observations

are consistent with the GR theory prediction. In particularly they looked for "the best fit of input data" having the Solar mass and the conserved total energy fixed, and the conserved angular momentum varied. However, those parameters are physically correlated and contain more than two independent ones, therefore, their solutions were over-constrained, while Einstein's equation has the unique one solution characterized by the two and only two independent sufficient parameters, as shown in our analysis. Also, it was shown there that the solution in Mercury's case is highly sensitive to numerical precision and rounding errors, especially with the usage of Tartaglia and Cardano formulas in [7]. To ensure stable numerical computations, we use the exact algebraic (dimensionless) solutions for roots in elementary functions.

5.2 Notion of time in GR and classical theories

Einstein's perihelion advance problem is an exceptional case in the GR gravitational theory, since it admits local conservation laws in the ideal planetary model, where planets are considered not interacting point-like particles (zero Ricci tensor solution). This is the one-body spherical symmetric problem. The time and angular variables are inalienably constrained by laws of the locally conserved angular momentum and total energy. Such a formulation is specific in GR because it admits the Lagrangian approach based on time translation and reverse symmetries yielding the conservation laws, in accordance with Noether's theorem [25].

Einstein considered the Mercury problem in terms of angular GR advance $\Delta\theta_{cen}$ accumulated for Earth's 100 years (about 415 orbital evolution). Assuming the equivalence of GR and classical time periods $T_{gr} = T_{cl}$, he obtained $\Delta\theta_{cen} = 43$ arcsec in a perturbation method (see also [10, 26, 27]. Interestingly, this number for the first time was obtained by a German teacher of Physics, Paul Gerber, in 1898, who derived the formula identical to Einstein's in article "Space and Time Propagation of Gravity" [28].

At that time, scientists and Gerber among them, tried to parallel gravitation and electrodynamics and use the concept of retarded potential. All tried to derive the value for the perihelion shift of Mercury's orbit already known from the French Astronomer Le Verrier. Likely, Einstein and Gerber were subconsciously attracted to the number too. But there was another hidden number, the equivalent time shift 1 sec, blowing the prediction.

Historic incidents are out of the scope of this work. The actual matter, which we are interested in, is the connection of GR Mercury's angular shift with the corresponding temporal relativistic effect. Mercury's time period calculated classically must be different from that predicted by GR, a difference being of the same order smallness as the angular shift.

Einstein [1] started with the approximate estimate of the perihelion advance $\Delta\theta$from the original equation (1) with $\alpha = 2\,r_g$, and geometrical parameters a - the semi-major axis, p - the semilatus rectum, e - eccentricity. Gerber's way was very different but final results occurred to be the same:

$$\Delta\theta = 2\,\pi\,\frac{3\,\alpha}{2\,p} \tag{33}$$

given Mercury's (classical) time period T_{cl}

$$T_{cl} = \left(\frac{8\,\pi^2\,a^3}{c^2\,\alpha}\right)^{1/2} \tag{34}$$

It follows

$$\Delta\theta = \frac{24\,\pi^3\,a^2}{T_{cl}^2\,c^2\,(1-e^2)}\,. \tag{35}$$

Historically, the GR Mercury's angular advance was studied in a separation with the time concept problem. In some works, it was suggested that a seemingly tiny difference of time period in GR and classical theories could be neglected in approximate solutions. For the first time, we solve the couples of GR angular and time dependent dynamics equations and the corresponding classical equations constrained by the common initial conditions.

Astronomers' observations of orbits cannot be conducted without time records. Therefore, the GR test of spatial (angular) shift is not definitive without connection with the temporal shift in the orbital cycle. The angular and temporal shifts are components of the effect having a common cause. In the Mercury case, the predicted GR time period is found about 1 sec smaller. This is extremely small relative effect (about 1.5×10^{-7}) on the background of 2 orders greater effects caused by forces from other planets. Observation of such effects anyway may seem to be beyond a technical imagination.

We use the test particle ideal model of orbital motion in GR and Classical theories, which are methodologically different. To compare the results of solutions, we choose the following initial conditions in both theories common: at $t = 0$ and $\tau = 0$, the planet is positioned at $\theta = 0$; this is a minimal distance (perihelion) from the Sun r_p with a maximal orbital (perihelion) speed of the particle β_0, when the radial speed is zero $\beta_r = 0$.

Next, the denotation of τ_{gr} is used for the time variable in GR Dynamics, and the time variable in the classical theory is denoted t_{cl}. Both time variables are dynamic ones measured with the use of standard clocks running uniformly, so all time-dependent calculations were conducted and compared in a universal time.

Generally, in field theories, standard atomic clocks at different locations cannot be synchronized, or their standard rates depends on a theory. In Mercury's case, a difference of time period in GR and Classical theories is due to the GR cubic term manifesting the 4-space curvature. The exact calculations showed that the classical time half-period is greater than the GR one by the amount $\Delta t = 0.555$ s. Therefore, the GR and classical time lines on a imaginary display are related to each other by the following linear connection: $t_{cl} = k\,t_{gr}$, where the coefficient k is the ratio of classical and GR time periods $k = T_{cl}/T_{gr} > 1$. We can interpret it as if the GR time unit is greater than the Classical unit that is, $k\Delta t_{gr} = 1$ s = $\Delta t_{cl} = 1$ s. Further, we demonstrate how both lines can be projected on each other in the example of different clock rates.

5.3 Input data for exact computations of full exact solutions of Mercury motion

For our exact calculations of space and time GR effects, we used recent input data taken from [29–31]:

- the speed of light $c = 299792458$ m/s;
- the Solar mass parameter (heliocentric gravitational constant) $\mu = 1.32712440041\times 10^{20}$ m^3/s^2, that makes Schwarzschild radius $r_{sch} = 2953.2500770$ m;
- Mercury's perihelion distance $r_p = 4.600\times10^{10}$ m;

- Mercury's aphelion distance $r_a = 6.982 \times 10^{10}$ m;

From these data, we have $\rho_0 = 3.21 \times 10^{-8}$, and $\beta_0^2 = 3.87 \times 10^{-8}$.

The value β_0^2 has been rounded to three significant figures for fixing identical initial conditions in both classical and GR computations. This makes Mercury's velocity at perihelion $v_p = 5.898 \times 10^4$ m/s, which agrees with [31]. The aphelion value then becomes $r_a = 6.9811764705882 \times 10^{10}$ meters in the classical theory with millimeter precision.

Having the initial conditions fixed, the three roots in the GR equation (13) are found exactly, as discussed. The first root, the inverse values of $r_p^{-1} = \xi_1 = 1$ corresponds to the perihelion. The second and the third roots $\xi_2 = 0.65891486$ correspond to the aphelion and the third GR term $\xi_3 = 1.5576322 \times 10^7$. Then the GR equation (13) is numerically specified (from here and below, we print up to eight significant digits while the calculations were performed with 600 digits):

$$\left(\frac{\mathrm{d}\xi}{\mathrm{d}\theta}\right)^2 = 6.42 \times 10^{-8}\,\xi^3 - \xi^2 + 1.6589147\,\xi - 0.65891479\,. \tag{36}$$

The corresponding Weierstrass form (26) of the above equation is

$$\left(\frac{\mathrm{d}x}{\mathrm{d}\theta}\right)^2 = 4\,x^3 - 0.083333307\,x - 0.0046296274 \tag{37}$$

with roots $x_1 = -0.083333317$, $x_2 = -0.083333323$, $x_3 = 0.16666664$. However, in SAGE and in PARI/GP we do not need to transform the equation into Weierstrass form in order to compute the periods. The software allows for arbitrary cubic polynomial with scaled major coefficient, produces the corresponding $\wp$ elliptic function and computes the semi-periods. For our input the half periods are $\omega_1 = 3.141592904530036$ and $\omega_2 = 20.40947598338886\,i$. Direct numerical integration reproduces the same result for the orbital half period ω_1 up to 300 significant digits, it is difficult to obtain higher precision for this type of numerical approximation. Taking into account Mercury's sidereal orbit period 0.2408467 Earth years, we obtain the known integral value of the Mercury's perihelion advance ≈ 42.98 arcsec per century.

Such apparently small GR integral effect is actually of the order of potential term ρ_0, but it is triggered by the GR cubic differential $\propto \rho_0\beta_0^2$, which is of the next order smallness in the non-linear equation of motion. It means that the cubic term could not be neglected in any of approximate solutions.

5.4 Numerical comparison of Mercury's motion in GR and Classical theories

It is instructive to see a picture of Mercury's motion in the vicinity of the half-period point $\theta = \pi$ in GR and Classical theories in comparison. For this purpose, three distinct time moments in the GR and classical theories are selected in *the three events scheme*, where exact values of main orbital characteristics are given. The values on the GR time line $\tau = \tau_{gr}$ are shown in relationship with similar classical characteristics on the classical time scale t_{cl}.

Events are selected in the first half period, as follows:

- Event 1 at the instant τ_1 when $\theta_{gr} = \pi$ (the aphelion is not reached yet).
- Event 2 at the instant τ_2 when the GR aphelion is reached.

- Event 3 at the instant τ_3 when the GR clock displays t_2 value of the classical aphelion (the equality of numbers of ticks of standard clocks in both theories, $\tau_3 = t_2$).

The corresponding time instants t_1, t_2, t_3 displayed by the classical clock follows, as next.

- The instant t_1 corresponds to τ_1 (when $\theta_{gr} = \pi$).
- The instant t_2 is when the classical aphelion is reached.
- The instant t_3 corresponds to τ_3 (when $\tau_3 = t_2$), t_2 is the classical aphelion moment.

5.5 Results of comparison

Let us sum up the results of three events comparison.

In Table 2, the input Mercury's data are presented. They are used in the initial conditions common for both theories. In the output, the main orbital characteristics are shown for each theory in comparison. Numbers characterizing the differences are rounded up to 4-5 significant digits.

In Table 3, the three-events comparison of the GR with respect to the classical theory is shown: the absolute values of main orbital characteristics at events 1, 2, 3, predicted in each theory, including the time, the radius, the angle, the particle orbital speed, and the passed length. The corresponding absolute and relative differences between the two theories are also given. To the precision of 4 significant digits, differences do not change over the time interval including the three events. From this fact, one can assess the precision requirements to the perihelion observations.

In Table 4, the absolute differences of the above variables between events (2, 1), (3, 2), and (3, 1) are shown for each theory.

Finally, in Table 5, the projections of each of the three events on GR time scale τ_{gr} to the corresponding classical scale t_{cl} are shown. The main predicted values of angular shifts and the corresponding time shift are seen in the intervals between events (2, 1), (3, 2), and (3, 1) on each of GR and classical time scales.

The remarkable results of exact solutions of Mercury's problem in GR and Classical theories are obtained for the first time. They include integral and differential data revealing the origin of GR effects due to the GR cubic term in the equation of orbital motion (13).

"The GR particle" compared to "the classical particle", moves on average faster, its aphelion is smaller, all together, its angular period is advanced by the value 5.019×10^{-7} rad/rev that is, the relative difference of the angle shift with respect to the classical value π is 7.988×10^{-8}; this is the known GR Mercury's perihelion advance in unclosed orbit. Correspondingly, the full time period of the GR orbit is 1.111 sec/rev shorter than the classical one; that makes a relative difference -1.461×10^{-7}. The temporal effect should be called "the GR temporal advance", which is a replica of the corresponding perihelion angular advance, - the effect of orbital plane precession.

With questions answered, more questions arisen: why approximate but not exact solution to Mercury's problem was pursued over triumphal hundred years, why two times in one space, what is my time, finally, is General Relativity for real? With these and more questions, let us continue reviewing GR Dynamics.

5.6 From Schwarzschild to Mercury and GPS.

5.6.1 Notes on Schwarzschild metric in GR Dynamics.

The key word in the GR Dynamics is "Schwarzschild" for the original (free of singularities) metric derived by Mathematician Schwarzschild, Einstein's counterpart (1916). After his unfortunate death, the metric has been modified and taken a form having a central singularity, in literature named "the Schwarzschild metric" [11].Actually, it should be called "the metric quadratic form", a metric tensor with vanishing off-diagonal terms. The corresponding 4-space metric is a square root of the quadratic form, as used in the Lagrangian (5). In GR Dynamics of curved space, it is constructed on the pseudo-Riemannian manifold, meaning that the quadratic form can be positive, negative, or zero. Typically, the time-like form is in use.

Two time variables τ and t were brought into one space by Schwarzschild upon his consideration of Einstein's ideas of curved space. He strongly criticized Einstein's equation of motion (1) derived from Einstein's field equations [1]. As emphasized before, the τ, by virtue of derivation, should be "world line affine time" in the abstract 4-space. In this work, we use a contemporary Lagrangian approach applied to the Schwarzschild metric to study Einstein's equation in terms of τ, closing our eyes on its weird meaning. In the final equations, the only time variableτ is left, the time t disappears.

Our physical formulation of the GR problem makes a difference. For the first time, exact spacial and temporal solutions were obtained from the equations defined by initial conditions with fixed physical parameters. The mathematical solution reveals a picture of forming an unclosed orbit, which exhibits "the advance effect" growing with a field strength. Under some specific conditions, a motion of particle speed eventually exceeds the speed of light. This is a violation of the Causality Principle. This fact is seen from our exact solutions of the GR strong field problem, as shown below.

In the following analyses of the GR approximations, we pretend that the τ in the problem of orbits has a meaning of SR coordinate time t, as physically should be in our exact solutions. There are literally hundreds of works, in which the GR Dynamics problems and their approximate solutions are discussed, such as Mercury's, GPS, and other problems. As concerns Mercury's anomaly, there are numerous different explanations in different versions of General Relativity, but always in agreement (not to speak about τ vs t dilemma), for example, in expertise works Bergmann [32] 1942, Fock [10] 1959, Landau [14] 1971, Moller [26] 1972, Weinberg [27] 1972, Misner, Thorn, Wheeler [33] 1973, Wald [34] 1984, Rindler [35] 2006.

5.6.2 Approximate evaluation of Mercury's perihelion advance.

The Mercury's anomaly problem plays a decisive role in the General Relativity value [36]: "The perihelion advance of the orbit of Mercury has long been one of the observational cornerstones of general relativity."

Historically, GR Dynamics has been investigated with the use of approximate methods applied to the Schwarzschild metric. It is the core of GR Dynamics. Having this noted, we reiterate our negative opinion about Schwarzschild metric being physical misconception, as also seen from analysis of specific approximations involving the metric.

We follow the works by the well-reputed authors Taylor and Wheeler [37], also Wald [34]. They compare the Newtonian effective potential $V_{ef}(r)$ with that derived

from the Schwarzschild metric in the PPN approximation [33] (see its exact expression in GR Dynamics (12)).

In general, the effective potential is a difference of the total energy and the kinetic energy of radial motion as a function of radius. Newtonian plot of $V_{ef}(r)$ has a form of the well showing a minimum at some point R between the roots r_1 (perihelion) and r_2 (aphelion). The two roots are connected by a horizontal line signifying a constancy of conserved total energy. The values of roots vary on the vertical sliding scale indicating a family of orbits of different total energies in the gravitational field due to a point source. The single root R is a solution for circular orbit characterized by a minimal total energy. The idea is to treat Mercury's orbital motion in terms of "harmonic oscillation" of frequencies ω of two types of periodic motion: radial and angular.

Next, we refer to the Pictures in Fig. 2 and Fig. 3 presented in [37]. In Fig. 2, the Newtonian picture of "potential well" is shown. The plot is designed to illustrate the idea of planet undergoing two types of "oscillation" between r_1 and r_2: the radial one of frequency ω_r, and the angular one of frequency ω_θ, which seem to be symmetric so that $\omega_r = \omega_\theta$. This is a picture of "rocking ball" in a static potential well.

In Fig. 3, the plot of GR function $V_{ef}(r)$ is shown in the same model of "rocking ball". It is obtained from algebraic elaborate work wit which the Schwarzschild metric (they call it "manipulations"). There are three roots, two of them are analogous to those in the Newtonian picture, r_1, r_2. Correspondingly, there are two oscillation frequencies ω_r, ω_θ, now, they are influenced by the third root r_3. The result is gladly desirable: it indicates the angular advance accompanied by the radial retardation, $(\omega_\theta$ - $\omega_r) > 0$. The difference of frequencies gives the wished number, - Mercury's perihelion advance 43 arcsec/cen, without hardships with Einstein's equation (1). Notice, they calculate a tiny relative difference of two frequencies, absolute values of which are not calculable.

Here is broken Physics, which is difficult to criticize, as commented next.

"The well" in Newton's case is far from being "symmetrical", and the oscillation cannot be even "approximately" the harmonic one; the same is true in the GR case.

On the plot, the horizontal line is the line of total energy constancy at any point of orbit. Hence, a ball (the planet) must move on the horizontal line between the root but not "oscillate" inside "the well". In the case of a circular orbit, the rocking ball comes to stop.

In reality, orbital motion is described by a rotating radius vector with two orthogonal components: the radial one (9) and the angular one (10). A separation of "radial and angular oscillation" in an orbital cycle is a nonsense. An orbit can be closed or unclosed but its radius vector cannot disintegrate in space and time.

Their "algebraic manipulation" is a piece of pseudo-Physics, what they say: "The GR approximate equations contain time τ instead of t, but this does not matter, since we have not yet decided which relativistic measure of time should replace Newton's universal time t... Second, the relativistic expression $(E = m^2)/2$ stands for the Newtonian expression $E = m$. However, both are constant quantities, which is all that matters in the analysis."

That is, "one Joule" equals " half squared Joule". A reader must be patient while reading absurdities.

6 GR Dynamics problems in Global Positioning System.

6.1 GPS Basic Physical Principles and Ashby's assumption

The current GPS network consists of satellite constellation and land reference stations, equipped with radio transmitters and computerized standard atomic clocks, while GPS users have specialized decoding receivers. The satellites continuously transmit coded data monitored by the land reference stations. The resulting orbital and time data are uploaded to the satellites for retransmission to GPS users. The data include satellite positions depending on time.

Specifically, each satellite continuously broadcasts a navigation message at 50 bits per second on the microwave carrier frequency of approx 1600 MHz. Historically, the GPS developers wanted to synchronize frequencies of sent and received messages in order to maintain a standard time line in the GPS network.

The Special Relativity postulate of constancy of the speed of light is considered there a fundamental principle on which GPS navigation works. In plain words, a position of the GPS receiver can be calculated from, at least, 4 algebraic triangulation equations. To solve them, a minimal information is needed, namely, satellite positions in space for 4 satellites, and times of signals they sent. A difference of time of sending and receiving a signal is calculated by a receiver. This procedure is true if the satellites are launched into known orbital positions in the Earth-fixed rotating reference frame. Therefore, the problem of high-precision synchronization of all atomic clocks, - of satellites, and GPS users, arises. Consequently, the concept of the standard atomic clock (SAC) must be formulated. This issue is discussed later.

Below, the role of GR Dynamics in the GPS performance is discussed. We follow publications of well reputed authors presenting a simplified model of Global Positioning System [37], also [38]. It is emphasized there that GPS navigation crucially depends on accuracy of synchronization of clocks carried by satellites and users. The required timing accuracy in GPS is so great that general relativistic effects are central to its operation. Now, let us look from inside how much the GPS is driven by Physical science.

The GPS physical model is based on the Schwarzschild metric approximations and assumptions in the GR Dynamics framework. We pay a special attention to the fundamental assumption [38]: the model is valid if the GR theory is correct (Ashby's assumption). In our continuing criticism of the GR Dynamics, the controversial (τ, t) issue is an indication of GR fallacy by Ashby's criterion.

6.2 GPS model of satellite motion in GR Dynamics

We know that Mercury's and GPS satellite orbit problems are the same GR Dynamics problem of precise accounting for relativistic effects. To analyze the GPS problem, we again follow publications [37], and [38], also, the book [**?**].

In the GPS model, Keplerian geometrical parameters are derived from the Schwarzschild metric in the so-called PPN approximation. We see the worst scenario of 'rocking ball" idea having radial and angular parts in the Keplerian approximation combined with the PPN Schwarzschild approximation. Notice, the idea does not work without doubly approximation.

The left term $\mathrm{d}s = \tau$ of Schwarzshcild metric is verbally assigned to two different times, - the time shown on "the shell clocks" of receivers *at rest*, and on "the shell

clocks" satellites *in motion*. The term of "shell clock" means that it shows observer's wristwatch (rest) time, which is measured by the bookkeeper using far-away time measurement. In the *let-it-be* manner, the Schwarzschild time τ becomes a uniformly running "proper time" in the equality $t = t_{shell} = \tau$ advised to all GPS participants. Notice, the *let-it-be* absurdity one can enjoy by making the equality directly in the Schwarzshcild metric.

Obviously, the Keplerian approximation erases Einstein's angular advance effect. We know that its relative value of angular advance per revolution of the GPS satellite is about $\delta\theta = 3r_g/R = 2 \times 10^{-9}$, compared to the Mercury's 8×10^{-8}, similar differences are in time shifts. Such seemingly small effects are detectable from the Earth with the use of nanosecond radio technology of the precision sufficient for the effective GPS operation. Besides, a short period of satellite orbit is advantageous over Mercury's time for accumulation of a relativistic shifts. The GPS satellite needs less than two months to make 415 revolutions, - equivalent to Mercury's time of one hundred years. This is good for conducting decisive GR tests. Unbelievably, in the multi-billion dollars GPS project, there was no room for scientific programs dedicated to the GR tests.

The fact that GR effect of perihelion advance is ignored in the GPS model is an additional evidence of fundamental deficiency of the GPS model and incompetence of its scientific advisers. Next, detailed analysis of the GPS problem in GR Dynamics and the Alternative theory is presented.

6.3 SR motional time dilation, Sagnac and Doppler effects

One of requested corrections in rates of GPS clocks is so-called "time dilation" known from the Special Relativity Kinematics. The concept is adopted as a piece of the Lorentz boost transformations in Minkowski (flat) 4-space in an abused form and a bad vocabulary. It says "the faster the clock moves, the slower it runs". The GR "experts" likely forgot that "the time dilation" is meaningless without "the length contraction". Having this said, reasonable physicists would be better to avoid those terms for the reason explained next.

Consider two coordinate systems in a relative motion, both carrying an imaginary observer. Each observer has the standard atomic clock of rate $\Delta\tau$, $\Delta\tau'$ and the standard length gauge (imaginary rod) Δl, $\Delta l'$. Let us fix initial conditions $x = 0$, $x' = 0$ at $t = 0$, $t' = 0$ and apply direct and inverse Lorentz transformations $\Delta t = \gamma\Delta\tau'$, $\Delta l' = \gamma\Delta l$. Ends of each rod are measured *simultaneously*. It says that a rest observer measures a time rate of a moving clock Δt occurred to be larger than it is at rest. At the same time, the length between two points at rest is shorter by the same Lorentz factor γ. The relative speed viewed by each observer is the same $\Delta l'/\Delta t = \Delta l/\Delta t' = \beta$. The Lorentz factor ensures constancy of the speed of light and the Causality Principle.

"Correction" of GPS clock rate for Lorentz transformations in the flat Minkowski space is a recurrent demonstration of non-criticizable GR absurdity.

The so-called Sagnac effect is in the list for "correction". It is referred to observations of light interference in the rotating ring, where a non-inertial (centripetal) force arises, and the light is viewed perpendicularly to the radius. Historically, the observation (1913) has been mistreated and claimed to be "a proof" of the Special Relativity wrongness. Such an opinion is still expressed in literature.

In the GPS conditions, the effect appears in the complex Doppler effect due to relative motions of rotating Earth and orbiting satellites in gravitational field. It is fully

explained in Special Relativity [39].

6.4 Gravitational time dilation and clock synchronization

The effect of gravitational time dilation is a phenomenon studied in SR Dynamics. It adopted in the GR Dynamics in abused way, along with other "relativistic effects" in the GR context of the clock synchronization in the current GPS model.

An attentive reader must understand that the GR relativistic terms are not physically defined, especially, when chosen by "let-it-be" assignment. The GPS problem of "clock synchronization" is ill posed. It cannot be "resolved" in principle, in particular, because of the notions of "time" and "standard atomic clock" are buried in numerous meaningless approximations and assumptions (not to speak about our mouth shut and eyes closed on the $(\tau - t)$ time dilemma).

As shown next, GPS Physics in the Special Relativity theory is very different. The concept of standard atomic clock is well defined in relation with the oscillator a generator and receiver of the radio waves. Let us consider an oscillator at rest at some point $r = r_i$ in the spherical symmetric gravitational well due to static potential $1/r$. The oscillator plays a role of emitter and detector of radio wave (a photon) of resonant frequency. The photon emitted from the SAC carries a coded information about a position of the SAC in space and time. Such information can be exchanged between the SACs.

The oscillators can be manufactured at one place and used in other places, or manufactured in different convenient locations for distributions. It is required, however, that all oscillators copy the natural inherent phenomenon called *the standard atomic clock*, SAC. Its standard rate should be agreed in terms of Earth-fixed gauge. It means that rates of all SACs will be naturally synchronous when brought in one place. The important thing is that the standard frequency is the matter of manufacturer's choice but their rates depend on the varying field strength. The question is whether their rates on the Earth should be "synchronized" with those on satellites by corrections of clock rates in the existing GPS network. To answer this question, let us first discuss the issue of clock synchronization in a static potential field $1/r$ in GR and SR Dynamics.

The SAC concept is defined in SR Dynamics. One should understand a physical process of information exchange between SACs in terms of transmitting and receiving radio signals, next we use the term "the photon". In the SR Dynamics, the SAC is the standard test particle of however small proper mass. By definition, the mass is gone from the equations of motion, but it is essential in the SAC concept of photon properties. Unlike in flat space, the mass of oscillator depends on the field strength, $m = m(r)$, its frequency is proportional $f(r) \propto (r_i)$ is a fixed point. Strictly speaking, the field is defined by exponential function. In Earth's conditions, $m(r)/m_i = f(r)/f_i = \exp(-r_g/r)$, where r_g is the gravitational radius of Earth. The values of quantities $c(r)$ and $f(r)$ increase with decrease of the field strength, and reach their maximal values c_0, and λ_0 as $r \to \infty$.

The change of proper mass energy $\Delta m(r)c_0^2$ is equal to the work required for particle displacement Δr with the corresponding change of potential energy. This is the particle energy conservation law for the static potential, consistent with the definition of the potential.

Having two synchronized SACs at the potential level r_2, let us put for a while one of them to the potential level of stronger field $r_1 < r_2$ and bring it back to $r = r_2$ to compare the records of elapsed time. As a result, the clock shows less ticks. This is the SR gravitational time dilation: in a stronger field, the SAC experiences slower rate; otherwise, faster rate.

It is clear that the clock synchronization in the GPS network is a misconception; doing man-made "clock corrections" is a violation of natural laws, the cause of abnormality of GPS performance. The model based on SR Physics will provide us with a rich description of the real Nature on the premises of fundamental physical laws. The GPS performance must be controlled by exact solutions of the differential equations of particle and photon motion in space and time. SR Kinematics and Dynamics are the theories, which revolutionized our understanding of Physical Nature, still their value in practical applications is not fully realized, and even ignored in the GPS projects.

6.4.1 Rediscovery of the gravitational redshift and bending of light

In accordance with the Special Relativity, energy of the photon is proportional to its frequency ν. The energy is originated from an equivalent quantum of the proper mass of the oscillator. Consequently, the frequency of the photon emerging from the SAC at some point $r = r_i$ is proportional to the proper mass $m(r) = m_i$ so that $\nu(r)/\nu_i = m(r)/m_i = \exp(-r_g/r)$. During its flight through the field, the photon keeps the frequency constant $\nu_i = c(r)/\lambda(r)$ by virtue of the photon energy conservation law. At the same time, the speed of light $c(r)$ and the wavelength $\lambda(r)$ remain field dependent, $\nu(r_i) = c(r)/c_i = \lambda(r)/\lambda_i = \exp(-r_g/r)$. The values of quantities $c(r)$ and $\nu(r)$ increase with decrease of the field strength, and reach their maximal values c_0, and ν_0 as $r \to \infty$.

Therefore, the photon emitted from the level r_1 is detected at the level $r_2 > r_1$ with the frequency shift toward a longer wavelength, - this is the redshift; otherwise, it would be the blue shift. At the quantum level, the wavelength phase must undergo half period shifts at instances of photon emission and absorption consistently with the frequency shift.

The above SR Dynamics case of the static potential demonstrates a perfect tuning of radio wave (photon) on sides of transmitter and receiver. Starting from $r = r_1$, the wavelength monotonously increases as $r \to \infty$, and decreases, when returned back from any point $r = r_2 > r_1$. The frequency remains constant during the photon flight, $\nu(r) = f(r_1)$ where r_i is an emission instance, while the frequency of the absorption is $\nu(r) = f(r_2) > \nu_1$. This is the gravitational redshift due to the conservation of photon energy.

The consequence of it is a dependence of the speed of light on the field strength r_g/r. In GPS Physics, the SAC concept is defined consistently with the gravitational time dilation and redshift concepts of Special Relativity. Both effects are considered under conditions of radial motion of the photon that is, the angular momentum is zero.

When the line connecting the transmitter and the receiver is not the radial one that is, the angular momentum of the photon is not zero, than a photon trajectory becomes curved. This is the SR effect of bending of light in gravitational field. The effect is caused due to the speed of light being dependent on the field strength.

Thus, we have a sketch of the SR theory of the statical model of information exchange between transmitters and receivers in the Earth Centered Fixed (ECF) frame without SACs corrections. A path of signal back and forth between pair of them is unique and synchronous at both sides, except the frequency shift. The theory is based on the conservation laws, so that the equations of particle and photon motion have a unique solutions. The conservation laws require the frequency shift $\Delta\nu$ and the corresponding time shift $N\Delta t$, where N is a number of clock ticks, Δt the time interval between two consequent ticks Δt, the concept of time t defined below.

The quantities ν and Δt are time-like parts of the 4-time-space vector X_μ and

the 4-momentum vector M^μ, which are complementary vectors. This means that one has a choice of a pair among many created by manufacturer or the Nature. Then, the 3-space part of complementary vectors would have the corresponding shift, both shifts are compensated in the 4-phase space vector. Its quadratic form is formed by a scalar product of X_μ and M^μ, representing the 4-phase vector conserving its value, the number of ticks N.

In the real GPS physical dynamics model, satellites are in orbital motion, and the Earth naturally rotates independently of gravitation. The concept of 4-vectors remains valid. The whole SR theory of motion of particles and photons is again governed by conservation laws, the two of them are special: the laws of conservation of total energy and angular momentum of satellites. According the famous Noether's theorem, the conserved total energy and angular momentum reflects the symmetry of 4-space: the uniform rate of clocks (the time like part) and the isotropy of 3-space (the spatial part). Therefore, the time rate is a theoretical (coordinate) uniform time. The observer at rest in his own frame having a wristwatch (SAC) must choose the initial conditions formulated in the problem of motion, while a receiver read the coded message and interprets it in terms of the coordinate time t in the Earth Centered Inertial coordinate system.

The GPS problem, including the information exchange between SACs, is exactly solvable in the Special Relativity theory. The ill posed problem of clock synchronization inevitably arises when a theory is not real, as in the GR case.

Let us compare the SR and GR theories in general and in the context of the GPS model.

- The speed of light c is determined by two quantities characterizing the space, (electric) permittivity ϵ and (magnetic) permeability μ, which are affected by a field of forces, $c^2 = \epsilon\mu$. Correspondingly, in SR Dynamics, the speed of light is field dependent. In GR Dynamics, the speed of light is a universal constant c_0.

- Proper (rest) masses of stable particles (neutral of charged) must be affected by a field of forces. Correspondingly, in SR Dynamics, the proper masses is field dependent. In GR Dynamics, rest masses of particles and material objects are not affected by forces.

- Frequency of the photon characterizes its energy, which is conserved in the gravitational field. Correspondingly, in SR Dynamics, the frequency is constant. In GR Dynamics, the photon in field behaves as if it has a mass. Correspondingly, its frequency increases with the field strength and decreases when it "climbs up" over potential levels.

- Wavelength of the photon decreases with the field strength in SR. In GR Dynamics, it does due to the fictitious conservation of photon energy consisting of potential and kinetic parts.

GR broken physics is clearly revealed in conceptions of redshift and light bending.

First, constancy of the speed of light makes the photon frequency rising with the field strength what is the blue shift. The gravitational redshift cannot be explained in General Relativity. The fake explanation in GR literature usually based on Pound-Rebka experiment treatment ignoring the relation $c_0 = \nu\lambda$. Notice, field dependence of photon frequency violates the energy conservation, as follows from SR Dynamics.

Second, the explanation of the light bending is impossible with the constancy of the speed of light. Dependence of speed of light on field strength is the known phenomenon of refraction in dielectric media. Remarkably, the gravitational field acts similarly causing the bending of light due to conservation of the energy and the angular momentum, as follows from SR Dynamics.

The bending effect was studied by German physicist Johann Soldner inspired by Newton's idea of corpuscular light. The results were published in 1804 [40]. In 1911, Einstein, who was aware of Soldner's work, derived the effect of the same value, arguing that his correct prediction was made in General Relativity. However, in 1915, he modified derivation and predicted the effect twice as high as previously found. Later on, his fake prediction was falsely confirmed in purely conducted observations of light grazing the Sun. The correct prediction is made in SR theory, which gives the value close to Soldner's. Roughly, he used Newtonian approximation, in which the speed of light can change up to the relative value of the effect.

Also, we state that Einstein's prediction of the Mercury's perihelion advance is wrong in its value and sign. Our correct prediction in SR theory shows not the advance but the retardation with the value of three times less than Einstein's.

6.5 GPS Science and paradigm shift

Our analysis of GR Physics and its GPS application is a demonstration of GR fictitious predictions. Fitishization of the General Relativity during the Century of its seemingly triumphal predictions plays a major role in the current Natural Sciences stagnation. This fact is denied by well funded mainstream, which propagates a blind belief in GR greatness and creates even greater scientific noise. Presented in this work verifiable rarely attended "details" reveal a pseudo-physical essence of the GR foundations.

The GPS has already a long history of performance darkened by multi-Billion budget expenditure. Yet, the current GPS is an unprecedented scientific failure still not realized by GPS scientific consultants, and managers. Neither this fact is realized by academic staff including Relativity experts, - advisers of next generation GPS promising the better precision and security albeit on the old premises and higher cost.

In GPS practice, dominating systematic errors are caused by a wrong theoretical model taken for real, to say more exactly, absence of Physical Science. To make GPS functioning, a continuous overloading process of multi-parameter adjustment is needed in solving basic equations for position and time determination. The process is fed by a stream of data from ground reference stations transmitting spoiled information about satellite orbits and the corresponding fictitious corrections. Any test of the GR Dynamics by GPS measurements would be useless because results could be any in the absence of a theory to be tested.

It is obvious that GR pseudo-physical methodology must be replaced by a theory of relativity, the only one having been abandoned by Einstein, unappreciated by his counterparts, and mistreated by the following generations, - the discussed above theory of Special Relativity. In this work, Special Relativity Dynamics is demonstrated as the Alternative to General Relativity, see Section 8.

Let us point out main theoretical fundamentals in our proposal of a new GPS project in the SR Dynamics framework.

- *GPS theory.* Terms such as Standard Atomic Clock, coordinate time, relativistic effects and others, are used in General Relativity, however, they have nothing to do with similar terms of physical concepts in Special Relativity Dynamics. In

our GPS project, a light (photon) path connecting transmitter and receiver is described by relativistic equations of an oscillator in relative motion in Minkowski 4-space. The theory is based on the empirically substantiated concept of field dependent proper mass proportional to the frequency of the oscillator, which is emitter and detector of the photon. A propagation of the photon and its properties in spherically symmetric gravitational field in Minkowski 4-space are described by the corresponding equations. The problem can be also formulated in terms of the complementary 4-momentum space, as well as the 4-phase space. The equations describe SR Dynamics effect of frequency shift and components of Doppler effect, which characterize conditions of locking of the receiver into a transmitted signal and allow to identify the unique path between transmitter and receiver. All equations are governed by conservation laws, which determine photon properties such as frequency, wavelength, and propagation speed depending on field strength.

- *Satellite orbit classification.* The GPS satellite orbit is described by SR Dynamics equations governed by conservation laws, similar to the Mercury's case. Their exact solutions are obtained by numerical methods. At the nano-second precision, classical elliptic classification of orbits in geometrical terms of eccentricity is not valid. Instead, the orbit is characterized by an amazingly simple physical criterion of $\sigma = r_g/\gamma_0^2\beta_0^2$ for type of sub-circle $\sigma > 1$, and over-circle $\sigma < 1$ orbit (similar to classical types in Figure 1). Those are also the criteria of orbital launching and adjustment to the required satellite position. There is a relativistic effect of precession of angular momentum vector about the plane axis. It makes the orbit unclosed with periodic retardation of angular and the corresponding temporal rates in comparison with classical (Keplerian) orbit. It is vitally important that the effects are taken into account.

- *Atomic clocks.* The Standard Atomic Clocks (SAC) is the natural oscillator based on quantum transitions in atoms. Therefore, we can create conditions allowing to count the number of transitions, what makes the oscillator the Atomic Clock. Its time rate and counting numbers are field dependent, therefore, the problem of SACs synchronization has no physical sense. However, in the spherical symmetric field, their synchronization can be understood in terms of resonant wave mode of the photon. In other words, radio waves are automatically tuned in harmony with natural laws on both sides of transmitter and receiver. A big question is: why do we need SACs, which are field dependent?

- *Frequency comparison.* In GPE User sector using SACs, navigation in passive regime ("do not ask satellite") can be performed without counting the delayed path time δt provided the satellite orbits are exactly known. It can be made by identifying a unique "passport" for path between transmitter and receiver. It can be found from analysis of frequency shift and components of Doppler effect. However, the Control sector needs full information to maintain the accuracy of satellites data by communication of ground reference stations with satellites in active regime ("I am here, you are there"). This is not possible without a high precision time service as the Universal Coordinate Time.

- *The Universal Coordinate Time.* As discussed, the existence of the uniformly running coordinate time UCT in the SR Dynamics is the consequence of time translation and space isotropy symmetries related to the conservation laws for

total energy and angular momentum. This concept is used in the Mercury's problem and is similarly valid in the GPS problem. There is a subtlety, though: the Earth's field is not ideally symmetric, firstly, it is not a sphere (oblateness effect), secondly, it rotates by inertia about its axis. Therefore, those effects should be separately accounted for. The Universal Coordinate Time should be first introduced in the Earth Centered Fixed frame (no rotation) prior to its adaptation in the Earth Centered Rotating Frame. UCT is the uniformly running and field independent time t. It is valid in the space of Earth's potential $1/r$ above Earth up to the radius of satellites and ballistic missiles not noticeably affected by forces from Sun and Moon. The UCT is theoretical (paper) time having a complex relationship with a set of imaginary SACs along a trajectory of moving object. Information about 3D coordinates of each satellite visible at any moment t must be composed in the Control sector. The GPS user must store it in a GPS navigating device to be available at any moment t before receiving a satellite signal. The same information must be received by each satellite and stored in its SAC block. Upon connecting with instantly recognized satellite, the user must receive a value of transmission time t_{tr} in addition to known information about satellite position and reception time t_{re} for each satellite. The navigation equations can be formulated in terms of the extremal action of photon travel from satellites to the user at instantaneous rest. In this approach, positioning navigation accuracy is essentially dependent on precision of parameters of satellites and UCT stability and scaling. Doppler analysis is helpful without SACs but their usage can improve the navigation precision. In the User segment, the navigating devises, rates of which are field dependent (such as genuine SACs), should not be used. The main problem is a generation and dissemination of field independent high precision UCT. Numerous companies claim that they resolve the this problem.

The above GPS project is radically different from the current GPS network in stability, precision, efficiency, scientific correctness, and cost of performance. The new GPS would be a long expected radical paradigm shift in Natural Sciences, Philosophy, and Mass Media.

7 GR strong field problem

7.1 Orbital motion

Equations of GR particle dynamics Section 2.2 are valid for the strong field conditions. In particular, the equation (13), metric being an exact solution of Einstein's field model (in the academic GR framework), is claimed to be valid not only under weak field conditions, but also in the whole range of field strength. So far, the equation has never been used for an exact description of the strong fields, particularly, in BH environment. Here, for the first time we use the equation for this purpose. Recall, the problem is formulated in the spherical symmetric geometry with the point-like source of mass $M \gg m$, where m is the the point-like mass of the test particle. As before, we use the equation of motion in the dimensionless form allowing to set the initial conditions.

The GR concept of point particles representing material bodies is a necessary requirement of the ideal model along with the concept of test particle of however small mass. In practice, the real size of the source, the radius R is taken into account in comparison with the gravitational radius r_g or the Schwarzschild radius $r_{sch} = 2\, r_g$.

In literature, the GR particle orbital motion in strong gravitational fields is often associated with the Black Hole environment. The concept of Black Hole used in Astrophysics suggests that a material spherical object having several solar masses, undergoes a process of gravitational collapse. This is a hypothetical phenomenon rather than a mathematical abstraction. The existence of infinite density of matter does not follow from the GR academic framework. Moreover, it is completely estranged from Fundamental Physics and the Standard Particle Model.

In full analogy to Mercury's problem, the GR equation of motion of test particle on BH environment implies the conservation laws and periodic time-reversal solutions, so that the particle never perish in a collision with an ideal point like center. Lagrangian properties are always preserved, particularly, in spiral fall orbits. As the parameter $\beta_0^2 \to 0$, the orbital precession frequency and the particle speed rapidly increase. The above GR picture of the strong field is very different from that GR literature.

An example of orbital motion in a moderately strong field is shown in Figure 7 with the following parameters: $\rho_0 = 0.05$, and $\beta_0^2 = 0.04$. As seen from orbit classification Table 1, it is of sub-circle type with notably precessing orbit. The angular half period there is about 4.53 radians, which is 44% larger than the corresponding classical value π, the time period is 7% smaller, the periapsis 38% smaller, and the velocity at periapsis 63% higher.

7.2 Spiral fall and the particle speed

The spiral fall orbit does not have an analogy in the classical theory. This is the GR phenomenon in the strong field in the sub-circle orbits, when the roots ξ_2 and ξ_3 approach each other. The case $\xi_2 = \xi_3$ is "the edge point" so that the spiral fall occurs in the region where the roots ξ_2 and ξ_3 become complex numbers, Figure 9. More details about spiral fall formation can be found in [3]. The particle can start from the initial weak field condition and fall upon the center under extremely strong fields before returning back with a huge angular advance. For $\rho_0 > 1/4$, the only possible type of Black Hole orbits is of spiral fall, as seen from tables and figures of orbit classification. An example of typical spiral fall orbit is shown in Figure 5.

The angular advance and total speed of the test particle increase with $\sigma = \rho_0/\beta_0^2$. There is no mechanism in GR Dynamics, which can restrict this tendency, hence, it is possible that the particle would move faster than light. This issue is discussed in the textbook [41] in connection with a radial fall (the exact full solution of the orbital motion problem was not available at the time when it was published). They correctly concluded that the superluminal motion can occur after the particle crossed the Schwarzschild surface of radius $r_{sch} = 2\, r_g$.

The existence of superluminal motion is one of results of our exact solutions of orbital motion. The infinite energy comes from the infinity of the potential $1/r$. From the conservation laws in the case of non-zero angular momentum, we obtain the expression for the total speed of the particle along an orbit:

$$\beta^2(\xi) = \beta_0^2 - 2\,\rho_0 - 2\,\rho_0\,\beta_0^2 + 2\,\rho_0\,\xi + 2\,\rho_0\,\beta_0^2\,\xi^3\,. \tag{38}$$

From this, the total speed at Schwarzschild radius is found in terms of elementary

functions

$$v^2(r_{sch}) = 1 - 2\,\rho_0 + \beta_0^2 \left(1 - 2\,\rho_0 + \frac{1}{4\,\rho_0^2}\right) \\ = (1 - 2\,\rho_0)\left(1 + \beta_0^2\right) + \frac{\beta_0^2}{4\,\rho_0^2}\,, \tag{39}$$

with radial and angular velocities given by Eq. (9), (10).

Under certain conditions, the full speed of the particle at Schwarzschild radius can be smaller than, equals to, or greater than the speed of light. Figure 13 shows combinations of parameters ρ_0 and β_0^2 when the speed is equal to the speed of light. Example of a spiral fall trajectory from case 3 of Figure 9 is shown on Figure 10. The particle crosses the Schwarzschild surface at the speed $\beta_{sch} = 1.982$ and continues to accelerate.

Let us consider the components of velocity for particle crossing the horizon $\xi_{sch} = 1/(2\,r_g) = 1/(2\,\rho_0)$, also in exterior and interior regions. On the horizon sphere, the GR effective potential always takes a zero value, $V_{eff}^2 = 0$ (straightforward verification). Consequently, the squared radial speed is equal to the total (squared) energy, $\beta_r^2 = \epsilon_0^2$ always taking values less than unit, $\beta_{sch}^2 = \epsilon_0^3 < 1$ in the whole range of interior region (including the Schwarzschild surface).

The orbital component could be any, depending on β_0^2. Indeed, $l_0 = r_0\,\beta_0 = r\,\beta_\theta$, $r = 1/\xi$ or

$$\beta_\theta(\xi) = \beta_0\,\xi\,, \quad \beta_\theta^2(\xi) = \beta_0^2\,\xi^2\,. \tag{40}$$

At a however small β_0^2, a however small (squared) addition to the radial speed makes the resultant speed less than the speed of light, $\beta < 1$, or, at some greater value, makes $\beta \geq 1$, as in the example of Figure 10.

Figures 11 and 12 demonstrate GR predictions of particle motion in the interior (and while crossing the horizon) with speed less and greater than the speed of light. In the example of field strength $\rho_0 = 0.050$, we have the following speed (squared) values at the horizon $\xi_{sch} = 10$:

- subluminal case, $\beta_0^2 = 0.0001$, Figure 12: $\beta^2 = 0.910$, $\beta_r^2 = 0.900$, $\beta_\theta^2 = 0.010$;
- superluminal case, $\beta_0^2 = 0.0080$, Figure 11: $\beta^2 = 1.707$, $\beta_r^2 = 0.907$, $\beta_\theta^2 = 0.080$.
- For a greater value of $\beta_0^2 = 0.030$ (still less than the edge value $\beta_0^2 = 0.03419$), it would be $\beta^2 = 3.927$, $\beta_r^2 = 0.927$, $\beta_\theta^2 = 0.300$.
- It is easy to find that the particle crosses the horizon at the speed of light for $\rho_0 = 0.005$, $\beta_0^2 = 0.0010$: $\beta^2 = 1.000$, $\beta_r^2 = 0.900$, $\beta_\theta^2 = 0.100$.

7.3 Free radial fall

As previously noted, GR Dynamic equations of orbital motion are influenced by the GR cubic term of interference of angular momentum with the potential energy is neglected. Because the angular momentum of the particle in free radial fall is zero by definition, the GR equation of the radial motion has to be automatically coincide with the corresponding classical one, provided the appropriate initial conditions are fixed.

In conventional GR Dynamics, the radial fall equation differs from the classical one. The reason for that is that the GR equation is derived with the use of GR expression of conserved total energy ϵ_{rad} (7) [33], also [41, 42]. Recall, unlike in orbital motions, in the GR case of a radial fall, we have two time variable, τ and t, having different meaning.

Below, we follow the conventional derivation of equations starting from the initial conditions in the expression for ϵ_{rad}:

$$\epsilon_{rad} = (1 - 2\,r_g/r)\,\mathrm{d}t/\mathrm{d}\tau = (1 - 2\,r_g/r_{ic})\,\mathrm{d}t_{ic}/\mathrm{d}\tau_{ic}\,. \tag{41}$$

Assume the initial conditions are fixed at "far away". To avoid the infinite time of motion from infinity, let us introduce the "far-away" distance r_{fa} however great but finite, and let the initial inward speed be $(\mathrm{d}r/\mathrm{d}t)_{fa} = (1 - 1/\gamma_{fa}^2)^{-1/2}$. Then, the inward speed of a particle in the radial fall is found:

$$(\mathrm{d}r/\mathrm{d}t)_{fa}(r) = (1 - 2r_g/r)\left(1 - (1 - 2r_g/r)/\gamma_{fa}^2)\right)^{1/2}\,. \tag{42}$$

Here, $\gamma_{fa} = E_0/m_0 \geq 1$ is considered the "far-away" total energy. Respectively, the formula is interpreted in terms of the "far-away" observer whose wristwatch shows the coordinate time t. At the same time, let us introduce the so-called "shell observer" placed at some point $r_{shell} < r_{fa}$, which is not fixed in the initial conditions, whose wristwatch must show the proper time τ_{shell}. Then, the radial speed $\mathrm{d}r_{shell}/\mathrm{d}\tau_{shell}$, viewed by the "shell" observer in accordance with (41), must be given by

$$(\mathrm{d}r/\mathrm{d}\tau)_{shell}(r) = \left(1 - (1 - 2r_g/r)/\gamma_{fa}^2)\right)^{1/2}\,. \tag{43}$$

One can suggest to treat the formula (42) from the viewpoint of "far-away" observer. The particle sent from infinity to the center begins to accelerate, but at some point, it starts decelerating. The motion looks "strange", however. The matter is that the particle, before approaching the Schwarzschild radius $r_{sch} = 2r_g$, at some point dependent on γ_{fa}, starts decelerating: the higher initial kinetic energy, the farther the deceleration point from the center. For $\gamma_{fa} \geq \sqrt{3/2}$, the particle will never accelerate in a gravitational field. The gravitational force exerted on the particle becomes repulsive in the entire space.

Quite differently, the formula (43) shows that, from the viewpoint of "shell" observer, the particle always accelerates. When crossing the Schwarzschild sphere, it reaches the speed of light. In the internal space, the particle is considered not observable (due to "light trap"), likely, its motion becomes superluminal till it "crashes" at the center. This picture is widely known in association with the particle radial fall onto Black Hall.

8 Special Relativity theory

8.1 Transition from the abstract proper 4-space to the observable coordinate space-time

In this work, we disagree with the statement that, unlike Einstein's General Relativity theory, the Special Relativity theory is not able to describe the Newtonian gravity [33]. They say that SR Dynamics failed to explain observations of Mercury's perihelion advance in the gravitational field of the Sun, and some other observations. The objection

points to the fact that the argument of incompatibility with gravitation is based on certain assertions and actually not strictly proven [43]. In particular, it is shown that an introduction of the relativistic concept of field dependent proper mass makes the difference.

SR Dynamics (motion in field of forces) starts from the concept of the abstract proper 4-space x^μ known in connection with the earlier developed SR Kinematics (motion by inertia with no forces). In both cases, the proper 4-space is converted to the coordinate space-time, in which SR Kinematics and Dynamics is formulated in the real physical space and time.

The starting point is the concept of a world line $s(x^\mu)$ characterized by the abstract proper time τ serving the role of affine parametrization of space and time variables (with a usual convention of speed of light at infinity $c_0 = 1$). The metric quadratic form in the *abstract* 4-space is given by

$$\mathrm{d}s^2(\tau) = c_0^2\,\mathrm{d}\tau^2\,. \tag{44}$$

The proper unit 4-vector $U^\mu = \mathrm{d}(x^\mu)/\mathrm{d}s$ is introduced, which is tangential to the world line, so that the metric tensor is diagonal:

$$U_\mu U^\mu = 1, \quad U_\mu(\mathrm{d}U^\mu/\mathrm{d}\tau) = 0\,. \tag{45}$$

The proper 4-coordinate infinitesimal displacement $\mathrm{d}x^\mu$ of the world line is defined in connection with the 4-space and the 4-momentum (complementary) space P^μ through U^μ:

$$\mathrm{d}x^\mu = \mathrm{d}\tau(x^\mu)U^\mu, \quad P^\mu = m(x^\mu)U^\mu\,. \tag{46}$$

Next, the 4-vector force in the abstract proper 4-space is defined

$$K^\mu = \mathrm{d}P^\mu(s)/\mathrm{d}s\,. \tag{47}$$

This is the Minkowski 4-force having, as any 4-vector, the proper (temporal) part and spatial components of 3-vector. One can proceed further in a formulation of the angular momentum, the torque, etc. in the tensor form similarly to that in Relativistic Electrodynamics.

Eventually, all abstract physical quantities are put in connections with real measurable or observable quantities in physical world. For example, the Minkowski 4-force is associated with the scalar, - the conserved total energy, and the components of "ordinary" force, - the vector in 3-space [13].

With the use of the Lorentz transformations, the abstract 4-space is converted to the coordinate space-time, what is *the observable* Minkowski space-time. Similarly, the abstract 4-momentum is connected with the corresponding real physical quantities. At the same time, the SR Lagrangian formulation of the problem is important in the generalization of SR Kinematics to the SR Dynamics.

With the transition to the coordinate (the observable) space-time, one can forget the abstract proper 4-space and the abstract equations there. Unfortunately, a terminology of "proper quantities" is used for observables also, – in a sense of the observables at rest with respect to imaginary observers exchanging their information with respect to each other in a relative motion. In the operational language, they do it using the standard (atomic) clocks serving also the role of the standard emitter/detector of the light signal.

8.2 Field dependent proper mass

In the conventional SR theory, the proper mass is constant. We consider it a weak field approximation, after Synge, [13], who developed the theory accounting for the proper mass variation in the field but thought the effect be practically negligible, as a reasonable approximation. This point of view is widely accepted among the Relativistic Mechanics community. The history of this issue and the consequences of the approximation are discussed in [43], also see [44].

The advanced SR particle dynamics is formulated in the coordinate space-time of observables, where the static mass or the mass in the comoving reference frame (both usually called the proper mass, as noted) are field dependent proper mass. In the static spherical symmetric field, a dependence of the proper mass on radius is given by

$$m(r) = m_{test} \exp(-\rho_0(r_0/r)) \,. \tag{48}$$

Here, m_{test} is the mass of the test particle having a limit $m(r) = m_{inf}$ as $r \to \infty$. As shown below, it can be considered in relations with the Einstein-DeBroglie's concept of the standard clock characterized by the frequency of ticks, what allows the comparing the time rate as the field strength (the potential function) changes. In the ideal (one body) model, the test particle mass is canceled on left and right sides of the SR equations of motion, similarly to that in Classical Dynamics.

Thus, the static potential function in the space-time coordinate space takes the form

$$V(r) = -\left(1 - \exp(-r_g/r)\right) \,, \tag{49}$$

which is reduced to Newtonian potential $V(r) \propto 1/r$ at $r_g/r_0 \ll 1$.

To consider the proper mass constancy "an approximation" would be actually methodologically wrong because the values of $\mathrm{d}t$ and m must be inversely proportional due to the complementarity of the SR space-time vector and $\mathrm{d}x^\mu$ and the 4-momentum vector P^μ, therefore, their scalar product is constant:

$$P^\mu \cdot \Delta x_\mu = m\Delta t \,. \tag{50}$$

It is the absolute value of constant 4-phase vector. It is consistent with the Einstein-de Broglie relationship. There, a period of a quantum oscillation is related to the frequency

$$mc_0^2 = h\, f, \quad \Delta\tau = 1/f \,, \tag{51}$$

where h is Planck's constant, $c_0 = 1$, $m_0 = 1$. Next, we take $\mathrm{d}t = \Delta t$ meaning a however small finite period of the standard quantum oscillator in (51) (the time interval between consequent clock's ticks).

We have to reiterate that SR Dynamics with the field dependent proper mass is fully relevant to the relativistic motion in the gravitational field, and it obeys the Causality Principle (as follows from the SR Dynamics formulation and the corresponding equations). Also, we make a strong statement that the known central infinities in the existing field theories would be naturally eliminated with the introduction of the field dependent proper mass in the spherical symmetric geometry. Consequently, the force on the test particle has a zero limit as the radius approaches the center. This fact is illustrated in Figure 14.

Remarkably, the picture reminds the QCD phenomenon of "quark rad/rad overrad/rad overconfinement" related to "the asymptotic freedom". The artificial mathematical procedures of "mass renormalization" became not needed. For this and other

reasons, we suggest SR Dynamics be considered the alternative to GR particle dynamics [2, 43, 45].

Next, the principles of advanced SR Dynamics applied to the spherical symmetric field, and the corresponding orbital motion equations are formulated.

8.3 Principles and equations of SR Dynamics

In brief, the SR Dynamics problem of orbits is formulated in the relativistic Lagrangian approach consistently with Noether symmetries of space-time (the 3-space isotropy, and the coordinate time translation and time reversal) in relationship with the conservation laws. Therefore, the coordinate time t runs uniformly while the comoving observer's time pace t_{com} is affected by the field.

In polar coordinates, the 4-coordinate displacement vector and the 4-momentum vector are defined, as follows: $\mathrm{d}X^\mu(r) = \gamma\,\Delta t\ (1, \beta_r, \beta_\theta)$ with the Lorentz factor $\gamma = (1-\beta^2)^{-1/2}$, β is the total orbital speed. The 4-momentum vector is $P^\mu(r) = \gamma\, m(r)\ (1, \beta_r, \beta_\theta)$, where 3-velocity components and the Lorentz factor are functions of r and θ, with a usual convention $c_0 = 1$.

We shall see that the equations of motions are characterized by two roots. In other words, the equation of motion in a dimensionless form is governed by two independent physical parameter. In this sense, there is a similarity of the GR and SR Dynamics but the results would be radically different because the principles of SR Dynamics do not allow superluminal motion in any circumstances.

In terms of initial conditions, there are only two independent physical parameters, which are parameters of the equations of motion, for example, the field strength ρ_0 and the squared angular speed β_0^2, their ratio being the classical orbit classification parameter $\sigma_0 = \rho_0/\beta_0^2$. Also, we may use the analogous relativistic parameter $\sigma_r = \gamma^2\sigma_0$.

There are two conservation laws, – the conserved total energy ϵ_0, and the conserved angular momentum L_0 given below for the initial conditions $r(r) = r_0$, $\theta = 0$, $\beta_r = 0$, $\beta_\theta = \beta_0$:

$$\epsilon_0 = \gamma_0\,\gamma_{r,0} = \gamma\,\gamma_r\,, \tag{52}$$

$$L_0 = \gamma_0\,\gamma_{r,0}\,r_0\,\beta_0 = \gamma\,\gamma_r\,r\,\beta_\theta\,. \tag{53}$$

Instead of (53), it is convenient to use a conserved quantity $l_0 = \epsilon_0/L_0$:

$$l_0 = r\,\beta_\theta\,. \tag{54}$$

Here, a squared inverted Lorentz factor is $1/\gamma^2 = 1 - \beta_r^2 - \beta_\theta^2$, and $\beta_r = \mathrm{d}r/\mathrm{d}t$, $\beta_\theta = r\,\mathrm{d}\theta/\mathrm{d}t$. To get the angular equation, consider $\beta_r = (\mathrm{d}r/\mathrm{d}\theta)(\mathrm{d}\theta/\mathrm{d}t)$, and transform (54) into $\beta_\theta^2 = l_0^2/r^2$. After introducing a variable $\xi = r_0/r$, we arrive to the exact relativistic equation of orbital motion of a bounded test particle. The equation is valid for a however strong field by the criterion r_g/r:

$$\left(\frac{\mathrm{d}\xi}{\mathrm{d}\theta}\right)^2 = \frac{1}{\beta_0^2} - \xi^2 - \frac{1}{\gamma_0^2\,\beta_0^2}\,\exp\left(\frac{2\,r_g}{r_0}\,(1-\xi)\right)\,. \tag{55}$$

The Newtonian limit, or weak field conditions, is given by a linear approximation of the exponential function:

$$(\mathrm{d}\xi/\mathrm{d}\theta)^2 = (1 - 2\,\sigma_r) + 2\,\sigma_r\,\xi - \xi^2 - 2\,\sigma_r\,(r_g/r_0)\,(1-\xi)^2\,, \tag{56}$$

By definition, there is a useful relationship

$$\mathrm{d}\xi/\mathrm{d}\theta = (\mathrm{d}r/\mathrm{d}t)/\beta_0\,, \tag{57}$$

where $(\mathrm{d}r/\mathrm{d}t)^2 = \beta_r^2(r)$ is the radial (squared) component to the total (squared) speed $\beta(r)$:

$$\beta^2(r) = \beta_r^2(r) + \beta_\theta^2\,, \tag{58}$$

with the angular speed term

$$\beta_\theta^2 = r_0^2\,\beta_0^2/r^2\,. \tag{59}$$

$$\beta(r) = \left(1 - (1/\gamma_0^2)\,\exp(-2\,r_g/r)\right)^{1/2}\,. \tag{60}$$

9 Mercury problem in SR Dynamics

In a full analogy with quantitative comparison of GR Dynamics with respect to Classical Dynamics of orbital motion, we introduce the three event scheme comparison of SR Dynamics with respect to Classical Dynamics. Unlike in GR, the SR events delay with respect to classical time instants. The three event instants on the base SR time line t_{sr} are defined, as follows.

- Event 1 at the instant $t_{sr,1}$, when SR clock displays the value of the classical aphelion, the event 2 (the equality of numbers of ticks of standard clocks in both theories, $t_{sr,1} = t_{cl,2}$).
- Event 2 at the instant $t_{sr,2}$, when the SR aphelion is reached.
- Event 3 at the instant $t_{sr,3}$, when the SR orbital angle is π.

The corresponding time instants t_1, t_2, t_3 displayed by the classical clock are specified, as well:

- The instant t_1 corresponds to $t_{sr,1}$ (when $t_{sr,1} = t_{cl,2}$).
- The instant t_2 is when the classical aphelion is reached.
- The instant t_3 corresponds to $t_{sr,3}$ (when the SR orbital angle is π).

Results of comparison based on the 3 events scheme for the exact combined solutions of the Mercury problem in SR and Classical Dynamics are presented in Table 6, Table 7, Table 8, Table 9.

In Table 6, the input and output data for computing Mercury's orbital characteristics in Classical and SR Dynamics are given. In the input, must be only two independent model parameters, for example, ρ_0 and β_0^2. In the output, absolute values of main classical characteristics integrated over the full period and their absolute and relative differences with respect to corresponding SR Dynamics results are given.

In Table 7, orbital characteristics q_{sr} computed at 3 events in SR Dynamics time scale t_{sr} in comparison with q_{cl} computed in the classical time scale t_{cl} starting with initial conditions. Also shown their absolute and relative differences $\Delta q = q_{sr} - q_{cl}$, $\delta q = (q_{sr} - q_{cl})/q_{cl}$. The following characteristics are computed: the time passed t_{sr}, t_{cl}, the radius r_{sr}, r_{cl}, the orbital angle r_θ, r_θ, the orbital speed v_{sr}, v_{cl}, the orbital length l_{sr}, l_{cl}.

In Table 8, absolute differences of orbital characteristics between events (2, 1), (3, 2), (3, 1) computed in SR Dynamics and Classical theory.

Finally, in Table 9, the projection of the three SR events on the base time line t_{sr} and the classical time line t_{cl} is shown. Notice, dealing with disparity of events on time and angular scales, one has distinguish between the angle π in Classical and and Relativistic theories.

Similarly to the GR Mercury problem, the corresponding SR time instants t_1, t_2, t_3 displayed on the time lines are specified, where the standard clocks run uniformly in both theories too. However, the standard "SR clock" on the base time line runs slower than "the classical clock". The SR and classical time lines are related to each other by the following linear expression: $t_{cl} = k\, t_{sr}$ where the new coefficient k is a ratio of classical and SR time periods $k = T_{cl}/T_{sr} < 1$. Again, it is a disparity of SR and classical time lines, which requires a necessity of difference in SR and classical time periods.

The relativistic SR effects characterize the retardation of the angular and temporal rates with respect to the classical theory predictions. Namely, in a first half period, starting from the initial conditions, the angular shift $\Delta\theta = -8.365 \times 10^{-8}$ rad, or the relative effect $\delta\theta = -2.663 \times 10^{-8}$, are delayed with respect to the classical theory. The effect is three times smaller but has an opposite sign than the corresponding GR effect. The about same factor of retardation is seen in the time half period where the difference is $\Delta t = 0.191613$ s, or the relative effect $\delta t = 5.042 \times 10^{-8}$.

Clearly, the SR retardation is due to the proper mass dependence on the field strength implemented into SR Dynamics. It must prevent the particle motion from the appearance of superluminosity under strong field conditions: with the rise of a field strength, the particle motion rise is restricted by SR laws. Moreover, the central infinity is naturally eliminated and more positive consequences follow, and the Black Hole GR concept and other String field phenomena are revised.

The retardation of SR angle is equivalent to the angular classical advance, so we suggest the following law of the angular shift under weak field conditions analogous to the GR angular advance,(32). The less the field strength, the greater the precision of this law.

$$\Delta\theta = \sigma_0\, \rho_0 \tag{61}$$

Here, $\Delta\theta = \theta_{cl}/\theta_{sr} - 1 = \sigma_0\, \rho_0$ is a relative angular advance rad/rad of the classical angle with respect to the SR angle (initially averaged over half a period), $\theta_{cl} = \pi$, $\sigma_0 = \rho_0/\beta_0^2$ for $\rho_0 \ll 1$. As opposed to GR, the value of the angular shift in SR Dynamics with respect to the Classical theory is exactly 3 times less than in GR, but has an opposite sign. The time period is greater in SR Dynamics by about the same factor 3.

In the SR based Dynamics, the GR controversies and problems, such as the superluminosity and Causality Principle breakage, infinities, τ vs t time problems, and others, do not arise. General Relativity is proven totally wrong conception, it is not even a theory. Doing our calculations in GR, we closed our eyes on this fact. As concerns Mercury's problem, the true relativistic effect is the retardation rather than advance.

10 New Hypothesis of Physical Cosmology, the Grand Universe Model

We propose a hypothetical Alternative Cosmology. Its physical principles and methodology are based on Special Relativity Dynamics of gravitating matter and its Newtonian limit. This is a model of steady-state, matter-antimatter symmetric Grand Universe consisting of an infinite number of matter and antimatter Typical Universes. They are floating in infinite space-time and interact with each other and with the Grand Universe relativistic background. The Grand Universe is self-sustained in an eternal process of matter-antimatter annihilation and recreation. The Model suggests different interpretation and conceptually consistent explanations of all basic Cosmological and Astrophysical observations. In particular, the enigmatic matter-antimatter asymmetry is naturally understood; the observed physically red-shifted light from observed flying away galaxies is considered an evidence of physical disintegration of a matter dominated Universe, we live in, in a result of its collision with some antimatter dominated Universe. Numerous longstanding and newly appearing problems of the Standard Cosmological Model do not arise in our Model, and physically unexplainable "new physics" does not appear.

10.1 Preamble

Next, we discuss challenges beyond the latest ΛCDM version of Standard Cosmological Model (SCM), which is currently considered the leading model among earlier proposed alternatives. There are literally thousands of observations and the corresponding theoretic works, which seem to support the statement that the Model is firmly proven a true one. From this, a conclusion could be made by "main stream experts" that any new alternatives would require a huge resources for testing and should not be accepted anymore. Even more extreme position is taken by some cosmologists and philosophers claiming that mathematically "elegant" model do not need a thorough empirical verification. In reaction to such philosophy, physicists call upon the scientific community to defend Physics Integrity [46].

In the recent work [47], a large database of basic observations was compiled and systematized in their historical order to allow a reader to judge independently on its role in validation of the SCM. It is stated that the main tenets of the Model have never been tested *directly*:

- the redshifts of the galaxies are due to the expansion of the Universe plus peculiar motions;
- the cosmic microwave background radiation and its anisotropies derive from the high energy primordial Universe when matter and radiation became decoupled;
- the abundance pattern of the light elements is explained in terms of primordial nucleosynthesis;
- the formation and evolution of galaxies can be explained only in terms of gravitation within a scenario of inflation, plus dark matter, plus dark energy.

We agree with this statement and also criticize the General Relativity and its applicaion to the SC Model, – the concept of metric space-time expansion [48, 49].

In its essence, the SC Model tells us that Physical world we live in was some time ago instantly created and expands in the whole space from nothingness and non-existence, and it actually going back to nothingness and non-existence. Meanwhile,

we got to know that everything now is made from "a mysterious non-observed matter", and only 5 percent of the matter is left to well known "ordinary matter", – the core of still respected Physics Foundations. Real gravitation plays only a minor role (if any) in the SCM. As for today, this is a model of absurdity, supporters of which deny new alternatives and their role of continuous empirical testing of theories at a deeper fundamental levels is in conflict with the real physical science.

Necessity of exploring alternatives is expressed in works of leading cosmologists, e.g. [50–56] and numerous other works. The evolution of modern cosmology over six decades, during which the ordinary matter was replaced with "dark hypothetical substances", as well as reality facts are vividly tracked in [50, 51]. In [52], a review of hundred years of the Cosmological Constant, from "Superfluous Stunt" to "Dark Energy", shows drastic changes of Big Bang Cosmology. Every new Big Bang version claims a perfect match of a model and observations. Evidently, it is maintained by increasing a degree of fitting freedom, when every new non-explained phenomenon is labeled and parametrized. Among many others, radical methodological alternatives are suggested in [53–55] in order to resolve historically arisen undeniable problems.

A piercing view of the ultimate cosmological problem is presented by Martin Rees, see [56] and his other works. What are there far beyond the horizon? Are there man "big bangs" rather than just one? If there are many, are they all governed by the same Physics? The questions are not new, but, if to exclude known versions of multiverse, or cycling, models, which are practically non-verifiable, the questions acquire a new deep meaning and priority. Indeed, decades of cosmological inquiries is a tiny instant of observing a tiny space-time slice of the Universe in its conundrum enormity, what is more than insufficient for proclaiming the assurance of great progress in our understanding the Nature. We need clear physical answers to the questions with ideas to allow interpreting observations and explaining observed physically unexplained phenomena consistently with the historical heritage of existing physical knowledge, rather than denying it. Ideally, the ideas must have not only explanatory but also predictive power. These line of thoughts is pursued in this work.

A new hypothetical model based on the methodology of Special Relativity Dynamics and its Newtonian limit is proposed, as described in [57] in more details. It is claimed that our new Alternative, called the Grand Universe Model (GU Model), is competitive and should be considered by cosmologists and physicists for further examination. This is the conceptual Hypothesis rather than the result of scrupulous studies of the observational database. Therefore, it needs new numerical tests through comparative analysis of basic observations. It is claimed that the Model suggests different interpretation and conceptually consistent explanations of all basic Cosmological and Astrophysical observations, and it is testable.

10.2 Physical Principles of the GU Model

We consider SC Model problems of Matter-Antimatter Asymmetry and Ultra-High Energy Cosmic Rays the ones of primary cosmological issues, which are forgotten and claimed to be resolved in a new Cosmology. From this starting point, one can come to the idea of steady-state, matter-antimatter symmetric Grand Universe (GU), which is attractive by its naturalness, and explanatory and predictive power.

The GU is a world of Newtonian gravitation and exists due to gravitation solely due to ordinary matter. The GU world always existed, and it is eternal with no spatial boundaries, – there is no question about its origin. The amenable scientific questions to be asked are about an evolution of its parts and a state on the whole. The GU is

in the equilibrium state due to a balance of continuous matter-antimatter annihilation and creation and a statistical mechanism of matter-antimatter separation on the largest cosmic scale [58].

The GU can be called a physical multiverse. It consists of finite bounded Typical Universes (TU) each equally made of, mostly, matter or antimatter. They are stable till destroyed in their random collisions. On the largest GU scale, the TUs can be considered either massive point particles, or, more exactly, insular systems characterized by masses, sizes, total energy, and angular momentum.

The TUs interact gravitationally at distance in the infinite space-time filled with the physical Ground Universe Background (GUB). The GUB is a high-energy relativistic medium for gamma rays, particles, as well as matter and antimatter fragments. This is a place for eternal evolution of Typical Universes interacting with each other and with the GUB itself. Notice, a physical process of matter annihilation and pair creation implies nuclear reactions between nuclear particles rather than bulk materials. From this, one can try to figure out about how huge is a lifetime of a TU.

10.3 Our Observed Universe in the GU Model

It is quite naturally to hypothesize that Our Observed Universe (OU) is an ordinary cosmological phenomenon resulting from a collision of two Universes of different masses, one contains matter, the other antimatter. Our collision scenario suggests that we observe consequences of the completed collision rather than the collision beginning and its peak.

This is not an explosive annihilation but rather a lengthy continuous disintegration. It is accompanied by releases of huge amount of radiation and relativistic particles as well as a huge amount of kinetic energy of flying away parts of the TUs due to loss of their binding energies. A radiation pressure creates radial forces and torques that makes Dynamics of Observed Universe quite complicated, when galaxies recede in both chaotic and somehow orderly manner. Possibly, some part of the OU would survive in the form of a cluster of galaxies or just single galaxies.

Not surprisingly, galaxies in the OU, in particular, in the Milky Way (discussed later), must be very different from freely floating TUs in the GU. The TUs are expected to be much more bounded to the central super-massive core, more densely packed, and rotate about the center, the closer to the core, the higher the speed. It should be noted that, due to the TU volume finiteness and the finiteness of lifetime of its luminous matter, the famous Olber's "dark night sky" paradox does not arise in the GU Model.

Our place in the Observable Universe occurred to be in a spatial region of initially large but limited volume containing the center of mass of colliding TUs. The OU is finite but too large to clearly detect edges. For this reason, the observed picture of receding galaxies is apparently isotropic, but it could be not exactly so. So far, we are talking about Newtonian Physics, in which receding galaxies are freely moving by inertia at a moderate speed. Our Observed Universe must have a resulting angular momentum and the corresponding axis of rotation. However, it is hard to directly observe it, since we belong to the rotating system of a huge volume. But it could be observed indirectly [59, 60].

There are long standing and newly appearing SC Model problems of fundamental importance. They are mostly listed in [47], and discussed in more details in this paper. Some of them can be naturally understood within the GU Model framework, namely, in the annihilating collision scenario. Examples with ideas of explanation are given below.

- *The matter-antimatter asymmetry of the Observed Universe.* Our Universe is observable in a post-collision era, it is matter-dominated decaying Universe, when the most of antimatter of the colliding pair have been burnt out, but still is present and observed but not recognized.

- *The physical nature of "unusual" phenomena, such as quasi-stellar objects (QSO) and gamma bursts*. Likely, antimatter clouds surrounding some super-massive objects slowly annihilate, what looks like a QSO characterized by huge luminosity varying in time. As for gamma bursts, they originate in processes of annihilation of in colliding antimatter solid pieces of various masses with massive matter objects.

- *"Mysterious" releases of radiation of huge energy in the Milky Way and distant galaxies.* Again, the likely cause could be annihilating antimatter clouds attracted to the central parts of galaxies.

- *The large scale matte spacious structure.* In the collision scenario, the structure was historically formed during a long process of non-uniform antimatter annihilation when original matter made TU was partially washed out.

- *The origin of galaxies.* In the GU concept, fluctuations of matter due to residual presence of antimatter (and vice versa) in Typical Universes must originate gravitational clustering due to original non-uniformity of matter density.

- *A diversity of properties of galaxies in the Observed Universe.* Again, in the collision scenario, observed galaxies are partially "washed out" by antimatter in various ways, so there must be diverse classes of their physical properties. Typically, they must be less bounded than in original states.

10.4 Main Observable Universe observables

Before discussions of physical treatment of observed physical phenomena and features, let us outline main observables in the OU.

The receding galaxies are observable in the red-shifted light coming to our place, which is significantly void of matter annihilated in a large space. We shall see how the observable redshifts are treated in terms of Special Relativity (SR) Dynamics, namely, the motional and gravitational time dilation effects, and some other factors. So we have to analyze statistical data in order to assess masses, distances, and time of flight of galaxies in a random picture of the collision.

We consider the observable Cosmic Microwave Background (CMB) the electromagnetic radiation in local thermal (Black Body) state. Its temperature is equal to the temperature of the cold matter absorbing energy of radiation from stars and other sources. "Cold matter" consists of solid fragments and dust in interstellar and intergalactic space. Presumably, the CMB temperature has been decreasing during the adiabatic process of matter and gas expansion in the collision scenario.

Cosmological nucleosynthesis observables (including all spectrum of chemical elements and isotopes) must reflect the result of nuclear reactions in the GU quasi-stationary state of cyclic recreation of matter and antimatter. The Cosmic Rays of ultra-high energy (discussed further) contribute to the nucleosynthesis of heavy nuclei.

The scientifically amenable questions are about the GU physical properties and OU past and future. To answer them, a complete reinterpretation of the observations is

needed concerning space and time scaling. As noted above, the picture of the OU as a result of two TUs collision should be studied, particularly, by statistical simulation methods. Overall conditions of TUs interactions with each other and with the GUB must be just right for the GU to be self-sustained in its continuous self-destruction and recreation of the GU eternal steady state. This would be a challenging project of testing the GU Model with the use of a full arsenal of Classical and Modern Physics and beyond.

Next, GU Physics is discussed in more details.

10.5 Matter-antimatter symmetry?

In literature, the problem is usually formulated in terms of Baryon Asymmetry, which should be "proved" by theorems appealing to "the fist principles". We are talking about the general concept of matter made up of basic particles such as positive protons (baryons) and negative electrons (leptons) with a change of sign of charge and space-time symmetries in anti-matter. Consequently, the neutron has its counterpart, the anti-neutron, and so forth. All non-stable particles from high-energy reactions have also their anti-particles, as they appear in the left or right coordinate systems (axes direction change) with an inversion of time direction. We consider the matter-antimatter symmetry one of the empirical "Fist Principles" not requiring "the proof".

Our Observed Universe is apparently a matter dominated Universe. The matter-antimatter asymmetry can be explained by admitting an existence of multiple Universes (TUs) symmetrically dominated by matter or anti-matter. First of all, there must be a mechanism of statistical separation of matter and antimatter in the process of annihilation and creation [58]. Yet, the TUs evolutions should be viewed in the process of their interaction with each other and with the Grand Universe Physical Background. The GUB must be a relativistic physical medium containing massive and massless matter and all products of TUs distraction in matter-antimatter collisions. At the same time, the GUB has to provide material for the TU evolving. As a result, TUs have a great variety of masses and sizes.

Thus, Our Observed Universe is an exemplary case of collision of two matter/antimatter TUs of different sizes; one of them or both have to perish. Consequently, we observe a picture of "receding galaxies", which can be thought "the Expanding Universe".

The question arises: is there a notable amount of antimatter in Our Observable Universe? We state that the antimatter is actually all around in a considerable amount, but it is hardly distinguishable from ordinary matter. Its indirect consequences can be falsely recognized as "unusual" phenomena not related to the presence of antimatter. The annihilation process can take different unprecedented forms, when a release of huge amount of energy from conversing mass to kinetic energy and radiation takes place in a short or prolong time. Particularly, can be matter-antimatter annihilating collisions of super-massive stars or ordinary stars, or collisions of a small objects making short gamma burst. It can be an annihilation of slowly colliding dust clouds and galaxy attractors, and more variants. In some cases, the initial matter-antimatter annihilation can ignite the fast thermo-nuclear explosion. We also believe that anti-matter debris occasionally fall into Earth atmosphere and can be detected, or have been already seen as "unusual phenomena".

To sum up, next is not a full list of "unusual" phenomena, which are explainable by matter/antimatter annihilation:

- annihilation of slowly colliding large clouds with gravitational attractors in quasars

- star "explosions" and gamma bursts with release of huge amount of high energy
- universe large scale structure: walls and filaments separated by immense voids
- unusual radiation flares around the center of Milky Way and other galaxies [61–64]
- X-ray busts of a huge intensity and strange phenomena of central Black Holes in galaxies [65–67]
- shining halos around QSO [68]

A full review of observable "strange" pictures and events, which could be considered the evidence of the antimatter presence in Our Observable Universe, is out of the scope of the present work.

10.6 Primary Cosmic Rays and the Causality Principle

There are numerous galactic and intergalactic contributions to the observed Cosmic Rays (CR). The problem is that they contain particles of ultra-high energies $E > 10^{18}$ eV reaching values 10^{21} eV and beyond, physical origin of which is a mystery [69, 70]. For decades, physicists tried to unveil a mechanism of particle acceleration up to such an inexplicably ultra-high energy, though, physical mechanism of such accelerations are beyond a technical imagination. We state that it cannot be explained by any physically reasonable mechanism assuming their origination within the Observed Universe, and suggest radically new idea consistent the GU Model.

The explanation of this phenomenon with no need of "acceleration" is, as follows. The Primary CRs come from the GUB radiation in the form of extremely high energy particles. During penetration through the Universe, they loose energy. The observed ultra-high energy tail is a contribution from the GUB radiation. The latter is transformed by the process of inelastic scattering leading to deceleration of primary GUB particles. Thus, the observed ultra-high energy particles come from the ultra-high relativistic tail of the GUB as a result of the deceleration within the Observable Universe rather than the acceleration.

We predict that the observed CR ultra-high energy tail contains antimatter particles, since the Primary CRs must be matter-antimatter symmetric, and it must contain equal amount of protons and anti-protons as well as electrons and positrons, in the whole, constituting a neutral particle radiation. It must also contain the corresponding gamma rays of ultra-high energy.

Many researchers try to understand "the precision observations" of Cosmic Rays, in particular, the power form of energy spectra in parts of the whole observable range. They pay attention to a discrete character of sources in the intergalactic space [71]. From the viewpoint of the GU conception, the original Cosmic Rays come from the GU Background beyond Our Observable Universe. Their observable power spectrum can result due CR deceleration processes in the Observed Universe while the high energy "tail" of particles and radiation essentially come from the non-observable GU Background of a continuous source distributions. At a lower energy domains, the observations, indeed, are sensitive to individual sources distributed in the Observable Universe, and their influence must be studied.

The question arises about the role of the Causality Principle in the GU containing infinite numbers of TUs and their groups, clusters, and likely further, and how it affects relativistic properties of the primary GUB Cosmic Rays. One can speculate that the GU

Steady State is maintained under conditions of weakening casual connections between GU members so that a total casual disconnection eventually occurs.

A breakage of the Causality Principle on the largest GU scale leads to some consequences. Particles departed from some, say, TU-1, can travel most of the time in the GU background at a distance exceeding a scale of casual connection that is, the time exceeding a TU lifespan. The particle could reach some another TU-2 having a relative speed with respect to the TU-1 however high. A relative velocity dispersion has to grow with a travel distance. This is the idea of a statistical formation of the Lorentz invariant energy spectrum of Primary CR with ultra-high energy particles.

10.7 Randomness of GU world

In the GU Model, the treatment of observational data is fully consistent with the Fundamental Physical Principles and laws. That does not mean that all observational data should lay exactly on the theoretical curve. As seen, the GU world admit chaotic pictures because of randomness of many natural phenomena, such as the TU life during collisions with other UTs. Thus, a development of the Model in its parts and as a whole should be conducted in terms of Statistics of randomness in complex scenarios to be tested. The complexity is also caused by the hierarchy of matter clustering. The are no observations beyond Our Observed Universe.

Reconstructions of the GU images have to be made from an extremely limited sample of the OU time and space database. The are no observations beyond Our Observed Universe. That is why, predictions of GU pictures would have inevitable limitations of confidence level. This is not a deficiency of the Model but rather a reflection of reality of Nature.

Statistical treatments of observations are usually made by stochastic and numerical methods of trial and error within the Bayesian approach by the maximum likelihood criterion.

A physical explanation of the gravitational hierarchy of clustering, the origin of galaxies, in particular, is one of the fundamental problems unsolved in the SCM. Its explanation in the GU Model we relate to “clustering seeds” originated by fluctuations of densities due to ubiquitous matter-antimatter annihilation.

11 SR Dynamics methodology in Grand Universe Model

11.1 SR theory applications in OU and the GU Model

In the GU Model, the GR methodology of particle dynamics is replaced with SR Dynamics of motion at a high speed or in strong fields, or both. Under the weak field conditions and slow motion, it is reduced to the Newtonian Physics. Comparison of GR and SR methodologies is discussed in [2, 43, 48, 57] and references there. There are different physical phenomena in the GU Model, which require the methodology of SR Kinematics and Dynamics on both GU large and TU local scales. Below, some examples of SR theory applications in the GU Model are given.

- Treatment of locally observed phenomena related to strong fields there. It can be small and big gravitational attractors, such as neuron stars, on one side, and super-massive objects, on the other side. The important example is the so-called Black Holes, which can be super-massive stars (of a mass notably exceeding the Solar mass). Since GR Black Hole concept assumes the gravitational collapse,

we prefer using the term of super-massive compact object. It can be free in space or located in a center of galaxy. In vicinity of such objects, matter can reach a speed of motion comparable with the speed of light in vacuum. Dynamics of galaxies, especially, their central parts, should be considered relativistically.

- Clustering and variation of physical constants is better understood in the SR theory.
- The SR methodology is needed for physical treatments of galaxy dynamical properties and the corresponding observables, for example, redshifts.
- "Unusual phenomena" characterized by a huge release of different types of energy are, basically, effects subjected to SR Dynamics treatment.
- Generally, high-energy Physics of matter-antimatter interactions is a part of Relativistic Physics.

11.2 Concept of field dependent proper mass and physical units in SR Dynamics

The term "proper" for a mass, time, and other quantities is related, first of all, to physical quantities formulated *in the abstract proper 4-space* assuming that there is no physical "observations" outside the proper world line.[1] The connection of proper and coordinate systems is made by means of Lorentz transformations. It should be noted that the standard clock frequency f being an inverse quantity of the proper time interval $\Delta t = 1/f$, is the standard measure of "one second" so that the elapsed time is $t = n\Delta t$, where n is a number of clock ticks. In the SR theory, the standard proper frequency f is related to the standard proper mass $m \propto f$.

In the coordinate (observable) space-time, we consider the concept of proper mass dependence on the field strength a fundamental physical concept, which should be introduced in theories of fields for any type of forces the core of contemporary SR Dynamics theory. Remarkably, it leads to the elimination of central singularity [2, 13, 43, 72], and literature there. In the conventional SR Dynamics, the constant proper mass is used, what is actually justified when the effect is negligible in a weak field. For the history of this issue and the consequences of the approximation, also see [44].

In the spherically symmetric gravitational field, consider the test point particle of the proper mass m however small comparing to the central mass, $M \gg m$. Then, the proper mass dependence on a radius is given by

$$m(r) = m_0 \, \exp(-\rho_0/r) \, . \tag{62}$$

Then the *static* potential function $V(r)$ in the radial motion is

$$V(r) = -\left(1 - \exp(-r_g/r)\right) \, , \tag{63}$$

where the field strength parameter $\rho_0 = r_g/r$ is fixed in the initial conditions $r = r_0$; $r_g = GM/c_0^2$ is the radius of gravitational interaction, $m_0 = m(r)$ at the initial value

[1] Unfortunately, the term "proper" is used also in the SR Kinematics and Dynamics in the frames of "comoving observer", who identify her wristwatch standard frequency and the standard rod length to be compared with the corresponding improper quantities of another observer observed in a relative motion. Further, proper quantities ascribed to the proper coordinate system (world line observation) are distinct from those in the corresponding coordinate quantities in the observed space-time.

$r = r_0$. As $r_0 \to \infty$, the proper mass increases up to $m(r) = m_{inf}$, the value of a free particle "at infinity" that is, in "the physical vacuum" space. Conventionally, proper masses of particles are considered physical constants. However, in the SR Dynamics they are field dependent, therefore, physical unit of mass (the kilogram) at rest is field dependent: it depends on a radial position in the field created by a central mass. Notice, the above radial dependence of the proper mass cannot appear in the proper coordinate space-time.

The proper mass variation $m(r)$ immediately leads to the corresponding variation the physical unit of the standard clock rate $f = f(r)$ (the Hz) and the corresponding time unit, the proper period of a quantum oscillation $\Delta\tau(r)$ (the second). This is seen from the Einstein-de Broglie relationship

$$mc_0^2 = h\, f, \quad \Delta t = 1/f\,. \tag{64}$$

The length unit $d = c_0\, \Delta t$ (m) should be field dependent. Now, from the concept of spatial "infinity hierarchy", we come to the hierarchy of physical unit gauges. At this point, we restrain from discussions of a possible variation of fundamental physical constants such as the universal gravitational constant G, Plank constant h, and others.

11.3 Relativistic Doppler effect and the gravitational time dilation

Consider two inertial systems in a relative motion with the speed β so that the emitter of photon is in one of them and the observer's detector in the other. Both the emitter and the detector are tuned to the same proper frequency f_0. When the angle between the line of detector motion and the line of observer's sight is θ, the observed frequency f (the Doppler effect) is given by

$$f/f_0 = \gamma(1 - \beta\, \cos\theta)^{-1}\,, \tag{65}$$

where $\gamma = (1-\beta^2)^{-1/2}$ is the Lorentz factor. At $-\pi/2 > \theta > \pi/2$, the emitter and the detector are flying away from each other. At $\theta = \pi$, a maximal decrease of frequency (the red shift) is observed. Since the photon wavelength is $\lambda = c_0/f$, it corresponds to the increased λ. The relative wavelength effect is

$$z = \lambda/\lambda_0 - 1 = (\gamma(1-\beta))^{-1} - 1\,. \tag{66}$$

At a small speed, it is reduced to $\delta\lambda \approx \beta$. If the light is observed at $\theta = \pm\pi/2$, we have the transverse Doppler effect, which does not depend on the direction of motion [39]

$$f/f_0 = 1/\gamma\,. \tag{67}$$

The gravitational frequency shift is a static effect. It is associated with the gravitational time dilation in the time interval $\Delta t(r) = 1/f(r) = \Delta t_{inf}\exp(r_g/r)$. This is the consequence of the mass/frequency decreases with the depth of the gravitational potential (62):

$$f_(r) = f_{inf}\exp(-r_g/r) \tag{68}$$

with respect to the observer's frequency f_{inf} "at infinity" as $r \to \infty$. Here, the emitted photon has a frequency $f(r)$ of the atomic resonance line, say, of the atom on the surface of a central body, which creates a field. This frequency is conserved during a photon flight before it is absorbed. The gravitational frequency shift is the consequence of the proper mass field dependence, – the phenomenon neglected in the conventional SR theory [13].

For the photon wavelength $\lambda(r) = c_{int}/f(r)$, the corresponding relative effect is

$$z = \delta\lambda = \exp(r_g/r) - 1\,. \tag{69}$$

12 Treatment of observed astrophysical and cosmological phenomena

12.1 Black Holes

As discussed previously, the Astrophysical concept of the Black Hole phenomenon of a matter collapse into a singularity point is flawed from viewpoint of SR Dynamics. Besides, it has nothing to do with the Academic GR framework. Our arguments for the rejection of such a gravitational collapse is actually in agreement with the Birkhoff's Theorem admitting the matter-filled internal solution of the Schwarzschild metric, also with the non-singular solution originally obtained by Schwarzschild himself [8].

Undoubtedly, the physical phenomena similar to "Black Holes" do exist and are observed but with no evidence of a central singularity whatsoever. We shall call them Super-Massive Compact Objects (SMCO), which create a strong field environment around them. Such gravitational, seemingly looking "compact", attractors are typically located in centers of galaxies, but could be located otherwise. The SMCO concept follows from SR Dynamics of particles having field dependent proper masses [73]. There is no any singularities in SR Dynamics. From (62), the SMCO binding energy is characterized by the proper mass defect $\Delta m = m(r) - m_0$, which could be a large part of its proper mass at infinity.

Astronomers try to find some evidence of star orbits approaching the no-return point,– the Schwarzschild radius $r_{sch} = 2\,r_g$, which is the GR event horizon. As of today, astronomical instrumentation allows them to observe such conditions when a star should be "swallowed" by the Black Hole at the r_{sch} point. In SR Dynamics, the event horizon does not exist in principle. We must completely ignore the GR concept of "gravitational collapse into a central point", and forget about the the GR Schwarzschild radius concept. Instead, we should accept the existence of material spheres of any radius and the finite mass density.

Our BH problem formulation and the corresponding observation goals are very different from that in the SC Model. For example, consider the so-called G2 object, observations of which showed its passing to the MW central SMCO (Sgr A*), probably, as close as $R \approx 1 \times 10^{12}$ m (and maybe closer), seemingly, to be "swallowed", but it has survived [61]. Observations, which are treated in the GR framework, allow to somehow evaluate the mass of Sgr A* about $5 \times 10^6\ M_\odot$. However, its radius R, therefore, the mass density d, remain uncertain. In the SR framework, having the mass of Sgr A* reasonably varied, one can assess the range of its mass density and then to evaluate the best possible values of R and the closest point the star could reach. This is a real goal to prove the existence of "the material sphere" inside the Schwarzschild internal region. The positive result would immediately disprove the validity of the GR theory.

12.2 Neutron Stars

A typical Neutron Star seems to be a very compact, high density object having a mass of several $M_\odot$. In GR terms, it is not considered the Black Hole. In our methodology, the Neutron Stars and the SMCO objects have one common property: they all are characterized by finite size and finite density. There could be a difference, however. Densities of the SMCO objects can be very low, what follows from mass-density curves.

Recall, the gravitational radius r_g of a massive body M depends only on mass

$$r_g = \frac{G\,M}{c^2}\,. \tag{70}$$

On the other side, given M, we have the radius of material object R as a function of the mass density d

$$R = \left(\frac{3\,M}{4\,\pi\,d}\right)^{1/3}\,. \tag{71}$$

Among r_g, R, M, and d, any two parameters can be considered independent variables. We are interested in the mass-density functions. The mass-radius relationship in Neutron Stars is subject to multi-aspect studies [74, 75].

In our methodology, it is natural to admit the existence of the maximal universal ("nuclear") density d_{nuc}. Let it be fixed under the condition $r_g = R(d_{nuc}) = \tilde{R}$. The assumption imposes a strong constraint on the parameter variations. Indeed, it determines a unique object of minimal mass and size, we would like to call the Neutron Star. Moreover, the devision of masses into two clear categories follows: the condition of $M < \tilde{M}$ leads to $r_g < \tilde{R}$, and the condition of $r_g > \tilde{R}$ leads to $r_g > \tilde{R}$. Consequently, the condition of strong field $r_g > R$ is satisfied for all SMCOs of masses $M > \tilde{M}$ of low densities, in accordance to the relationship

$$\rho = r_g/R = \frac{G}{c^2}\left(\frac{4\,\pi\,d\,M^2}{3}\right)^{1/3}\,. \tag{72}$$

It is seen now that the term of "super-massive compact objects" is justified by the fact that they are "seen too small to be super-massive".

12.3 High redshifts

The "high redshift" phenomenon must be treated in terms of gravitational shift of atomic lines under the condition $\rho_0 = r_g/r > 1$, which all SMCOs satisfy. The redshift is defined in accord with the wavelength shift $z = \delta\lambda = \exp(r_g/R) - 1$ (69). The z values for typical SMCO rapidly grow with M. It should be noted, however, that the equation is obtained for statical conditions and a non-rotating object. Correct redshifts from sources in highly strong fields should be found from the SR Dynamics equations of matter motion in the vicinity of SMCO.

For decades, many famous Astronomers, such as Arp, Burbidge, and others, argued that some QSO with high redshifts are, actually, linked to close objects such as nearby galaxies of low redshifts [76–78]. They introduced the notion of "intrinsic redshift", unfortunately, they could not explain the physical nature of it. In the GU Model, the high redshifts depend on SMCO masses, so that objects of high redshifts *statistically* can be located closer than objects of lower redshifts or even be linked to them. Now, there is some understanding among Physical community that the Universe must have some disordered, which is actually observed but not widely recognized [79].

13 Physical properties of the Observed Universe

13.1 Milky Way before and after the collision

Our galaxy, the Milky Way, we live in, is a well studied part of Observed Universe. This is a type of spiral disc with a massive "Black Hole", – SMCO$_{mw}$, called Sgr A*, at the

center surrounded by a bulge [80–82]. There is no evidence of the Sgr A* gravitational collapse, physical reality of which is actually argued in literature, [73, 83]. In our methodology, the SMCO$_{mw}$ has a finite size, and a finite mass density.

Stars orbiting Sgr A* have been studied for a long time. It was assumed that the observed orbits are not close to the center, hence, can be described by Keplerian model (see discussions and references in [48]). There are more new information is expected from the continuous observations, including the G2 object, with progressing precision.

In the collision scenario, the age of the observed MW galaxy could be approximately assessed, provided the random statistics of the complex history taken into account. Likely, the Galaxy had existed in some mature form before the collision of the two TUs. It is reasonable to suggest that the original MW had been old enough and reached a state of maximal mechanical stability. Such a state requires optimal conditions of reconciling an extreme binding energy, on the one hand, and the extreme angular momentum, on the other hand. Then, a system of stars could rotate about the central attractor of a great mass and density, while the stars comprised a thick galaxy disc and had orbits characterized by minimal eccentricities with no bulges, no spiral arms.

The observed MW structure has been developing during the collision when the galaxy matter was significantly washed out by antimatter. What is survived is currently observed as the galaxy in a nearly decaying state. The Sgr A* has the mass appreciably less then the rest of the galaxy, because the original SMCO$_{mw}$ of much greater mass was destructed during the collision. The bulge formation, flares, and "strange phenomena" are examples of still observed annihilation.

Likely, the SMCO$_{mw}$ mass was about two orders greater than at present; the total mass of stars was greater as well. Originally, the MW was a strongly bounded system, but the collision dramatically changed it. Its binding energy significantly decreased while a great amount of matter lost. Spiral arms were formed in the weakest parts of the disc.

13.2 Space-time scaling of the receding galaxies in the Observed Universe

The Observed Universe has limits in space and time. Assume, arbitrarily, that we (the Observer) has stayed in the center of mass of the two colliding TUs, $r = 0$, in some MW space, which has a low matter density due to an intense matter annihilation. "Right now", at $t = 0$, we see a picture of galaxies at points in the whole range of radii r, from which the light may come back to us.

There is a principal relativistic limit of observable space-time due to a finite speed of light (the event horizon). There is also a practical today's limit $r = R$ of depth of observations due to space opacity and "fading" of light signal with r (the matter of observational technology). Let it be $R = 60$ light Gyr so that the light was emitted from galaxies there at at the time $t = -100$ Gyr. "The collision peak" might happened somehow earlier or later, while the colliding galaxies might have initial sizes, say, $20 - 30$ light Gyr across, so that the volume of "the collision peak" could be some sphere $R_{col} < R$.

We expect a slow motion (Newtonian Dynamics) picture of receding galaxies with various radial velocities, let it be mainly within the range $\beta < 0.1$. Hence, some survived galaxies from the both colliding TUs would have enough time to reach the maximal distance R. Clearly, such a slow motion will make small corrections to a

static picture, hence, should not significantly change our measurements of time-space scales.

The Observable Universe must look very much like a statical picture made by an instant snap. We detect light (photons) coming from galaxies located on spheres of radii in the range $r < R$. Measurements should give us a function $r(t)$ describing slow motion Kinetic of the receding galaxies. Very roughly, assuming the initial condition $t = 0$, $r = 0$, we have a simple expression for $r(t)$ in the range $r < R$

$$r = t \tag{73}$$

with the corresponding maximal time of photon flight $T = R$, $c = 1$.

From the above imaginary and simplified picture of galaxies in the suggested TU collision scenario, it is seen that direct measurements of space-time Kinematics of receding galaxies would reveal only a very small part of the collision history.

Having this said, we did not yet specify the methods of measurements of real function $r(t)$. In practice, one needs to determine directly observable physical variables of the model, such as velocities β, luminosities L, redshifts z, and others, in their interplay in the GU Model based on the SR theory and its Newtonian limit.

Besides, one needs to account for randomness of observable events. Due to randomness of the collision process, there cannot be strict correlation of r, t, L, z, β. Ideally, one would want to independently parametrize every single observed galaxy to unfold GU physical images from the GU predicted physical images.

At the same time, there must be a tendency of order, as noted before. For example, the galaxies, which had a greater chance to escape, might fly farther away being less damaged. Originally, they were more massive and more compact objects, than we observe. Still, they are local sources of strong field. Consequently, their light must be observed from longest distances and greatly red-shifted, up to maximal values of z.

13.3 Anti-matter in Milky Way

This issues is previously discussed in the context of observed "unusual" flares and releases of huge amount of energy in Milky Way and distance galaxies, as well as in intergalactic space. We relate such natural phenomena with matter antimatter annihilation, which could be realized in different forms provided the antimatter material objects are present and involved. For example, collision of pair of matter and antimatter stars, a matter star and antimatter debris and dust clouds, and vice versa, the same could be true with antimatter neutron stars, and, at the next level, antimatter SMCOs (Black Holes). Reports on observations and study of such events grow fast. Not surprisingly, this happens all the time in the Sgr A* area. A typical example is the QSO objects. In the largest scale, we explain the large matter structure of the Observed Universe by matter being burnt out during the collision.

We state that the annihilation phenomena must be observed and, likely, have been so numerous time, in the Earth's atmosphere, for example, due to the presence of antimatter-made asteroids, meteors, meteorites, and debris. It is still hard to assess the relative amount of antimatter in the Observed Universe; however, there is much more of it than previously thought.

13.4 Dark Matter issue

The history and all aspects of contemporary status of Dark Matter is most thoroughly presented in the book [84] by Peebles, 1993. Since then, numerous works devoted

to explanations of their physical nature appeared in press with more questions than answers. The Dark Matter, similarly to the Dark Energy, is a name for phenomenon, existence of which is suspected but never confirmed by direct observations. Moreover, suspicions became beliefs that it is real but remains a legend beyond the apprehension of people doing science.

Professor Peebles, among numerous arguments supporting the Dark Matter legend, put the straightforward question whether Newton's Physics of gravity failed in explanation of rotational structure of galaxies, which were suspected in being affected by mysterious Dark Matter, or contrarily, Newton's Physics was right but incorrectly applied and mistreated in making conclusion. Sadly, he inclined to blame Newton's Physics for failure and open the door to searching for alternative explanations, which were many and taken blindly. As of today, nothing changed after Peebles verdict.

In the first place, the existence of the gravitating invisible matter was suspected due "flat rotation curves" measured by the Doppler effect technique from observations of stars' orbital velocities. Long before Peebles, workers argued that the observed rotational curve cannot be explained by Newtonian (Keplerian) model of orbits. The "Dark Matter halo" is needed to explain the observed picture of the Milky Way and other spiral galaxies. They did not care that the Keplerian model is valid only for non-interacting stars of small masses, what is not true in the galaxy case. The correct description requires a model, in which a huge number of interacting stars creating collective gravitational field numerical calculations. Some authors showed that the flat rotational curve can be explained in a simplified approximate model with some additional assumptions about the galaxy physical structure, [85–87].

"To explain" the Dark Matter, many models of modified Newtonian Gravity are proposed, among them, versions of Milgromian MOND [88, 89]. The latter fits many particular galactic observations under special assumptions but not all of them. Yet, it is abstracted from many related issues with promises to develop in future "the full MOND theory". Overall, it is in conflict with Fundamental of Physics, and it actually rejects the tenets of the SC Model including its GR methodology in exchange of removal the Dark Matter concept.

Regardless of problem with galaxies, the Dark Matter along with the Dark Energy is needed in the SC Model, first of all, to reconcile numerous contradictions in the GR concept of metric space expansion in a description of the whole Universe history and the CMB concept of relic radiation.

Our "collision scenario" brings final clarity to the problem. First of all, it explains a great variety of galaxy types resulting in the annihilation process. In particular, spiral galaxies and their central cores became depleted to the extent of bounding energy loss and formation of flat rotation curve. It happens when the radial density approaches the $1/r^2$ law. It causes spiral disruption and leave the galaxy in the hyperbolic motion. Those galaxies are slowly decaying in the process of decay of the galaxy. The Milky Way is the example.

13.5 Clustering and galaxy evolution in the GU Model

The GU collision scenario suggests that, in any mature TU before collision happened, galaxies must be dynamically much more stable that is, more bounded and have a higher angular momentum, compared to what we see in the MW. In other words, in a physically "normal" (typical) Universe, the concept of gravitational clustering at the galaxy level should depict pictures essentially different from what we observe and study in the SC Model. Central attractors in galaxies must have a greater mass and

a mass density, the galaxies must be more compact and heavy, their stars must strongly interact with each other, and for this reason, the galaxies must not have spirals. Each galaxy has its own lifetime evolution, generally, from the "embryonic" state to the age of maturity till collision catastrophe. The destroyed galaxies are replaced with newly born ones originated from remnants. This picture gives a clue for the solution of the galaxy origin problem. Also, it makes the GU as a whole self-sustained and recreating.

The question arises, though, how the hierarchy of clustering, including the galaxy formation, is theoretically explained. In our view, the cluster hierarchy exists due to *gravitation* in combination with a low scale matter non-uniformity. The latter is produced under conditions of presence of antimatter (matter) in a galaxy made of matter (antimatter). In other words, the matter-antimatter asymmetry at some low level must be a natural property of galaxies. During an annihilation in a collision, matter-antimatter tends to statistically separate rather than being completely destroyed. This makes the continuous process of annihilation and particle pair creation in a perfect balance in the largest GU scale. To confirm this picture, one needs to mathematically simulate the GU Model using the whole arsenal of Fundamental Physics and Applied Mathematics.

14 Concluding Remarks

In our quest for comprehension of physical world at a new level, we respect the succession of Physical knowledge, and hope that methodological novelties of the proposed GU Model will shed light on relationship of Cosmological Science with Fundamentals of Classical Physics as well as Modern Physics branches. In brief, we claim:

- The GU Cosmological Model is radically different from other models. It has an explanatory and predicting power owing to its conceptual methodology based on Newtonian Physics and contemporary SR Dynamics. The Model gives a physical explanation of "expansion" of the Observable Universe and its "Beginning".
- The GU Model is constructive since questions are formulated in the form revealing the roots of certain unsolved problems in Cosmology; it gives clues for their resolutions.
- The GU Model is enlightening since physical issues are raised in greater generality to the extent, where validity of Fundamental Physics Principles become questionable. It opens a new room for deeper exploration and comprehension of the harmonious Physical Nature.

Good conceptual ideas having a common sense are rarely completely new. Working on our proposal of the Alternative Cosmology, we have recognized them, one after one, in old alternative models, listed below. The wonderful thing is that those ideas are harmoniously reconciled in the GU Model, which is drastically different from any of old ones:

- matter-antimatter symmetry (the Plasma Universe)
- "The Beginning" with the following "space expansion" (Lemaître's primeval atom, and the Big Bang)
- continuous matter recreation (the Steady State Cosmology, and string collisions in "Brane world")

- Multiple Universes in different cosmological versions.

The proposed Alternative outlines the new cosmological framework for further numerical studies required for any new physical model or a theory. It is a source of different perspective project proposals. A complete reinterpretation of space-time scales is needed on a basis of the observational database and the corresponding concepts of observables. Yet, one can try to unfold, beyond observations, the likely statistical pictures of GU past and future, particularly, with the use of known methods of numerical simulation. A special practically important project must be devoted to the presence of antimatter in the Observed Universe, and yet more.

We hope to find many interested supporters and critics of the Alternative among scientists involved in Cosmological and Modern Physics researches, first of all, Astronomers and Astrophysicists as well as Physicists, Mathematicians, and Philosophers.

15 Final conclusion

In this work, we combined interconnected problems revealing a true picture of General Relativity as a whole and its scientific application to Astronomy, Astrophysics, and Cosmology. This is the main part of Modern Physics praised in literature and mass media for its tremendous successes in understanding the Nature and practical technological applications such as Global Positioning System. Though they are selected from a huge list of problems, they are sufficient for showing in one paper pseudo-physical and anti-scientific essence of General Relativity and Big Bang Cosmology. Scientists listening to their common sense know that something is very wrong with Modern Physics. We tried to show what and why is wrong, actually, without discussing the GR foundations, - Einstein's field equations, which have never been mathematically and physically solvable. We did not discussed Big Bang Planck's 10^{-43} sec. stage nonsense and many others absurdities. Instead, we suggest Alternatives having common sense for us and all scientists, who consciously avoided 'main stream brainwashing and chaos. Any messages from them are welcome.

References

[1] Albert Einstein. Erklrung der Perihelbewegung des Merkur aus der allgemeinen Relativittstheorie. Sitzungsberichte der Kniglich Preussischen Akademie der Wissenschaften zu Berlin, 1915. See also The Collected Papers of Albert Einstein. vol. 6, Princeton University Press, (1996).

[2] Anatoli Vankov. General Relativity Problem of Mercury's Perihelion Advance Revisited. arXiv:1008.1811 [physics.gen-ph], 2010.

[3] Kirill Vankov. The Problem of Particle Motion in the Schwarzschild Field: Critical Methodological Analysis, Exact Numerical Solution, and the Alternative. *The General Science Journal*, 2016.

[4] Kirill Vankov. General Relativity Mercurys Anomaly Prediction: What and How to Test? *The General Science Journal*, 2016.

[5] Yusuke Hagihara. Theory of the relativistic trajectories in a gravitational field of Schwarzschild. *Annales de l'Observatoire astronomique de Tokyo*, 31:67176, 1931.

[6] Subrahmanyan Chandrasekhar. *The mathematical theory of black holes*, volume 69 of *International Series of Monographs on Physics*. Clarendon Press/Oxford University Press, New York/Oxford, 1983.

[7] Georgios Kraniotis and Steve Whitehouse. Compact calculation of the perihelion precession of Mercury in general relativity, the cosmological constant and Jacobi's inversion problem. *Classical and Quantum Gravity*, 20(22):4817, 2003.

[8] Karl Schwarzschild. On the Gravitational Field of a Mass Point According to Einstein's Theory. *General Relativity and Gravitation*, 35(5):951959, 2003. ber das Gravitationsfeld eines Massenpunktes nach der Einsteinschen Theorie. Sitzungsberichte der Kniglich Preussischen Akademie der Wissenschaften zu Berlin, Phys.-Math. Klasse 1916, 189196.

[9] Peter Gabriel Bergmann. *Introduction to the Theory of Relativity*. Kessinger Publishing, 2008.

[10] Vladimir Fock. *The Theory of Space, Time and Gravitation*. Pergamon, 1959.

[11] Anatoli Vankov. Explanation of the Perihelion Motion of Mercury from General Relativity Theory. *The General Science Journal*, 2014.

[12] John Lighton Synge. *Relativity: the General theory*. North Holland Publishing Company, Amsterdam, 1964.

[13] John Lighton Synge. *Relativity: the special theory*. North Holland Publishing Company, Amsterdam, 1965.

[14] Lev Davidovich Landau and Evgenii Mikhailovich Lifshitz. *The classical theory of fields*. Pergamon Press, Oxford, 1971.

[15] Yvonne Choquet-Bruhat. *General relativity and the Einstein equations*. Oxford University Press, 2009.

[16] Edmund Taylor Whittaker and George Neville Watson. *A Course of Modern Analysis*. Cambridge University Press, 1927.

[17] Richard Courant and Adolf Hurwitz. *Funktionentheorie*. Verlag von Julius Springer, Berlin, 1929.

[18] Claus Lmmerzahl. Testing Basic Laws of GravitationAre Our Postulates on Dynamics and Gravitation Supported by Experimental Evidence? In *Mass and Motion in General Relativity*, page 2565. Springer, 2011.

[19] Henri Cohen. *A course in computational algebraic number theory*, volume 138 of *Graduate Texts in Mathematics*. Springer, 1993.

[20] John Cremona. *Algorithms for modular elliptic curves*. Cambridge University Press, 1997.

[21] Jean-Benot Bost and Jean-Franois Mestre. Moyenne arithmtico-gomtrique et priodes des courbes de genre 1 et 2. *Gaz. Math*, 38:3664, 1988.

[22] John Cremona and Thotsaphon Thongjunthug. The complex AGM, periods of elliptic curves over C and complex elliptic logarithms. *Journal of Number Theory*, 133(8):28132841, 2013.

[23] W. A. Stein et al. *Sage Mathematics Software (Version 6.4)*. The Sage Development Team, 2014. http://www.sagemath.org.

[24] The PARI Group. *PARI/GP version 2.7.1*. Bordeaux, 2014. available from http://pari.math.u-bordeaux.fr/.

[25] Emmy Noether. Invariante Variationsprobleme. *Nachr. D. Knig. Gesellsch. D. Wiss. Zu Gttingen, Math-phys. Klasse*, (2):235257, 1918.

[26] Christian Mller. *The theory of relativity*. Clarendon Press, Oxford, 1972.

[27] Steven Weinberg. *Gravitation and cosmology: principles and applications of the general theory of relativity*. Wiley New York, 1972.

[28] Paul Gerber. The spatial and temporal propagation of gravity. *Zeits.f.Math.u.Phys*, 43:93–104, 1898.

[29] K.A. Olive and Particle Data Group. Review of Particle Physics. *Chinese Physics C*, 38(9):090001, 2014.

[30] U.S.NAVY. The Astronomical Almanac. Constants., 2017. Avaialable at http://asa.usno.navy.mil/SecK/Constants.html.

[31] NASA. Lunar and planetary science. Mercury fact sheet., 2016. See http://nssdc.gsfc.nasa.gov/planetary/factsheet/mercuryfact.html, accessed on 2017-08-03.

[32] Peter Gabriel Bergmann. *Introduction to the Theory of Relativity*. Prentice-Hall, Inc, Englewood Cliffs, New Jersey, 1942.

[33] Charles W. Misner, Kip S. Thorne, and John Archibald Wheeler. *Gravitation*. W. H. Freeman and Co, San Francisco, 1973.

[34] Robert Wald. *General Relativity*. University of Chicago Press, 1984.

[35] Wolfgang Rindler. *Relativity: special, general, and cosmological*. Oxford University Press, 2006.

[36] Anna M Nobili and Clifford M Will. The real value of Mercury's perihelion advance. *Nature*, 320:3941, 1986.

[37] Edwin F Taylor, John Archibald Wheeler, and Edmund William Bertschinger. *Exploring Black Holes: Introduction to General Relativity, Second Edition*. The Internet Archive, 2018.

[38] Neil Ashby. Relativity and the global positioning system. *Physics Today*, 55(5):4147, 2002.

[39] Anatoli Vankov. Mass, Time, and Clock (Twin) Paradox in Relativity Theory. arXiv:physics/0603168 [physics.class-ph], 2006.

[40] JGV Soldner. On the deflection of a light ray from its rectilinear motion, by the attraction of a celestial body at which it nearly passes by. *Berliner Astronomisches Jahrbuch*, 161, 1804.

[41] Edwin F Taylor, John Archibald Wheeler, and Edmund William Bertschinger. *Exploring Black Holes: Introduction to General Relativity*. Addison-Wesley, 2010.

[42] S. I. Blinnikov, L. B. Okun, and M. I. Vysotskii. Critical velocities $c/\sqrt{3}$ and $c/\sqrt{2}$ in the general theory of relativity. *Physics-Uspekhi*, 46(10):10991103, 2003.

[43] Anatoli Vankov. On Relativistic Generalization of Gravitational Force. *Foundations of Physics*, 38(6):523545, 2008.

[44] Netsivi Ben-Amots. A new line element derived from the variable rest mass in gravitational field. arXiv:0808.2609 [physics.gen-ph], 2008.

[45] Anatoli Vankov. Different Look at Relativistic Gravity and Related Phenomena. In Valeriy Dvoeglazov, editor, *Relativity, Gravitation, and Cosmology: New Developments*, Contemporary Fundamental Physics, page 167194. Nova Science Publishers, 2010.

[46] George Ellis and Joe Silk. Scientific method: Defend the integrity of physics. *Nature*, 516(7531):321323, 2014.

[47] Martn Lpez-Corredoira. Tests and Problems of the Standard Model in Cosmology. *Foundations of Physics*, 47(6):711768, Jun 2017.

[48] Kirill Vankov. Physics Tomorrow: New Cosmology and Gravitation in Modern Physics. hal-01399327, Nov 2016.

[49] Kirill Vankov. Particle Orbits in General Relativity: from Planetary Solar System to Black Hole Environment. hal-01571766, Aug 2017.

[50] Jayant V Narlikar. The evolution of modern cosmology as seen through a personal walk across six decades. *The European Physical Journal H*, 43(1):4372, 2018.

[51] Jayant V Narlikar and Geoffrey Burbidge. *Facts and speculations in cosmology*. Cambridge University Press, 2008.

[52] Cormac O'Raifeartaigh, Michael O'Keeffe, Werner Nahm, and Simon Mitton. One hundred years of the cosmological constant: from superfluous stunt to dark energy. *The European Physical Journal H*, 43(1):73117, 2018.

[53] Fred Hoyle, Geoffrey Burbidge, and Jayant Vishnu Narlikar. *A different approach to cosmology: from a static universe through the big bang towards reality*. Cambridge University Press, 2000.

[54] Jian Liang Yang. Criticism to Universal Big Bang. *Journal of Astrophysics & Aerospace Technology*, 4(1):15, 2016.

[55] Nikodem J. Popawski. Matter-antimatter asymmetry and dark matter from torsion. *Phys. Rev. D*, 83:084033, Apr 2011.

[56] Martin Rees. *Cosmology and the multiverse*, page 5776. Cambridge University Press, 2007.

[57] Kirill Vankov. Physics Tomorrow: The Proposal of New Cosmology, the Grand Universe Model. hal-01567117, Jul 2017.

[58] Anatoli Vankov. On matter-antimatter separation in open relativistic material system. arXiv:astro-ph/9906279, 1999.

[59] Borge Nodland and John P Ralston. Indication of anisotropy in electromagnetic propagation over cosmological distances. *Physical Review Letters*, 78(16):3043, 1997.

[60] Ratbay Myrzakulov. *The Universe Rotation: Pro and Contra*. Nova Science Publishers, 2017.

[61] Gunther Witzel, Andrea M Ghez, Mark R Morris, Breann N Sitarski, Anna Boehle, Smadar Naoz, Randall Campbell, Eric E Becklin, Gabriela Canalizo, Samantha Chappell, et al. Detection of Galactic Center source G2 at 3.8 μm during periapse passage. *The Astrophysical Journal Letters*, 796(1):L8, 2014.

[62] MA Nowak, J Neilsen, SB Markoff, FK Baganoff, D Porquet, N Grosso, Yuri Levin, J Houck, A Eckart, H Falcke, et al. Chandra/HETGS observations of the brightest flare seen from Sgr A*. *The Astrophysical Journal*, 759(2):95, 2012.

[63] Masayoshi Nobukawa, Syukyo G Ryu, Takeshi Go Tsuru, and Katsuji Koyama. New Evidence for High Activity of the Supermassive Black Hole in our Galaxy. *The Astrophysical Journal Letters*, 739(2):L52, 2011.

[64] G Ponti, B De Marco, MR Morris, A Merloni, T Muoz-Darias, M Clavel, D Haggard, S Zhang, K Nandra, S Gillessen, et al. Fifteen years of XMMNewton and Chandra monitoring of Sgr A*: evidence for a recent increase in the bright flaring rate. *Monthly Notices of the Royal Astronomical Society*, 454(2):15251544, 2015.

[65] Jimmy A Irwin, W Peter Maksym, Gregory R Sivakoff, Aaron J Romanowsky, Dacheng Lin, Tyler Speegle, Ian Prado, David Mildebrath, Jay Strader, Jifeng Liu, et al. Ultraluminous X-ray bursts in two ultracompact companions to nearby elliptical galaxies. *Nature*, 538(7625):356358, 2016.

[66] G. Dubus and B. Cerutti. What caused the GeV flare of PSR B1259-63? *Astronomy & Astrophysics*, 557:A127, 2013.

[67] Benoit Cerutti, Gregory R Werner, Dmitri A Uzdensky, and Mitchell C Begelman. Gamma-ray flares in the Crab Nebula: A case of relativistic reconnection? *Physics of Plasmas*, 21(5):056501, 2014.

[68] Elena Borisova, Sebastiano Cantalupo, Simon J. Lilly, Raffaella A. Marino, Sofia G. Gallego, Roland Bacon, Jeremy Blaizot, Nicolas Bouch, Jarle Brinchmann, C. Marcella Carollo, Joseph Caruana, Hayley Finley, Edmund C. Herenz, Johan Richard, Joop Schaye, Lorrie A. Straka, Monica L. Turner, Tanya Urrutia, Anne Verhamme, and Lutz Wisotzki. Ubiquitous Giant Lyα Nebulae around the Brightest Quasars at $z \sim 3.5$ Revealed with MUSE. *The Astrophysical Journal*, 831(1):39, 2016.

[69] Maurizio Spurio. *Particles and Astrophysics*. Springer, 2015.

[70] A.A Watson. Chasing the highest energy cosmic rays: From 1948 to the present. *Astroparticle Physics*, 53:107114, 2014. Centenary of cosmic ray discovery.

[71] Genolini, Y., Salati, P., Serpico, P. D., and Taillet, R. Stable laws and cosmic ray physics. *Astronomy and Astrophysics*, 600:A68, 2017.

[72] Anatoli Vankov. On Problem of Mass Origin and Self-Energy Divergence in Relativistic Mechanics and Gravitational Physics. arXiv:gr-qc/0311063, 2003.

[73] Kirill Vankov. Black Holes in Einstein's General Relativity versus Modern Theoretical Astrophysics, and Observations. hal-01150644, Mar 2015. Essay written for the Gravity Research Foundation 2015 Awards for Essays on Gravitation.

[74] Andrew W Steiner, James M Lattimer, and Edward F Brown. The neutron star mass-radius relation and the equation of state of dense matter. *The Astrophysical Journal Letters*, 765(1):L5, 2013.

[75] Feryal zel, Dimitrios Psaltis, Tolga Gver, Gordon Baym, Craig Heinke, and Sebastien Guillot. The dense matter equation of state from neutron star radius and mass measurements. *The Astrophysical Journal*, 820(1):28, 2016.

[76] Halton C Arp. *Quasars, redshifts and controversies*. Cambridge University Press, 1988.

[77] Pasquale Galianni, E. M. Burbidge, H. Arp, V. Junkkarinen, G. Burbidge, and Stefano Zibetti. The discovery of a high-redshift X-ray-emitting QSO very close to the nucleus of NGC 7319. *The Astrophysical Journal*, 620(1):88, 2005.

[78] Martn Lpez-Corredoira. Pending Problems in QSOs. *International Journal of Astronomy and Astrophysics*, 1(2):7382, 2011.

[79] W. M. Stuckey, Timothy McDevitt, A. K. Sten, and Michael Silberstein. End of a dark age? *International Journal of Modern Physics D*, 25(12):1644004, 2016.

[80] Ortwin Gerhard. Structure and Mass Distribution of the Milky Way Bulge and Disk. In Jos G. Funes and Enrico Maria Corsini, editors, *Galaxy Disks and Disk Galaxies*, volume 230 of *ASP Conference Series*, page 2130, 2001.

[81] Richard B. Larson. Galaxy Formation and Evolution. In G. Tenorio-Tagle, M. Prieto, and F. Sanchez, editors, *Star Formation in Stellar Systems*, page 125. Cambridge University Press, 1992.

[82] Hans-Walter Rix and Jo Bovy. The Milky Ways stellar disk. *The Astronomy and Astrophysics Review*, 21(1):158, 2013.

[83] Stephen William Hawking. Information Preservation and Weather Forecasting for Black Holes. arXiv:1401.5761 [hep-th], 2014.

[84] Phillip James Edwin Peebles. *Principles of physical cosmology*. Princeton University Press, 1993.

[85] Niall Ryan. Galactic Disc Rotation: Analytic models and asymptotic results. arXiv:1301.5233 [astro-ph.GA], 2013.

[86] Jonathan Davies. A Heavy Baryonic Galactic Disc. arXiv:1204.4649 [astro-ph.GA], 2012.

[87] X. X. Xue, H. W. Rix, G. Zhao, P. Re Fiorentin, T. Naab, M. Steinmetz, F. C. Van den Bosch, T. C. Beers, Y. S. Lee, E. F. Bell, et al. The Milky Ways Circular Velocity Curve to 60 kpc and an Estimate of the Dark Matter Halo Mass from the Kinematics of ∼2400 SDSS Blue Horizontal-Branch Stars. *The Astrophysical Journal*, 684(2):1143, 2008.

[88] Mordehai Milgrom. Road to MOND: A novel perspective. *Phys. Rev. D*, 92(4):044014, 2015.

[89] Benot Famaey and Stacy S. McGaugh. Modified Newtonian Dynamics (MOND): Observational Phenomenology and Relativistic Extensions. *Living Reviews in Relativity*, 15:10, 2012.

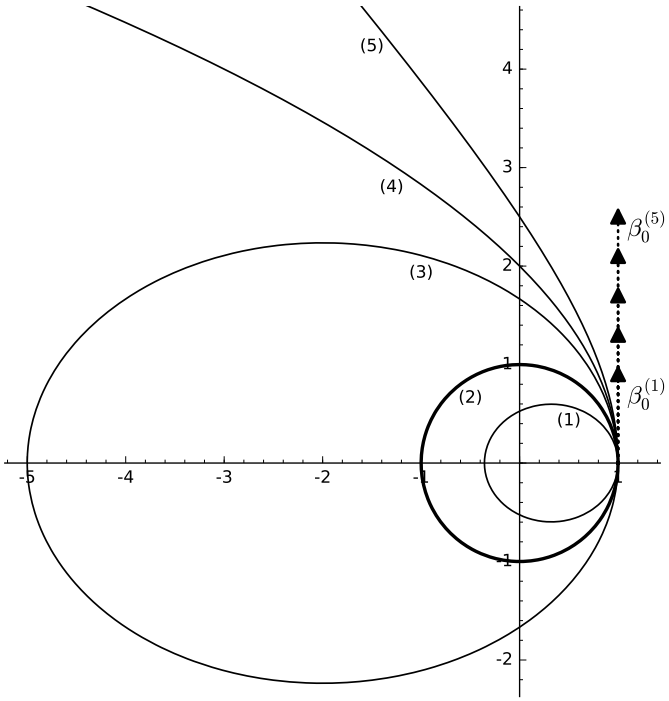

Figure 1: Classical orbits plotted in $(x,\ y)$ plane, $r = \sqrt{x^2 + y^2}$. Illustration of the σ family of orbits: (1) Sub-circle ellipse, $\sigma = 1.9$; (2) Circle, $\sigma = 1$; (3) Over-circle ellipse, $\sigma = 0.6$; (4) Parabola, $\sigma = 0.5$; (5) Hyperbola, $\sigma = 0.4$. The gravity center is placed at the coordinate origin, which is at rest with respect to the far-away stars (an inertial coordinate system). All orbits are produced by launching a test particle at the point $x_0 = 1$ with different initial speed $\beta_0 = \sqrt{r_g/\sigma}$, the arrow shows the geometry without value specification. The meaning of terms "subcircle" and "overcircle" follows from the the orbit classification, and is illustrated in the picture, see the text.

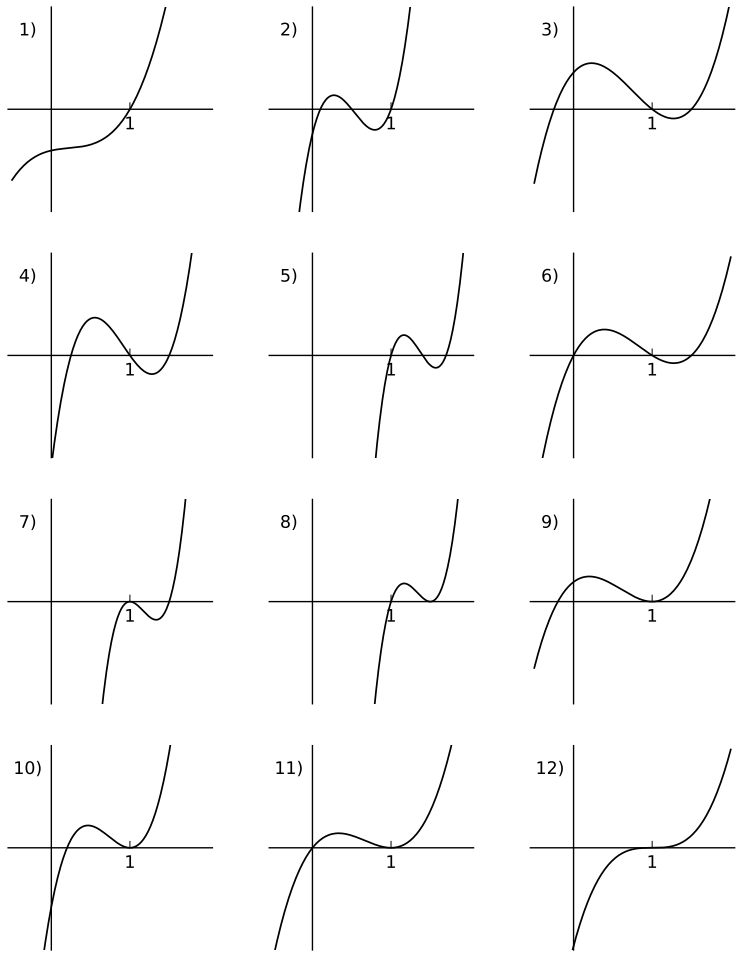

Figure 2: All possible roots of a cubic r.h.s. of (13):
1) complex ξ_2, ξ_3 roots; 2) $\xi_3 \leqslant \xi_2 < 1$; 3) $\xi_2 < 0, \xi_3 > 1$;
4) $0 < \xi_2 < 1, \xi_3 > 1$; 5) $1 < \xi_2 < \xi_3$; 6) $\xi_2 = 0, \xi_3 > 1$;
7) $\xi_2 = 1, \xi_3 > 1$; 8) $1 < \xi_2 = \xi_3$; 9) $\xi_2 < 0, \xi_3 = 1$;
10) $0 < \xi_2 < 1, \xi_3 = 1$; 11) $\xi_2 = 0, \xi_3 = 1$; 12) $\xi_2 = 1, \xi_3 = 1$.

Table 1: GR orbit classification: SF – spiral fall, H – hyperbola, P – parabola, C – circle, OC – over-circle, SC – sub-circle.

condition on ξ_2, ξ_3	relation between β_0^2 and ρ_0	orbit type	Figure 2 ref.
ξ_2, ξ_3 not real or $\xi_3 < 1$	$\rho_0 < \frac{1}{6}\,, \quad \beta_0^2 < \frac{16\,\rho_0^2}{1+4\,\rho_0-12\,\rho_0^2}$ or $\frac{1}{6} < \rho_0 < \frac{1}{3}\,, \quad \beta_0^2 < \frac{\rho_0}{1-3\rho_0}$ or $\rho_0 \geqslant \frac{1}{3}$	SF	1), 2)
$\xi_2 < 0,\ \xi_3 > 1$	$\rho_0 \leqslant \frac{1}{4}\,, \quad \beta_0^2 > \frac{2\rho_0}{1-2\rho_0}$ or $\frac{1}{4} < \rho_0 < \frac{1}{3}\,, \quad \beta_0^2 > \frac{\rho_0}{1-3\rho_0}$	H	3)
$\xi_2 < 1 < \xi_3$	$\rho_0 < \frac{1}{4}\,, \quad \frac{\rho_0}{1-3\,\rho_0} < \beta_0^2 < \frac{2\rho_0}{1-2\rho_0}$	OC	4)
$1 < \xi_2 < \xi_3$	$\rho_0 < \frac{1}{6}\,, \quad \frac{16\,\rho_0^2}{1+4\,\rho_0-12\,\rho_0^2} < \beta_0^2 < \frac{\rho_0}{1-3\rho_0}$	SC	5)
$\xi_2 = 0,\ \xi_3 > 1$	$\rho_0 < \frac{1}{4}\,, \quad \frac{2\rho_0}{1-2\rho_0}$	P	6)
$\xi_2 = 1,\ \xi_3 > 1$	$\rho_0 < \frac{1}{6}\,, \quad \beta_0^2 = \frac{\rho_0}{1-3\,\rho_0}$	C	7)
$1 < \xi_2 = \xi_3$	$\rho_0 < \frac{1}{6}\,, \quad \beta_0^2 = \frac{16\,\rho_0^2}{1+4\,\rho_0-12\,\rho_0^2}$	SC, SF	8)
$\xi_2 < 0,\ \xi_3 = 1$	$\frac{1}{4} < \rho_0 < \frac{1}{3}\,, \quad \beta_0^2 = \frac{\rho_0}{1-3\,\rho_0}$	H, C, SF	9)
$0 < \xi_2 < 1 = \xi_3$	$\frac{1}{6} < \rho_0 < \frac{1}{4}\,, \quad \beta_0^2 = \frac{\rho_0}{1-3\,\rho_0}$	OC, C, SF	10)
$\xi_2 = 0,\ \xi_3 = 1$	$\rho_0 = \frac{1}{4}\,, \quad \beta_0^2 = 1$	P, C, SF	11)
$\xi_2 = \xi_3 = 1$	$\rho_0 = \frac{1}{6}\,, \quad \beta_0^2 = \frac{1}{3}$	C, SF	12)

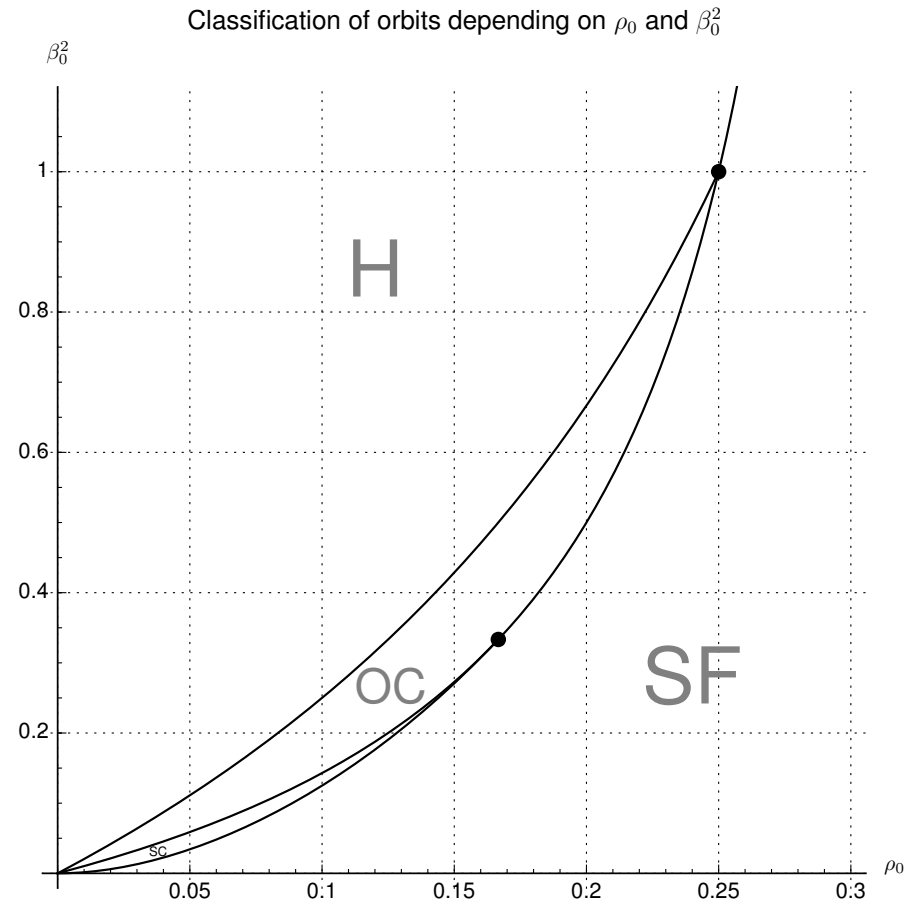

Figure 3: GR orbit classification on (ρ_0,β_0^2) plane: H – hyperbolic type; OC – over-circular type; SC – sub-circular type; SF – spiral fall type; parabolic type – line next to H; circular orbits – middle curve from 0 till $\rho_0 = 1/6$ continuing to $\rho_0 = 1/4$.

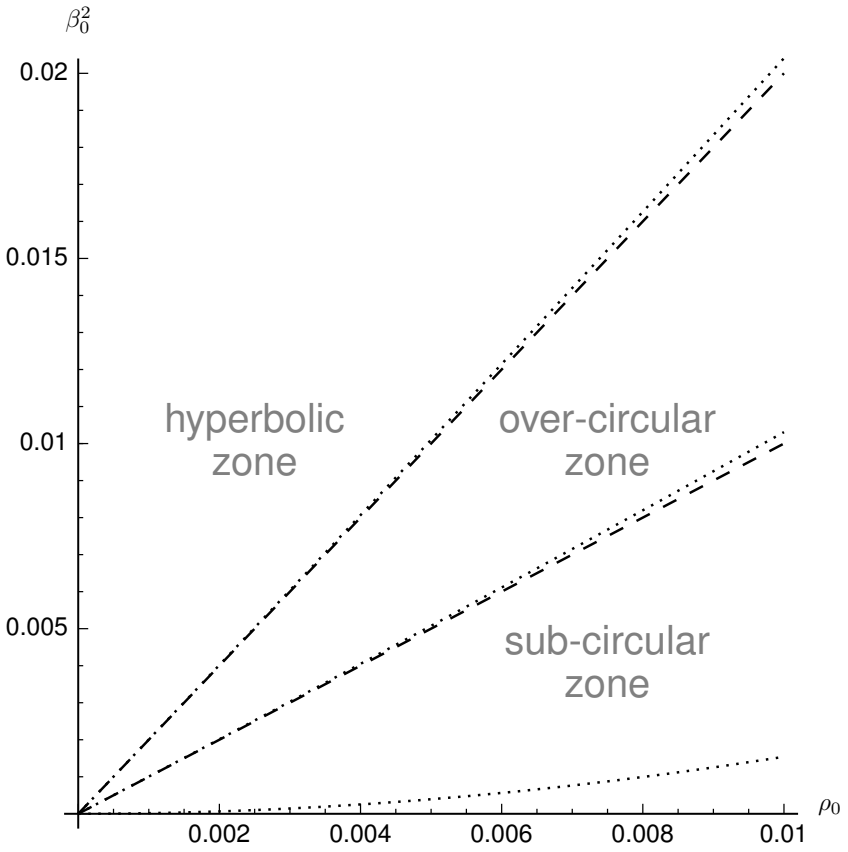

Figure 4: Orbit classification in classical mechanics (dashed lines): the top region corresponds to hyperbolic orbits, the top dashed line – parabolic orbits, in between the dashed lines – over-circular orbits, the bottom dashed line – circular orbits, below – sub-circular orbits. In GR theory (dotted curves) there is an additional (at the very bottom, below the dotted line) region with spiral-fall type of orbits. When ρ_0 and β_0^2 are small, the orbit classification in classical mechanics becomes similar to that in GR.

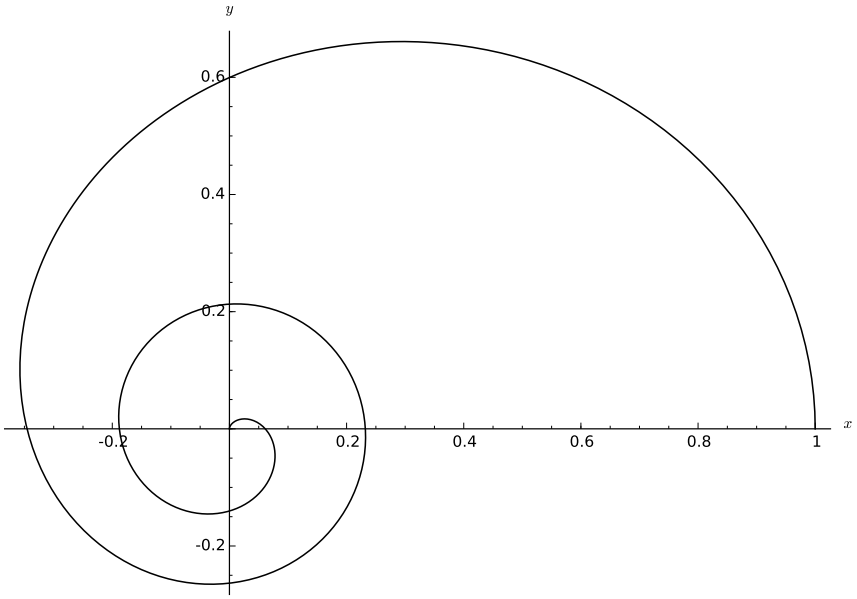

Figure 5: Spiral fall trajectory for $\rho_0 = 0.05$, $\beta_0^2 = 0.03$. Shown only half period.

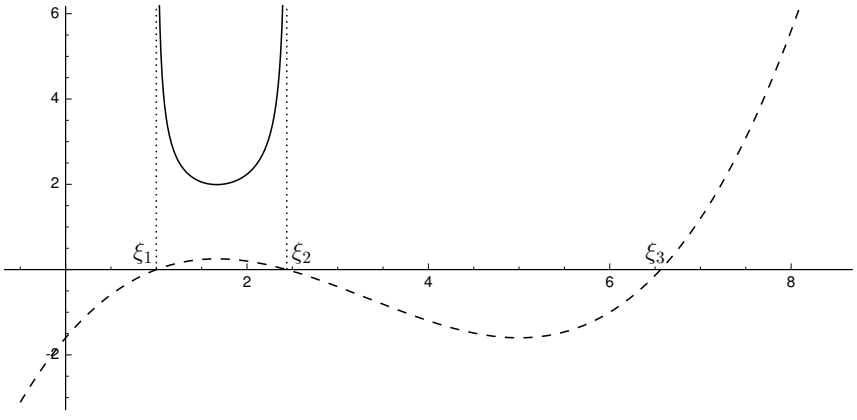

Figure 6: Typical case of polynomial $f(\xi)$ with three roots (here $\rho_0 = 0.05$, $\beta_0 = 0.04$, the dashed line). The integration is performed from $\xi_1 = 1$ to ξ_2 under the solid line.

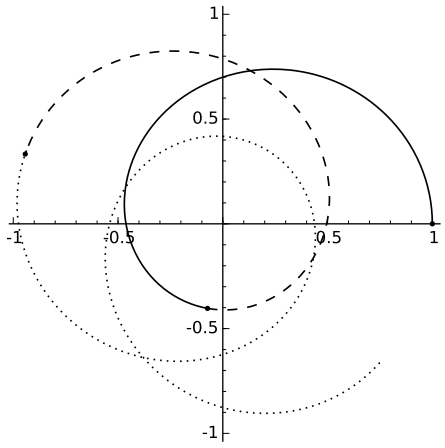

Figure 7: Orbit for $\rho_0 = 0.05$ and $\beta_0 = 0.04$. Starting point (1,0), following solid line first periapsis at point (0.41,4.53), following dashed line first period completed at point (1,9.07), continuing by dotted line for another period. All points are given in polar coordinates.

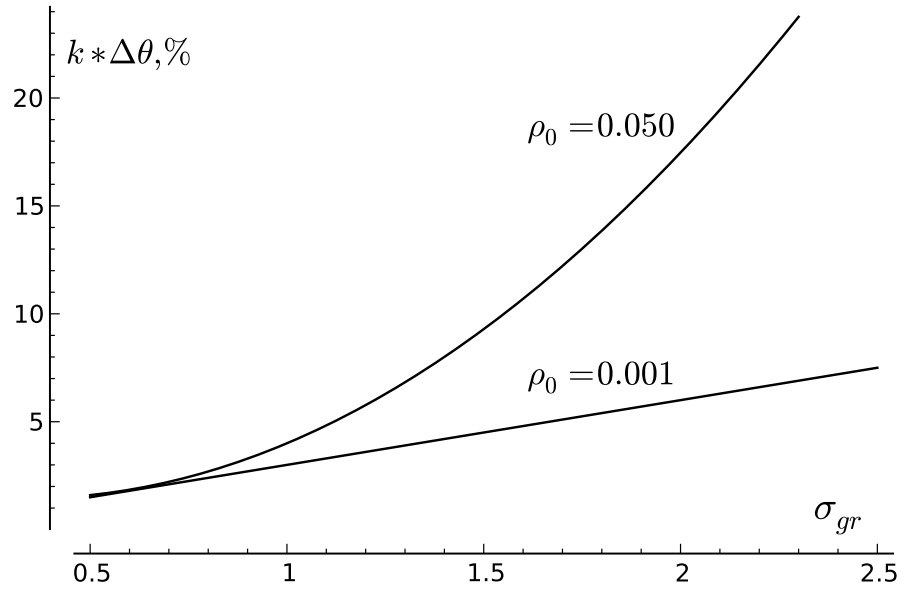

Figure 8: Dependence $\Delta\theta = 3\,\rho_0\,\sigma_{gr}$ of relative precessional advance on σ_{gr} as ρ_0 varies (exact numerical integration). Two curves are normalized to the same vertical plotting scale. Normalization coefficient $k = 10$ for $\rho_0 = 0.001$ (weak-field), and $k = 1/5$ for $\rho_0 = 0.050$ (mildly strong field) so that all lines for $\rho_0 < 0.001$ with proportionally however smaller effect coincide with the line for $\rho_0 = 0.001$. Deviated curves appear as the field strength rises with $\rho_0 > 0.001$.

Input parameters from the initial conditions:			
dimensionless $\rho_0 = r_g/r_0$	3.21×10^{-8}		
dimensionless β_0^2	3.87×10^{-8}		
dimensionless r_0	1		
Scaling quantities:			
The speed of light c	299792458 m/s		
Sun's standard gravitational parameter $\mu_0 = r_g c^2$	$1.32712440041 \times 10^{20}$ m^3/s^2		
Perihelion $r_0 = r_p$	4.6×10^{10} m		
Velocity at perihelion	58976 m/s		
Output:			
Computed characteristics	Classical theory q_{cl}	Absolute difference $q_{gr} - q_{cl}$	Relative difference $q_{gr}/q_{cl} - 1$
Aphelion radius r_a	69811764705.882 m	-14237.080 m	-2.039×10^{-7}
Velocity at aphelion	38860.233 m/s	7.924×10^{-3} m/s	2.039×10^{-7}
Angular full period	$2\,\pi$ rad	5.019×10^{-7} rad	7.988×10^{-8}
Time full period	7599967.916 s	-1.111 s	-1.461×10^{-7}
Full period orbit length	3.600×10^{11} m	-12603.073 m	-3.501×10^{-8}

Table 2: Mercury's problem in GR and Classical theories: input and output data. In the input, we fixed perihelion and velocity at perihelion as well as the gravitational field strength in the initial conditions, which chosen common for the GR and the classical theory. The output includes the main exactly calculated values of classical characteristics q_{cl} of the orbit, also the absolute differences of the corresponding GR values $q_{gr} - q_{cl}$ and the relative differences $q_{gr}/q_{cl} - 1$ with respect to the classical values.

	Event 1: at $\theta_{gr} = \pi$	Event 2: GR aphelion	Event 3: $\tau_3 = t_2$
τ	3799982.951801 s	3799983.402610 s	3799983.957976 s
r_{gr}	69811750468.802 m	69811750468.802 m	69811750468.801 m
θ_{gr}	$\pi = 3.141592654$ rad	$pi + 2.509 \times 10^{-7}$ rad	$\pi + 5.600 \times 10^{-7}$ rad
v_{gr}	38860.241 m/s	38860.241 m/s	38860.241 m/s
l_{gr}	179978550169.643 m	179978567688.220 m	179978589269.852 m
t	3799983.507166 s	3799983.957976 s	3799984.513341 s
r_{cl}	69811764705.882 m	69811764705.882 m	69811764705.881 m
θ_{cl}	$\pi - 2.509 \times 10^{-7}$ rad	$\pi = 3.141592653$ rad	$\pi + 3.091 \times 10^{-7}$ rad
v_{cl}	38860.233 m/s	38860.233 m/s	38860.233 m/s
l_{cl}	179978556471.180 m	179978573989.757 m	179978595571.387 m
Absolute differences of GR and classical theory values			
$\tau - t$	-0.555365 s	-0.555365 s	-0.555365 s
$r_{gr} - r_{cl}$	-14237.080 m	-14237.080 m	-14237.080 m
$\theta_{gr} - \theta_{cl}$	2.509×10^{-7} rad	2.509×10^{-7} rad	2.509×10^{-7} rad
$v_{gr} - v_{cl}$	0.007925 m/s	0.007925 m/s	0.007925 m/s
$l_{gr} - l_{cl}$	-6301.538 m	-6301.537 m	-6301.535 m
Relative differences of GR with respect to classical values			
$(\tau - t)/t$	-1.461×10^{-7}	-1.461×10^{-7}	-1.461×10^{-7}
Δr	-2.039×10^{-7}	-2.039×10^{-7}	-2.039×10^{-7}
$\Delta\theta$	7.988×10^{-8}	7.988×10^{-8}	7.988×10^{-8}
Δv	2.039×10^{-7}	2.039×10^{-7}	2.039×10^{-7}
Δl	-3.501×10^{-8}	-3.501×10^{-8}	-3.501×10^{-8}

Table 3: Three-events data in GR and classical theories. Shown are the absolute values of main orbital characteristics at events 1, 2, 3, predicted in each theory, including the time τ, t, the radius r_{gr}, r_{cl}, the angle θ_{gr}, θ_{cl}, the full orbital speed v_{gr}, v_{cl}, and the passed length along orbital trajectory l_{gr}, l_{cl}. Here and in the next tables, they are calculated in the first half-period starting from the initial conditions. The corresponding absolute values $q_{gr} - q_{cl}$ and relative differences of GR values with respect to classical ones $q_{gr}/q_{cl} - 1$ are also given. To the precision of 4 significant digits, differences do not change over the time interval, which includes the three events.

	classical theory	**GR**
Difference of values at event 2 and event 1		
time	0.450810 s	0.450810 s
radius	5.689×10^{-4} m	5.689×10^{-4} m
polar angle	2.509×10^{-7} rad	2.509×10^{-7} rad
full speed	-4.002×10^{-10} m/s	-3.986×10^{-10} m/s
trajectory length	17518.577 m	17518.578 m
Difference of values at event 3 and event 2		
time	0.555365 s	0.555365 s
radius	-8.634×10^{-4} m	-8.634×10^{-4} m
polar angle	3.091×10^{-7} rad	3.091×10^{-7} rad
full speed	6.039×10^{-10} m/s	6.050×10^{-10} m/s
trajectory length	21581.630 m	21581.631 m
Difference of values at event 3 and event 1		
time	1.006175 s	1.006175 s
radius	-2.945×10^{-4} m	-2.945×10^{-4} m
polar angle	5.601×10^{-7} rad	5.601×10^{-7} rad
full speed	2.064×10^{-10} m/s	2.064×10^{-10} m/s
trajectory length	39100.207 m	39100.209 m

Table 4: Three-events. Shown are the absolute differences of values of main orbital characteristics at events 1, 2, 3, predicted in each theory, including the time, the angle, the radius, the particle orbital speed, and the passed length, starting from the common initial conditions. Notice similarity of two columns.

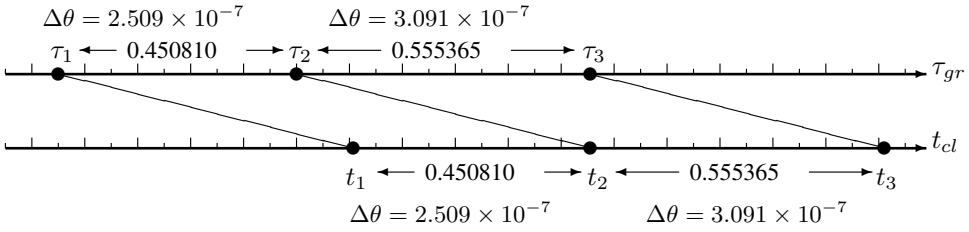

Table 5: Projections of GR three events to the classical time line. The GR angular advance $\Delta\theta = 2.509 \times 10^{-7}$ rad and the temporal advance $\Delta\tau = 0.555$ s are caused by the common reason, – the cubic term in GR Dynamics equations. The time shift is formed between events (3, 2), while the GR angular shift between the events (2, 1).

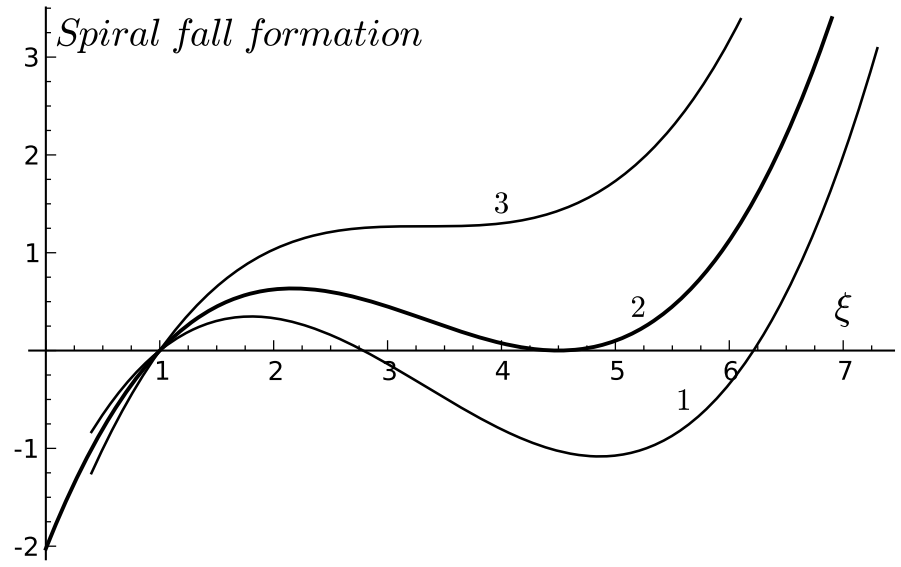

Figure 9: Plotted $f(\xi)$ (see text) for $\rho_0 = 0.050$. The curve 2 shows the edge point $\xi_2 = \xi_3 = 4.5$, with initial squared velocity $\beta^2_{edge} = 0.0341880$. The curve 1 is a sub-circle orbit with $\beta^2_0 = 0.038$. The curve 3 is an over-edge orbit, with $\beta^2_0 = 0.030$ and it illustrates the spiral fall trajectory that begins with $\beta^2_0 < \beta^2_{edge}$, when the roots ξ_2 and ξ_3 become complex.

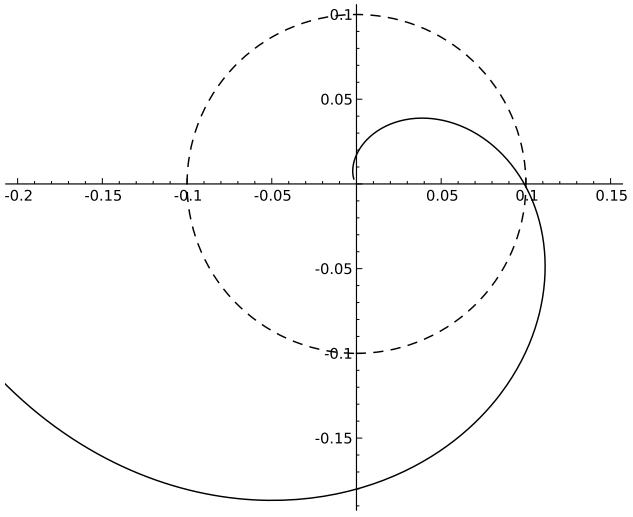

Figure 10: Spiral fall onto the center: crossing the Schwarzschild surface ($\xi = 10$, $r = 0.10$, $r_0 = 1$) in an over-edge orbit, $\rho_0 = 0.0500$, $\beta^2_0 = 0.300$, the case 3) in Figure 9. This figure shows proximity of a spiral sharp-dive onto the point center $r = 0$. The trajectory shown from some point before crossing of the Schwarzschild surface (dashed line). A particle crosses the Schwarzschild surface at the speed $\beta_{sch} = 1.982$, and, as shown in the picture, ended up deep inside the Schwarzschild sphere, at $r = r_g/15$ ($\xi = 300$), having a speed $\beta(1/300) = 285$.

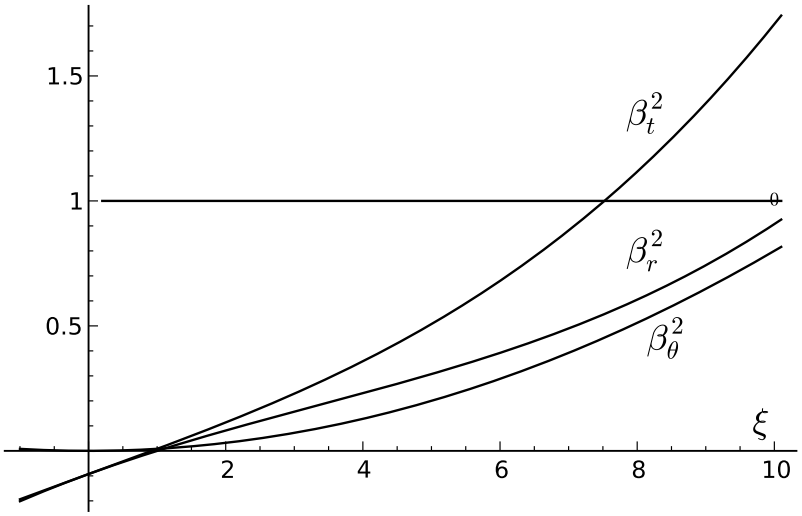

Figure 11: Example of over-edge motion: a spiral fall onto the center; $\rho_0 = 0.050$, $\beta_0^2 = 0.008$. Shown squared relative velocities of the test particle $\beta_r^2(\xi)$ Eq. (9), $\beta_\theta^2(\xi)$ Eq. (10), $\beta^2(\xi)$ Eq. (38); a conserved (squared) total energy $\epsilon_0^2 = 0.907$ (that is, a bounded motion). The particle crosses the Schwarzschild surface $\xi_{sch} = 10$ ($r_{sch} = 0.10$) at the resultant speed $\beta = 1.304$ (faster than light) with the kinetic energy $\beta_r^2 = 0.907$. The angular component of speed is $\beta_\theta^2 = 0.800$ (in this example, it is less than the speed of light), and the resultant one $\beta^2 = 1.707$ (faster than light). The particle reaches the resultant speed equal to the speed of light $\beta = 1$ at the radial point $\xi = 7.54$ ($r = 0.133$), that is outside the interior region.

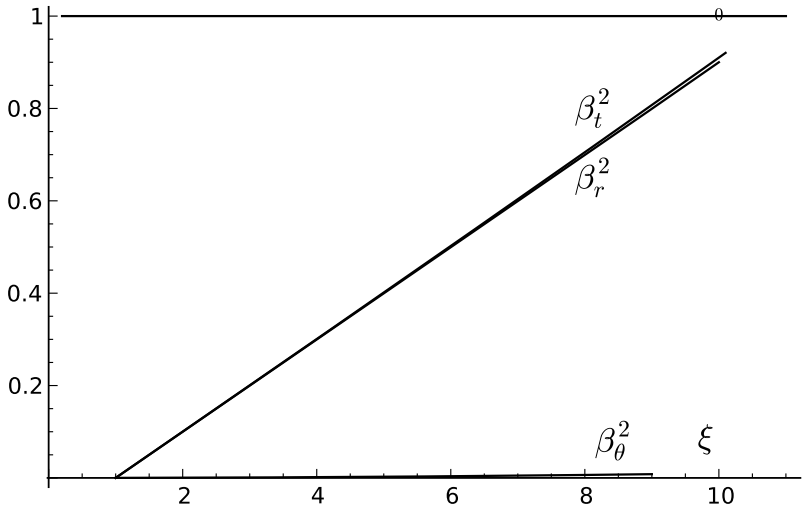

Figure 12: The case of subluminal motion: spiral fall onto the center; $\rho_0 = 0.050$, $\beta_0^2 = 0.0001$. Shown squared relative velocity components $\beta_r^2(\xi)$ Eq. (9), $\beta_\theta^2(\xi)$ Eq. (10), $\beta_t^2(\xi)$ Eq. (38); a conserved (squared) total energy $\epsilon_0^2 = 0.900$. The particle crosses the horizon at the resultant speed $\beta_t = 0.910$ (less than speed of light) with velocity (squared) components $\beta_r^2 = 0.900$, $\beta_\theta^2 = 0.010$.

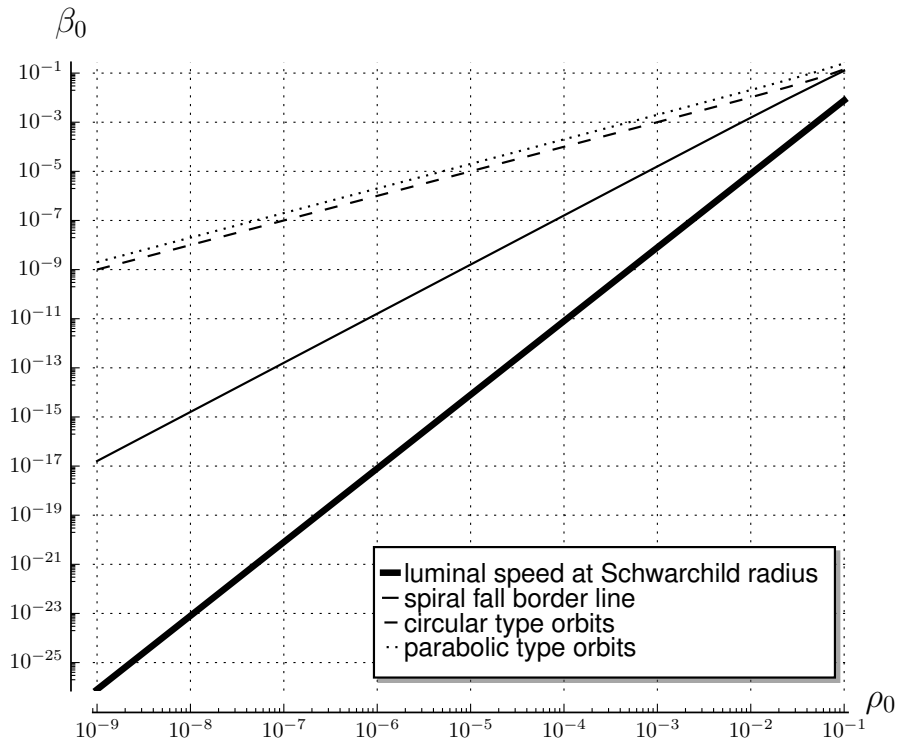

Figure 13: Conditions of the luminal speed at Schwarzschild radius. For the values (ρ_0, β_0^2) below the thick line the full speed of a particle at Schwarzschild radius is lower than the speed of light, between the thick and the solid lines, the speed is greater than the speed of light.

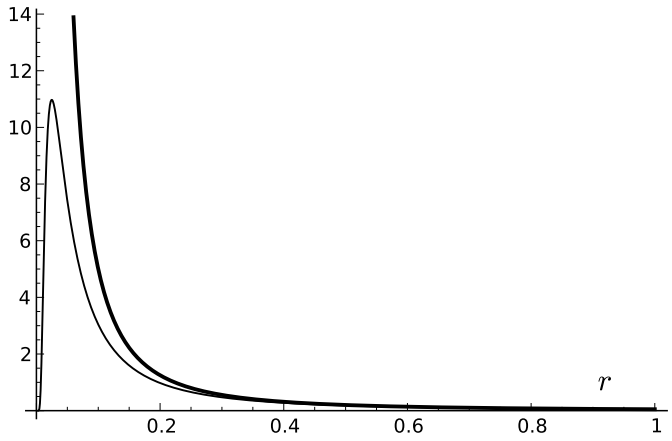

Figure 14: Newtonian attractive force $F(r) \sim r_g/r^2$ (thick line) and its relativistic generalization $F_R(r) \sim r_g/r^2 \exp(-r_g/r)$ in the concept of field-dependent proper mass, in the example of a strong interaction $r_g = 0.05$. It has a maximal absolute value at $r = r_g$, and $F_R(r) \to 0$ as $r \to 0$; in the range $r < r_g$, it rises with distance and asymptotically $F_R(r) \to F(r)$ as $r \to \infty$.

Input parameters:			
dimensionless $\rho_0 = r_g/c^2$		3.21×10^{-8}	
dimensionless β_0^2		3.87×10^{-8}	
dimensionless r_0		1	
Scaling quantities:			
The speed of light c		299792458 m/s	
Sun standard gravitational parameter $\mu_0 = r_g c^2$		$1.32712440041 \times 10^{20}$ m^3/s^2	
Perihelion r_p		4.6×10^{10} m	
Velocity at perihelion		58976 m/s	
Output:			
Computed characteristics	Classical theory q_{cl}	Absolute difference Δq	relative difference δq
Aphelion r_a	69811764705.882 m	4877.583 m	6.987×10^{-8}
Velocity at aphelion	38860.233 m/s	-2.715×10^{-3} m/s	-6.986×10^{-8}
Angular full period	$2\,\pi$ rad	-1.673×10^{-7} rad	-2.663×10^{-8}
Time full period T	7599967.916 s	0.383 s	5.042×10^{-8}
Full period orbit length	3.600×10^{11} m	4510.132 m	1.253×10^{-8}

Table 6: The input and output data for computing Mercury's orbital characteristics in Classical and SR Dynamics are shown. In the input, there are only two independent model parameters, ρ_0 and β_0^2, from the initial conditions common for both theories. In the output, absolute values of main classical characteristics q_{cl} integrated over the full period, and their absolute and relative differences $\Delta q = q_{sr} - q_{cl}$, $\delta q = q_{sr}/q_{cl} - 1$ with respect to corresponding Classical Dynamics, are given.

	Event 1: $t_{sr}(1) = t_{cl}(2)$	Event 2 SR aphelion	Event 3: SR $\theta = \pi$
t_{sr}	3799983.957976 s	3799984.149588 s	3799984.299859 s
r_{sr}	69811769583.465 m	69811769583.465 m	69811769583.465 m
θ_{srd}	$\pi - 1.903 \times 10^{-7}$ rad	$\pi - 8.364 \times 10^{-8}$ rad	$\pi = 3.141592653$ rad
v_{sr}	38860.230 m/s	38860.230 m/s	38860.230 m/s
l_{sr}	179978568798.694 m	179978576244.823 m	179978582084.349 m
t_{cl}	3799983.766362 s	3799983.957976 s	3799984.108246 s
r_{cl}	69811764705.882 m	69811764705.882 m	69811764705.882 m
θ_{cl}	$\pi - 1.066 \times 10^{-7}$ rad	$\pi = 3.141592653$ rad	$\pi + 8.364 \times 10^{-8}$ rad
v_{cl}	38860.233 m/s	38860.233 m/s	38860.233 m/s
l_{cl}	179978566543.628 m	179978573989.757 m	179978579829.283 m
Absolute differences between SRD and classical theories			
Δt	0.191613 s	0.191613 s	0.191613 s
Δr	4877.583 m	4877.583 m	4877.583 m
$\Delta\theta$	-8.365×10^{-8} rad	-8.365×10^{-8} rad	-8.365×10^{-8} rad
Δv	-0.002715 m/s	-0.002715 m/s	-0.002715 m/s
Δl	2255.066 m	2255.066 m	2255.066 m
Relative differences between SRD and classical theories			
δt	5.042×10^{-8}	5.042×10^{-8}	5.042×10^{-8}
δr	6.987×10^{-8}	6.987×10^{-8}	6.987×10^{-8}
$\delta\theta$	-2.663×10^{-8}	-2.663×10^{-8}	-2.663×10^{-8}
δv	-6.987×10^{-8}	-6.987×10^{-8}	-6.987×10^{-8}
δl	1.253×10^{-8}	1.253×10^{-8}	1.253×10^{-8}

Table 7: Orbital Mercury's characteristics q_{sr} computed at 3 events in SR Dynamics time scale t_{sr} in comparison with q_{cl} computed in the classical time scale t_{cl} starting with the common initial conditions are shown. Also shown their absolute and relative differences $\Delta q = q_{sr} - q_{cl}$, $\delta q = q_{sr}/q_{cl} - 1$. The following characteristics are computed at each event: the time passed t_{sr}, t_{cl}, the radius r_{sr}, r_{cl}, the orbital angle θ_{sr}, θ_{cl}, the orbital speed v_{sr}, v_{cl}, the orbital length l_{sr}, l_{cl}.

	Classical theory	**SR theory**
Difference between Event 2 and Event 1		
Time	0.191613 s	0.191613 s
Radius	1.028×10^{-4} m	1.028×10^{-4} m
Polar angle	1.067×10^{-7} rad	1.067×10^{-7} rad
Full speed	-7.276×10^{-11} m/s	-7.202×10^{-11} m/s
Trajectory length	7446.129 m	7446.129 m
Difference between Event 3 and Event 2		
Time	0.150270 s	0.150270 s
Radius	-6.321×10^{-5} m	-6.321×10^{-5} m
Polar angle	8.365×10^{-8} rad	8.365×10^{-8} rad
Full speed	4.366×10^{-11} m/s	4.429×10^{-11} m/s
Trajectory length	5839.526 m	5839.526 m
Difference between Event 3 and Event 1		
Time	0.341883 s	0.341883 s
Radius	3.957×10^{-5} m	3.957×10^{-5} m
Polar angle	1.903×10^{-7} rad	1.903×10^{-7} rad
Full speed	-2.773×10^{-11} m/s	-2.773×10^{-11} m/s
Trajectory length	13285.655 m	13285.654 m

Table 8: Absolute differences of orbital characteristics between events (2, 1), (3, 2), (3, 1) computed in SR Dynamics and Classical theory.

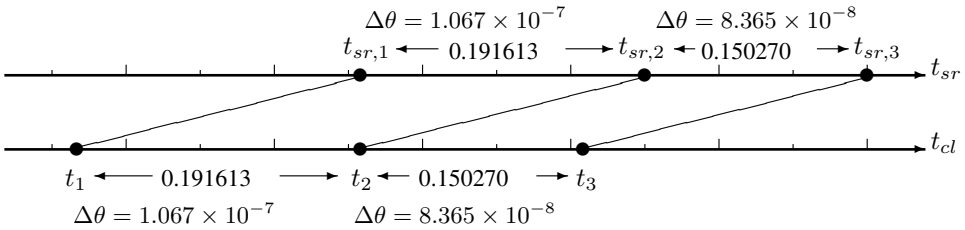

Table 9: The projections of the three SR events on the base time line t_{sr} and the classical time line t_{cl} are shown, which, again, demonstrate the disparity of angular and temporal shifts on the uniform time scales. The retardation of SR time clock and angular shift, as opposed to the GR advance, is demonstrated. It makes a tremendous positive impact on SR Physics of orbits, see the text